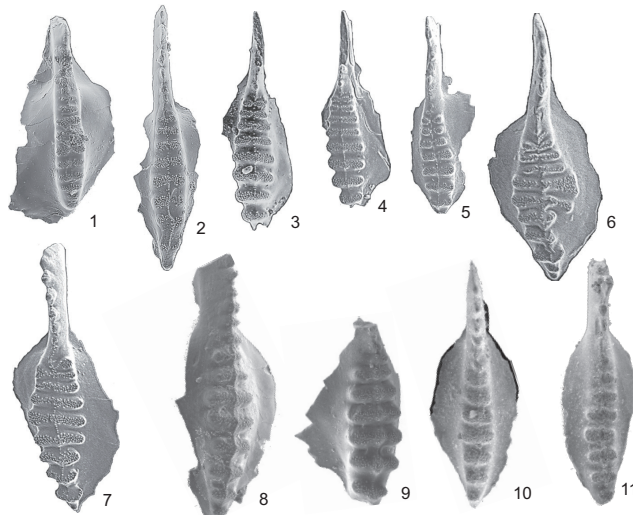
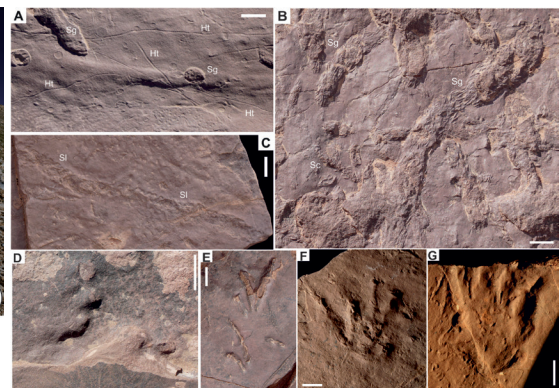




# Permophiles

International Commission on Stratigraphy



Newsletter of the  
Subcommission on  
Permian Stratigraphy  
Number 70  
ISSN 1684-5927  
January 2021

## Table of Contents

|   |           |
|---|-----------|
| <b>Notes from SPS Secretary</b>   | <b>3</b>  |
| Yichun Zhang  |           |
| <b>Notes from SPS Chair</b>   | <b>3</b>  |
| Lucia Angiolini   |           |
| <b>Annual Report 2020</b>   | <b>4</b>  |
| <b>Report of SPS corresponding members meeting on 13 November 2020</b>  | <b>7</b>  |
| <b>TO BE OR NOT TO BE <i>Sweetognathus asymmetricus</i>?</b>  | <b>10</b> |
| Charles M. Henderson, Valery V. Chernykh  |           |
| <b>Permian substages</b>  | <b>13</b> |
| Spencer G. Lucas  |           |
| <b>Permian continental trace fossils of Morocco: first record from the Jebilet massif</b>   | <b>16</b> |
| Amal Zouicha, Sebastian Voigt, Hafid Saber, Lorenzo Marchetti, Abdelkbir Hminna, Ahmed El Attari, Ausonio Ronchi, Joerg W. Schneider  |           |
| <b>Tectono-sedimentary evolution of the Upper Paleozoic Mulargia-Escalaplano molassic basin (Sardinia, Italy) in the collapsing Variscan chain: matching the pull-a-part model of the W Europe basins</b>   | <b>19</b> |
| Luca G. Costamagna  |           |
| <b>Latest Carboniferous to Early Permian volcano-stratigraphic evolution in Central Europe: U-Pb CA-ID-TIMS ages of volcanic rocks in the Thuringian Forest Basin (Germany) - summary of the original paper in Int. J. Earth Sci. (Geol. Rundsch.), 2020.</b>                                   | <b>23</b> |
| Harald Lützner, Marion Tichomirova, Alexandra Käßner, Reinhard Gaupp  |           |
| <b>Guadalupian and Lopingian transgression of the Khuff Formation carbonate sea in the Middle East and Levant</b>   | <b>27</b> |
| Michael H. Stephenson, Dorit Korngreen  |           |
| <b>One step closer to understanding the Permian-Triassic mass extinction</b>  | <b>29</b> |
| Hana Jurikova   |           |
| <b>Report of fieldtrip to northern Tibet: Permian successions in blocks of the Qinghai-Tibet Plateau</b>  | <b>31</b> |
| Yichun Zhang, Hua Zhang, Quanfeng Zheng, Mao Luo, Wenkun Qie, Dongxun Yuan, Feng Qiao, Haipeng Xu, Qi Ju, Biao Gao  |           |
| <b>Comment to Chen et al., 2020: Abrupt warming in the latest Permian detected using high-resolution in situ oxygen isotopes of conodont apatite from Abadeh, central Iran. Importance of correct stratigraphic correlation, reporting of existing data and their scientific interpretation</b> | <b>33</b> |
| Micha Horacek, Leopold Krystyn, Aymon Baud  |           |
| <b>Compilation of selected papers published on Permian topics in 2020</b>   | <b>36</b> |
| <b>SUBMISSION GUIDELINES FOR ISSUE 71</b>   | <b>43</b> |



Fig. 1. Artist's reconstruction of the onset of the Permian-Triassic mass extinction, Jurikova, this issue.  
 Fig. 2. Field views in the Duoma area, Shuanghu County, Tibet, Zhang et al., this issue.  
 Fig. 3. Trace fossils from the Koudiat El Hamra Formation, Zouicha et al., this issue.  
 Fig. 4. *Sweetognathus asymmetricus* Sun and Lai, Henderson and Chernykh, this issue.

## Notes from the SPS secretary

Yichun Zhang

### Introduction and thanks

During this busy time, Lucia Angiolini and I prepared this issue of *Permophiles* 70 via frequent email communications, as we had no opportunity to meet due to severe Covid-19 virus restrictions around the world. Even if the interval between the last issue and the current issue was very short, we received many contributions for this issue. It is clear that Permian scientists are very active in Permian research and keen to discuss significant Permian topics!

During the last months, I worked to design and organize a new Permian website (<http://permian.stratigraphy.org/>). I would like to thank Nicholas Car (webmaster of ICS) who assisted me in building our new website. I also thank many researchers who kindly provided the photos for the website. The new website will be released soon. In the new website, besides an update on the Objectives, Members, Working groups, GSSPs, Time scale, Publications, there is a new section with topics of interest to all the members. At the moment it comprise a compilation of the papers published on Permian topics in 2020. This work was commissioned to Claudio Garbelli by the SPS executive. Thanks to Claudio for his hard work. The 2020 reference list will also be included at the end of this *Permophiles* issue. Here, I would like to encourage Permian workers to share their work on the website at any time, and suggest publications to be added to the list (for the moment just papers published in 2020).

This issue of *Permophiles* contains contributions covering many aspects of our Permian study including biostratigraphy, high-resolution dating, palaeogeography, end-Permian mass extinctions and field reports. Many thanks to the contributors of this issue: Charles M. Henderson, Valery V. Chernykh, Spencer G. Lucas, Amal Zouicha and co-authors, Luca G. Costamagna, Harald Lützner and co-authors, Michael H. Stephenson and Dorit Korngreen, Hana Jurikova, Micha Horacek and co-authors.

### Permophiles 70

This issue contains fruitful contributions on diverse aspects related to Permian studies. Charles Henderson and Valery Chernykh have agreed to use *Sweetognathus asymmetricus* to replace *Sw. whitei* to define the base of the Artinskian stage. The emended description of *Sw. asymmetricus* and its wide distribution and potential global correlation hold promise for defining GSSP at the Dal'ny Tulkas Section.

Spencer G. Lucas reviewed the substages of Permian. He strengthened that subdividing the substages of Permian is the future work of SPS. We acknowledge such proposal.

Amal Zouicha and co-authors reported tetrapod ichno-assemblages from the Koudiat El Hamra-Haiane basin of Morocco. These trace fossils suggest the age to be Artinskian to Capitanian for the red beds in the basin.

Luca G. Costamagna reported his work in the Mulargia-Escalaplano molassic basin in Sardinia, Italy. By studying the depositional facies of the Rio Su Luda and Mulargia formations, he proposed a pull-a-part basin model.

Harald Lützner and co-authors reported recent high-resolution TIMS ages on the volcanic rocks in the Thuringian Forest Basin of Germany. These new data allow to update the ages of many formations in the basin and help in defining the Carboniferous-Permian Boundary in the basin. More significantly, the duration of the volcanic activity in this basin was shorter than previously recognised.

Michael H. Stephenson and Dorit Korngreen have reported their recent work in the Permian of the Negev desert of Israel and Jordan. The correlations of Permian sequences among Israel, Jordan, Saudi Arabia and Oman allowed the authors to recognise a significant diachronous onset of marine limestones from Oman to Israel.

Hana Jurikova summarised the key findings and implications of a recent geochemical work on the Permian-Triassic mass extinction. The modelling based on pH data from brachiopods and global carbon isotope records suggests a sudden and steep release of CO<sub>2</sub>, which triggered the end-Permian mass extinction.

Yichun Zhang and co-authors reported their recent fieldwork in northern Tibet. The different Permian sequences and faunas are significant for palaeobiogeographic and palaeogeographic reconstructions.

This issue ends with a last minute contribution by Micha Horacek and co-authors which contains a discussion about a paper by Chen et al. recently published on the famous Abadeh section in Iran. We welcome and wait for a reply by Chen and co-authors and remind all Permian workers that *Permophiles* is a forum for discussion on Permian topics.

### Future issues of *Permophiles*

The next issue of *Permophiles* will be the 71st issue.

We welcome contributions related to Permian studies around the world. So, I kindly invite our colleagues to contribute harangues, papers, reports, comments and communications.

The deadline for submission to Issue 71 is 31 July 2021. Manuscripts and figures can be submitted via email address ([yczhang@nigpas.ac.cn](mailto:yczhang@nigpas.ac.cn)) as attachment.

To format the manuscript, please follow the TEMPLATE on Permian website.

---

## Notes from the SPS Chair

Lucia Angiolini

In last *Permophiles* issue, the new executive was presented, along with the main goals for the next term. The new SPS executive started to work to promote collaboration among Permian workers and to widen the Permian community, by organizing two webinars. The first (22 October 2020) was restricted to voting members and has been already reported in *Permophiles* 69, while the second (13 November 2020) was open to the corresponding members and it is described in the present issue.

The results of these webinars are now coming to fruition, as demonstrated by the conspicuous contributions presented for this issue. This is an important step forward for the completion of the

GSSPs for the Permian System.

The work of Valery Chernykh and Charles Henderson, presented in this issue with the evocative title “TO BE OR NOT TO BE *Sweetognathus asymmetricus*?””, allows the executive to turbocharge the Artinskian-base GSSP.

The candidacy of the Dal’ny Tulkas section to define the Artinskian-base GSSP was published many years ago in *Permophiles* 58 (Chuvashov et al., 2013) and updated in *Permophiles* 69 (Chernykh, 2020). The section and point are promising, as sedimentation is continuous and there are several bioevents to mark the boundary and use for correlation: conodonts, fusulines, ammonoids. There are geochronologic ages, and C and Sr isotope data. The main problem, discussed in the SPS voting member webinar, was the name of the defining conodont species *Sweetognathus whitei*.

However, based on the important contribution published in this issue, it is clear that the successful collaboration between Valery and Charles lead to the solution of the main objection regarding this taxon and thus the removal of the main obstacle in defining the GSSP at Dal’ny Tulkas.

I thus kindly ask all SPS voting and corresponding members to read carefully the taxonomic agreement of the two conodont specialists and provide comments and contributions by the end of February.

A revised proposal will be sent to voting members by April, with a request for comments before voting, followed by call for a vote of voting members in summer 2021.

Other ongoing activities include the construction of the new SPS website by the SPS secretary Yichun Zhang with the help of Nicholas Car, of SURROUND Australia. For this, I warmly thank Yichun for his very hard work (also in editing *Permophiles*) and those of you who have provided photos for the website and the revised working group descriptions.

The website is available now to all of you and it will be supplemented by a video to advertise the Permian to a wide audience. This is still under construction.

Last, but not least, the vice-chair Mike Stephenson and I have discussed the topics of the next webinars.

The first already scheduled will be “Uses and abuses of radiometric data for Permian workers” by Mark Schmitz, Boise State University and will be held on 1st April 2021 at 16.00 European time with the help of organization by Jeanine Newham of BGS.

The second will be held after the summer and will be focused on “Uses and abuses of palaeogeographic reconstructions for Permian workers” by Giovanni Muttoni, Università di Milano.

We will keep you informed on all ongoing activities also through the new website.

---

## ANNUAL REPORT 2020

### 1. TITLE OF CONSTITUENT BODY and NAME OF REPORTER

International Subcommission on Permian Stratigraphy (SPS)

Submitted by:

Lucia Angiolini, SPS Chairman

Dipartimento di Scienze della Terra “A. Desio”

Via Mangiagalli 34  
20133 Milano, Italy  
E-mail: [lucia.angiolini@unimi.it](mailto:lucia.angiolini@unimi.it)

### 2. OVERALL OBJECTIVES, AND FIT WITHIN IUGS SCIENCE POLICY

**Subcommission Objectives:** The Subcommission’s primary objective is to define the series and stages of the Permian by means of internationally agreed GSSPs and establish a high-resolution temporal framework based on multidisciplinary (biostratigraphical, geochronologic, chemostratigraphical, magnetostratigraphical etc.) approaches, and to provide the international forum for scientific discussion and interchange on all aspects of the Permian, but specifically on refined intercontinental and regional correlations.

**Fit within IUGS Science Policy:** The objectives of the Subcommission involve two main aspects of IUGS policy: 1) The development of an internationally agreed chronostratigraphic scale with units defined by GSSPs where appropriate and related to a hierarchy of units to maximize relative time resolution within the Permian System; and 2) the establishment of framework and systems to encourage international collaboration in understanding the evolution of the Earth and life during the Permian Period.

### 3. ORGANISATION - interface with other international projects / groups

#### 3a. Officers for 2020-2024 period:

##### Current Officers (from 1 August 2020):

###### **Prof. Lucia Angiolini (SPS Chair)**

Dipartimento di Scienze della Terra “A. DESIO”  
Via Mangiagalli 34,  
20133 Milano, Italy  
E-mail: [lucia.angiolini@unimi.it](mailto:lucia.angiolini@unimi.it)

###### **Prof. Michael H. Stephenson (SPS Vice-chair)**

British Geological Survey  
Kingsley Dunham Centre  
Keyworth, Nottingham NG12 5GG  
United Kingdom  
E-mail: [mhste@bgs.ac.uk](mailto:mhste@bgs.ac.uk)

###### **Prof. Yichun Zhang (SPS Secretary)**

State Key Laboratory of Palaeobiology and Stratigraphy  
Nanjing Institute of Geology and Palaeontology  
39 East Beijing Road  
Nanjing, Jiangsu 210008, China  
E-mail: [yczhang@nigpas.ac.cn](mailto:yczhang@nigpas.ac.cn)

##### Officers until 1 August 2020:

###### **Prof. Shuzhong Shen (SPS Chair)**

School of Earth Sciences and Engineering  
Nanjing University,  
163 Xianlin Avenue, Nanjing, Jiangsu 210023, China  
E-mail: [szshen@nj.edu.cn](mailto:szshen@nj.edu.cn)

**Prof. Joerg W. Schneider (SPS Vice-Chair)**

Freiberg University of Mining and Technology  
Institute of Geology, Dept. of Palaeontology,  
Bernhard-von-Cotta-Str.2  
Freiberg, D-09596, Germany  
E-mail: [Joerg.Schneider@geo.tu-freiberg.de](mailto:Joerg.Schneider@geo.tu-freiberg.de)

**Prof. Lucia Angiolini (SPS Secretary)**

Dipartimento di Scienze della Terra “A. Desio”  
Via Mangiagalli 34, 20133  
Milano, Italy  
E-mail: [lucia.angiolini@unimi.it](mailto:lucia.angiolini@unimi.it)

**4. EXTENT OF NATIONAL/REGIONAL/GLOBAL SUPPORT FROM SOURCES OTHER THAN IUGS**

Shuzhong Shen and Michael Stephenson are investigating the possibility of support for SPS through the Deep-time Digital Earth (DDE) Big Science Program of IUGS focused on informatics support for biostratigraphic data management and palaeogeographic reconstructions.

**5. CHIEF ACCOMPLISHMENTS IN 2020 (including any relevant publications arising from ICS working groups)**

- General proposals for the bases of the Artinskian and Kungurian stages have been prepared and published in the SPS Newsletters *Permophiles* 69 by Chernykh (2020).
- A multidisciplinary study of the Mechetlino Quarry section (Southern Urals, Russia), the GSSP candidate for the base of the Kungurian Stage has been published by Chernykh et al. (2020, *Palaeoworld* 29).
- The Sakmarian-base GSSP by Chernykh et al. has been accepted for publication in *Episodes* in April 2020.
- Two issues of *Permophiles* have been published (SPS Newsletters *Permophiles* 68 and 69)
- The Guadalupian timescale has been refined based by Wu et al. (2020, *Palaeogeography, Palaeoclimatology, Palaeoecology*, 548). A comprehensive paper on the three GSSPs and their correlation of the the Guadalupian Series has been published (Shen et al., 2020, *Earth-Science Review*, 211)
- A comprehensive review of the terrestrial Permian stratigraphy has been provided by Schneider et al. (2020, *Palaeoworld*, 29).
- A voting members webinar has been organized on 22 October 2020.
- A corresponding members webinar has been organized on 13 November 2020.

**6. SUMMARY OF EXPENDITURE IN 2020**

No expenditure was incurred in 2020 due to the health emergency for Covid-19 which prevented travel for congresses and field trips.

**7. SUMMARY OF INCOME IN 2020**

An amount of Euros 3356,84 was allocated from ICS.

**8. BUDGET REQUESTED FROM ICS IN 2021\*\*\***

We apply for 5700 US\$ from ICS for SPS activities in 2021. This will be mainly for the activities to turbocharge

first the establishment of the base-Artinskian GSSP at Dal’ny Tulkas section, Russia and then the base-Kungurian GSSP at Mechetlino, Russia, and to organize (if possible depending on the development of the Covid-19 emergency) a voting members field trip in the area.

We will use a part of the money for producing a professional video to advertise SPS and eventually for some publication costs.

**9. WORK PLAN, CRITICAL MILESTONES, ANTICIPATED RESULTS AND COMMUNICATIONS TO BE ACHIEVED NEXT YEAR:**

- We plan to ratify the GSSP of the base of Artinskian and start to work on that of the base of Kungurian.
- We plan to produce a video to advertise SPS.

**10. KEY OBJECTIVES AND WORK PLAN FOR THE PERIOD 2020-2024**

- Establish the Artinskian and Kungurian GSSPs.
- Revise the Permian timescale where it needs to be improved (Guadalupian stages, replacement GSSP section of the base-Lopingian).
- Establish a robust palaeogeographic frameworks for the Permian and focus on N-S correlations.
- Propose DDE-sponsored informatics support for biostratigraphic data management and palaeogeographic reconstructions.
- Organize webinars to increase the size, diversity and international coverage of the Permian Community
- Publish at least two *Permophiles* issues each year

**APPENDIX [Names and Addresses of Current Officers and Voting Members]**

**Prof. Lucia Angiolini (SPS Chair)**

Dipartimento di Scienze della Terra “A. DEsio”  
Via Mangiagalli 34, 20133, Milano, Italy  
E-mail: [lucia.angiolini@unimi.it](mailto:lucia.angiolini@unimi.it)

**Dr. Alexander Biakov**

Northeast Interdisciplinary Scientific Research Institute  
Far East Branch, Russian Academy of Sciences,  
Portovaya ul. 16, Magadan, 685000 Russia  
E-mail: [abiakov@mail.ru](mailto:abiakov@mail.ru)

**Dr. Valery Chernykh**

Institute of Geology and Geochemistry  
Urals Branch of Russian Academy of Science  
Pochtovy per 7, Ekaterinburg 620154 Russia  
E-mail: [vtschernich@mail.ru](mailto:vtschernich@mail.ru)

**Dr. Nestor R. Cuneo**

Museo Paleontologico Egidio Feruglio  
(U9100GYO) Av. Fontana 140,  
Trelew, Chubut, Patagonia Argentina  
E-mail: [rcuneo@mef.org.ar](mailto:rcuneo@mef.org.ar)

**Prof. Charles M. Henderson**

Dept. of Geoscience, University of Calgary

Calgary, Alberta, Canada T2N1N4  
E-mail: [cmhender@ucalgary.ca](mailto:cmhender@ucalgary.ca)

**Dr. Valeriy K. Golubev**  
Borissiak Paleontological Institute, Russian Academy of Sciences  
Profsoyuznaya str. 123, Moscow, 117997 Russia  
E-mail: [vg@paleo.ru](mailto:vg@paleo.ru)

**Prof. Spencer G. Lucas**  
New Mexico Museum of Natural History and Science  
1801 Mountain Road N. W., Albuquerque, New Mexico 87104-1375 USA  
E-mail: [spencer.lucas@state.nm.us](mailto:spencer.lucas@state.nm.us)

**Prof. Ausonio Ronchi**  
Dipartimento di Scienze della Terra e dell'Ambiente  
Università di Pavia - Via Ferrata 1, 27100 PV, ITALY  
voice +39-0382-985856  
E-mail: [ausonio.ronchi@unipv.it](mailto:ausonio.ronchi@unipv.it)

**Dr. Tamra A. Schiappa**  
Department of Geography, Geology and the Environment  
Slippery Rock University, Slippery Rock, PA 16057 USA  
E-mail: [tamra.schiappa@sru.edu](mailto:tamra.schiappa@sru.edu)

**Prof. Mark D. Schmitz**  
Isotope Geology Laboratory  
Department of Geosciences  
Boise State University, 1910 University Drive  
Boise, ID 83725-1535, USA  
E-mail: [markschmitz@boisestate.edu](mailto:markschmitz@boisestate.edu)

**Prof. Joerg W. Schneider**  
Freiberg University of Mining and Technology  
Institute of Geology, Dept. of Palaeontology,  
Bernhard-von-Cotta-Str.2, Freiberg, D-09596, Germany  
E-mail: [Joerg.Schneider@geo.tu-freiberg.de](mailto:Joerg.Schneider@geo.tu-freiberg.de)

**Prof. Shuzhong Shen**  
School of Earth Sciences and Engineering  
Nanjing University, 163 Xianlin Avenue,  
Nanjing, Jiangsu 210023, P.R. China  
E-mail: [szshen@nju.edu.cn](mailto:szshen@nju.edu.cn)

**Prof. Guang R. Shi**  
School of Life and Environmental Sciences,  
Deakin University, Melbourne Campus (Burwood),  
221 Burwood Highway, Burwood, Victoria 3125, Australia  
E-mail: [guang@uow.edu.au](mailto:guang@uow.edu.au)

**Prof. Michael H. Stephenson (SPS Vice-Chair)**  
British Geological Survey, Kingsley Dunham Centre  
Keyworth, Nottingham NG12 5GG  
United Kingdom  
E-mail: [mhst@bgs.ac.uk](mailto:mhst@bgs.ac.uk)

**Prof. Katsumi Ueno**

Department of Earth System Science  
Fukuoka University, Fukuoka 814-0180 JAPAN  
E-mail: [katsumi@fukuoka-u.ac.jp](mailto:katsumi@fukuoka-u.ac.jp)

**Prof. Yue Wang**  
Nanjing Institute of Geology and Paleontology,  
39 East Beijing Rd. Nanjing, Jiangsu 210008, China  
E-mail: [yuewang@nigpas.ac.cn](mailto:yuewang@nigpas.ac.cn)

**Prof. Yichun Zhang (SPS Secretary)**  
Nanjing Institute of Geology and Palaeontology  
39 East Beijing Road, Nanjing, Jiangsu 210008, China  
E-mail: [yczhang@nigpas.ac.cn](mailto:yczhang@nigpas.ac.cn)

**Working group leaders**  
1) Artinskian-base and Kungurian-base GSSP Working Group;  
Chair-Valery Chernykh.  
2) Correlation between marine and continental Guadalupian  
Working Group; Chair-Charles Henderson.  
3) Correlation between marine and continental Carboniferous-  
Permian Transition Working Group; Chair-Joerg Schneider.

---

## Honorary Members

**Prof. Giuseppe Cassinis**  
Dipartimento di Scienze della Terra e dell'Ambiente  
Università di Pavia  
Via Ferrata 1, 27100 PV, Italy  
E-mail: [cassinis@unipv.it](mailto:cassinis@unipv.it)

**Dr. Boris I. Chuvashov**  
Institute of Geology and Geochemistry Urals Branch of  
Russian Academy of Science  
Pochtovy per 7  
Ekaterinburg 620154 Russia  
E-mail: [chuvashov@igg.uran.ru](mailto:chuvashov@igg.uran.ru)

**Prof. Ernst Ya. Leven**  
Geological Institute  
Russian Academy of Sciences  
Pyjevskyi 7  
Moscow 109017 Russia  
E-mail: [erleven@yandex.ru](mailto:erleven@yandex.ru)

**Dr. Galina Kotylar**  
All-Russian Geological Research Institute  
Sredny pr. 74  
St. Petersburg 199206 Russia  
E-mail: [Galina\\_Kotlyar@vsegei.ru](mailto:Galina_Kotlyar@vsegei.ru)

**Prof. Claude Spinosa**  
Department of Geosciences  
Boise State University  
1901 University Drive  
Boise ID 83725 USA  
E-mail: [cspinosa@boisestate.edu](mailto:cspinosa@boisestate.edu)

## Report of SPS corresponding members meeting on 13 November 2020

On 13 November, 2020, the SPS Chair Lucia Angiolini and Vice Chair Mike Stephenson, with the help of Jeanine Newham (BGS), organized a zoom webinar for the corresponding members.

Twenty-six persons from different parts of the world attended the webinar: Deepa Agnihotri, Lucia Angiolini, Sylvie Bourquin, Simonetta Cirilli, Luca Costamagna, Eliana Coturel, Giusy Forte, Claudio Garbelli, Charles Henderson, Hana Jurikova, Leopold Krystyn, Evelyn Kustatscher, Ruslan Kutygin, Lance Lambert, Lorenzo Marchetti, Giovanni Muttoni, Tadeusz Peryt, Ausonio Ronchi, Tamra Schiappa, Joerg W. Schneider, Lucas Spencer, Amalia Spina, Mike Stephenson, Geoff Warrington, Liz Weldon, Dungxun Yuan and Yichun Zhang.

The agenda of the meeting comprised the following topics: an Introduction to the SPS by Lucia Angiolini, a presentation on the continental Permian by Joerg W. Schneider, a presentation on the marine Permian by Charles Henderson, Break Out sessions to discuss issues of the Permian, and final comments.

In the introduction, Lucia Angiolini presented the main objectives of SPS which are: 1) to define the series and stages of the Permian by means of internationally agreed GSSPs and to establish a high resolution temporal framework based on multidisciplinary approaches; 2) to provide the international forum for scientific discussion and interchange on all aspects of the Permian, specifically on refined intercontinental and regional correlations. Then, she presented the already ratified Permian GSSPs and the two missing ones, the Artinskian and Kungurian GSSPs.

The main goal of the Executive for next year is to turbocharge the Artinskian-base and Kungurian-base GSSPs to complete the Permian System. The candidates are: Dal'ny Tulkas section, Bashkortostan, Russia for the base-Artinskian and Mechetlino, Bashkortostan, Russia for the base-Kungurian. Additional goals are to frame all Permian events into the time scale: evolution, climate, palaeogeography, marine and continental correlations, to revise the timescale where it needs to be improved and to increase the size, diversity and international coverage of the Permian Community. The Break Out sessions were organized for this purpose, to discuss together issues of the Permian, stimulate circulation of ideas and thoughts, and receive more contributions from a larger number of researchers.

After the introduction, two very interesting presentations were given by Joerg W. Schneider and Charles Henderson. These are summarized below in the two abstracts they kindly provided.

### Summary of the SPS Webinar presentations

#### Permian nonmarine-marine correlations: State of the art – future tasks

By Joerg W. Schneider and the Late Carboniferous - Permian - Early Triassic Nonmarine-Marine Correlation Working Group

The presentation provided an overview of the progress made by the members of the Late Carboniferous - Permian - Early

Triassic Nonmarine-Marine Correlation Working Group since 2013/2014. Details are published in the report of the group given by J.W. Schneider in *Permophiles* 69 (2020). The most important outcome was a compilation of nonmarine biostratigraphic methods suitable for long-range correlations and the connection of nonmarine sections to the marine Standard Global Chronostratigraphic Scale (SGCS), published by an international team of 18 authors (Schneider et al., 2020). Based on this, the following conclusions were drawn in the Webinar:

1) Climate results from interference between processes in the oceans and on the continents. We need to understand this coupled land-sea system for the understanding of ancient ecosystems and for the prediction of present and future processes on Earth.

2) Late Pennsylvanian, early to middle Cisuralian as well as Lopingian and Early Triassic nonmarine-marine correlations have already reached a good level. Late early Cisuralian and Guadalupian nonmarine biostratigraphy and connections to the SGCS are still unsatisfactory. Among other regions, the well exposed and fossiliferous late early Permian to Early Triassic deposits on the East European Platform bear a high potential for the solution of this problem.

3) The most challenging future task for nonmarine-marine correlations in the Late Carboniferous–Middle Triassic are global north-south correlations. Biostratigraphic correlations among the biotic provinces of Euramerica, Angara, Cathaysia, and Gondwana are still in a very unsatisfactory state. Sections of the East European Platform and Siberia in Russia, those of the Karoo basin in South Africa, sections in North China, in Jordan and North Africa as well as in the Paraná basin of South America should be a focus of further research of the SPS.

To promote progress a call for global cooperation in the correlation of the most important and well investigated continental and mixed marine-continental basins as well as for the establishment of regional continental reference sections will be published in the next issue of *Permophiles*.

#### References

Schneider, J.W., 2020. Summary report of the Nonmarine-Marine Correlation Working Group and notes from the former Vice-Chair of the SPS. *Permophiles*, v. 69, p. 37-40.

Schneider, J.W., Lucas, S.G., Scholze, F., Voigt, S., Marchetti, L., Klein, H., Opluštil, S., Werneburg, R., Golubev, V.K., Barrick, J.E., Nemyrovska, T., Ronchi, A., Day, M.O., Silantiev, V.V., Rößler, R., Saber, H., Linnemann, U., Zharinova, V., and Shen, S.Z., 2020. Late Paleozoic-early Mesozoic continental biostratigraphy – Links to the Standard Global Chronostratigraphic Scale: *Paleoworld*, v. 531, p. 186-238. doi.org/10.1016/j.palwor.2019.09.001

#### The Marine Permian

by Charles Henderson

The presentation started with an historical review of the establishment and subdivisions of the Permian system, from Murchison in 1841 to the heated debate on the number of series at the 1991 Perm meeting and finally to the paper by Jin et al., 1997 in *Episodes*, a classic compromise that has directed the activities of SPS ever since. An important aspect of the original Permian and all modifications was “looking at the rocks”, as

there are common signatures, for example, cycloths of the Asselian and major 3rd order sequences and flooding surfaces in the Sakmarian and Artinskian and above. The importance of not being detached from the rock record while we also consider taxonomic issues was underscored in the webinar and several sections were shown: the SW Ellesmere Island sections, which includes 1100 metres of cyclic (glacial-eustatic control) upper Kasimovian to lowermost Sakmarian; the GSSP at the Aidaralash section; the GSSP for the base-Sakmarian at the Usolka section, which includes facies that are similar to the central Sverdrup Basin Hare Fiord Formation; the proposed base-Artinskian GSSP at Dalny Tulkas in the southern Urals characterized by a strong rock signature and many fossils and U-Pb age dates and stable isotopic signals, all available for broader correlation; and the proposed base-Kungurian GSSP Mechetlino section, with a conodont succession identical at the Rockland section in Nevada and also in the Sverdrup Basin, demonstrating widespread, but not global, correlation for this Cisuralian (Lower Permian) stage.

Above this level in Russia, the succession is dominated by non-marine facies with some restricted marine, so the presentation moved to west Texas to define the Middle Permian or Guadalupian. In a recent paper, Shen et al. (see *Permophiles* 69 for Guadalupian report) show the geochronologic ages and fossils that assist correlation between south China and west Texas, but they conclude that the base-Roadian, base-Wordian and base-Capitanian GSSP definitions may need some minor revision or fine-tuning in the area. The outcrops in the Guadalupe Mountains National Park are outstanding as shown by the slides, for instance that of stratotype canyon, the GSSP for the base-Roadian, and these carbonates are subject to many sequence stratigraphic analyses (Kerans et al., 2014). The recognition of conodont geographic clines within transgressive facies allows the correlation of the base-Roadian into the Canadian Arctic, but strong provincialism limits correlation of younger units. The Middle Permian includes extensive carbonate platform deposits in the Maokou Formation of south China.

The Delaware Basin in west Texas became isolated, resulting in the deposition of evaporites, so the presentation moved to South China for the best Upper Permian (Lopingian) fossiliferous carbonates, deposited within the equatorial zone. The base-Lopingian (base-Wuchiapingian) GSSP at the Penglaitan section along the Hongshui River (Laibin, Guangxi) was flooded due to a new dam, but a nearby site is being intensively studied as a substitute. The GSSP at Penglaitan is really a natural boundary as it occurs near the correlative conformity within lowstand deposits. By having the GSSP within the lowstand, it means that rocks above the sequence boundary in other parts of the world are always Lopingian. The base-Changhsingian GSSP was celebrated at Meishan in 2006 at the same site where the base-Induan (base-Triassic or top-Permian) was celebrated in 2001. A Geopark was created to recognize these two GSSPs, which makes the location the body stratotype for the Changhsingian.

The presentation transported participants through 47 million years from the base Permian at 298.9 Ma to the top at 251.9 Ma. The greatest mass extinction in Earth history (EPME) occurred just before the end (251.94 Ma), and briefly the world was dominated by microbial units that span the PTB. The talk

concluded that there is still work to do, first to complete the Permian GSSPs (base-Artinskian, base-Kungurian). But when we do, the Permian community should focus on looking at the entire Permian rather than focusing on only the boundaries. With the completion of the marine Permian time scale, there should be a renewed focus to consider marine-continental correlations. The final statement was “don’t forget the rocks”.

A series of Break Out sessions were held as part of the webinar, where each of the Break Out groups was assigned a questions to discuss and answer. A spokesperson from each group then reported back. The reports are provided in note form below.

### **Comments from Group 1**

Reported by Evelyn Kustatscher

Question: What is the most important scientific question to be answered in the Permian?

A synopsis of the group’s answers: The most important scientific questions are 1) Accessibility of Palynological data: Data from palynology from the oil drilling companies are not accessible. 2) Most of the charts (Palaeogeography, biomes, palaeoclimate maps) that we are dealing with are some 20 years old but we still use them because there are few or no alternatives at the moment. 3) Correlation marine/no-marine successions. 4) How/why and when of the end of the Permian glaciation? Also when and how of the Permian glaciations? 5) What about the Guadalupian/Lopingian extinction? 6) Vegetation changes that might influence sedimentational rates? 7) Sea-level changes: what effect does it make on preservation/environmental of fossils in the sediments? 8) How does the climate change, how can we get to much higher resolution correlation? The seasonality, the latitudinal gradients? How can we improve/track this? 9) Why not reconsider the Permian from the scratch: produce new palaeographic maps based on sedimentologically sensible datasets that are updated?

### **Comments from Group 2**

Reported by Charles Henderson

Question: What are the main palaeontological gaps in Permian studies?

The following gaps were discussed. 1) The Middle and Upper Permian continental record in Russia and South Africa (and other regions), especially of the vertebrate succession. 2) The correlation of marine and continental successions, especially where they interfinger, through increased use of palynostratigraphy. 3) Middle Permian provincialism means we should be looking more at the similarities (clines) rather than the differences (taxonomic over-splitting) of conodonts and fusulinaceans, but also other invertebrates to reduce correlation gaps. This could mean a North-South consideration as mentioned by Joerg W. Schneider in his presentation on the continental Permian record. 4) It was noted that one gap is with taxonomy, this must still be emphasized, for microflora, but also all fossil groups. 5) There could be a concerted paleontologic focus on better integrating some of the regional scales (e.g. Wolfcampian and Leonardian) with the global time scale. 6) Finally, the fact that we have focussed on boundaries to define GSSPs has left

many gaps – in other words, we agreed that it is important to emphasize the entire Permian, including how the biotic record is affected by climate change and paleogeography.

### Comments from Group 3

Reported by Hana Jurikova

Question: Is it important to have an updated website for the Permian? How should *Permophiles* be developed?

A synopsis of the group's answers: 1) We need a website to include all Permophile issues, collect all submission work, all Permian works published, have a forum, etc. We need a members' page as well a page for the general public. 2) How to build it? We need an infrastructure, and regular updates are very important. ICS needs to be consulted to see if possible to make it in the framework of the ICS website. Eventually organize a call to find people who can help in structuring and managing the website. 3) *Permophiles*: we need more contributions, for example summaries / advertisements of recently published works and we need to attract younger researchers.

### Comments from Group 4

Reported by Spencer Lucas

Question: How do we build the Permian community? How do we get young researchers interested in Permian stratigraphy?

A synopsis of the group's answers: 1) Identify important and interesting problems of Permian Earth history that can only be resolved with a strong grasp of timescale and correlations. 2) Emphasize that Permian timescale problems are global problems that require integration of marine and nonmarine datasets, necessary to the ordering of Permian Earth history—in other words, “sell” the timescale research based on its great relevance to all aspects of understanding the Permian World.

### Comments from Group 5

Reported by Liz Weldon

Question: What do we do next, after the establishment of GSSPs?

A synopsis of the group's answers: 1) Focus on north-south correlations. 2) In several countries (e.g. India) it is difficult to find boundaries and there are no radiometric dates, in others (e.g. UK, Australia) there are problems of correlation with the International Time Scale. 3) Focus on breaks in sequences. 4) Focus on land-marine correlation to make the Permian more relevant. 5) *Permophiles* should continue to provide a forum for discussion and amendments of boundaries.

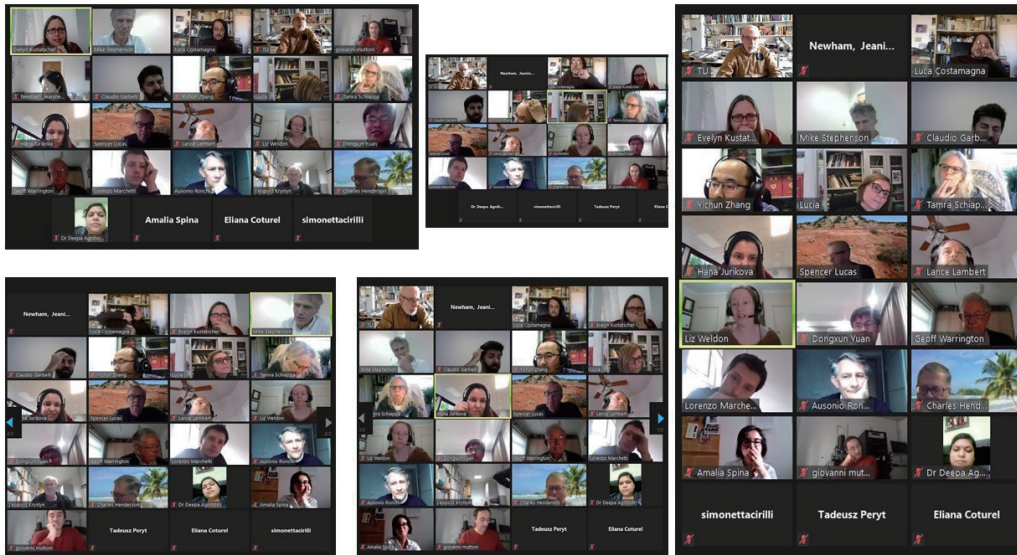
To conclude, the Break Out sessions were really stimulating and many topics were discussed and proposed to continue the studies of the Permian.

Among the most relevant issues that should be addressed in the near future to “fit the whole Permian world into this timescale” (cit. Spencer Lucas), are for certain North-South correlation, correlation of marine and continental successions, especially where they interfinger, and correlation of regional scales with the global time scale. These were the most reported topics during the Break Out sessions. Correlation is the watchword. However, to achieve correlation we need more robust and up-to-date palaeogeographic maps. Palaeogeography is thus the other main topic to develop. Palaeoclimate is also of concern and it also requires a good palaeogeographic base.

To build the community and attract young scientists we need to better advertise timescale research and show how this is important to understand the Permian world. We need also a good, attractive and interactive website not only for Permian researchers but for the wider audience. And finally, we need to keep *Permophiles* going as a great forum for Permian discussion, and for soliciting and providing more and more contributions.

As additional information, immediately after the webinar, the ICS executive was contacted on the website question, and the SPS website is currently being deployed and updated in the main ICS site by Nick Car (Canberra, Australia) with Yichun Zhang.

Lucia Angiolini, Michael Stephenson and Yichun Zhang



Screenshots from the 13 November webinar

## TO BE OR NOT TO BE *Sweetognathus asymmetricus*?

**Charles M. Henderson**

Department of Geoscience, University of Calgary, Calgary, Alberta, Canada T2N 1N4.

Email: [cmhender@ucalgary.ca](mailto:cmhender@ucalgary.ca)

**Valery V. Chernykh**

Zavaritskii Institute of Geology and Geochemistry, Ural Branch, Russian Academy of Sciences, Pochtovyi per. 7, Yekaterinburg, 620219 Russia.

Email: [chernykh@igg.uran.ru](mailto:chernykh@igg.uran.ru)

### Introduction

A preliminary proposal to define the base of the Artinskian GSSP at the Dal'ny Tulkas section was published in *Permophiles* 58 in 2013 (Chuvashov et al., 2013). There have been few objections regarding the proposed section and point because there are many markers for correlation including conodonts, fusulinaceans, ammonoids, sequence stratigraphy, stable isotopes and geochronology. The main objection was the name of the defining taxon (*Sweetognathus whitei*) as well as the need for details regarding its lineage (see Henderson, 2020).

This short note confirms that Valery Chernykh and Charles Henderson agree that the defining taxon is not *Sw. whitei*, but rather it should be referred to *Sw. asymmetricus*. We provide details regarding this conclusion below.

### Stratigraphic occurrences and homeomorphy

The sediments of the Artinskian Stage in the Dal'ny Tulkas section proposed as the GSSP of the base of this stage contain forms originally identified as *Sweetognathus whitei* (Rhodes). The low quality depiction of the holotype and paratype in the work of Rhodes (1963) make direct comparison difficult. Furthermore, the first description of *Spathognathodus whitei* Rhodes from the top of the Tensleep Formation in Wyoming, did not provide the full range of morphology. The assignment of the Uralian forms to this species was not determined by their comparison with specimens from Tensleep (Wyoming). Rather, the work of Ritter (1986, 1987) was used to identify the Uralian specimens. The Uralian forms correlated well with the Artinskian forms from the Riepetown Formation, Moorman Ranch (Nevada), which were identified by Ritter as *Sweetognathus whitei*. However, we now know that those Riepetown specimens differ in morphology and occurrence from specimens associated with the Tensleep Formation and Florence Limestone in Kansas.

This homeomorphy remained unrecognized for a long time. In retrospect, it should have been recognized that equating specimens of *Sw. whitei*, recovered from cyclothsems in association with species of *Streptognathodus*, with specimens of *Sw. whitei* from non-cyclothemtic succession without *Streptognathodus* was a problem. The first hint of this taxonomic and stratigraphic problem appeared when Mark Schmitz dated zircons in ash beds from Bolivia that demonstrated that some species of *Sweetognathus* were Asselian in age (Henderson et al.,

2009). After considerable research, Henderson (2018; online in 2016), determined that there were two lineages and two forms referred to as *Sweetognathus whitei*; he referred the younger new species initially to *Sw. aff. whitei*. From this point, the species independence of Artinskian sweetognathids from Uralian sections was clear. This new species was named by Sun and Lai (Sun et al., 2017) from lower Chihsia strata at Tieqiao section in South China as *Sweetognathus asymmetricus* (note: we have changed specific adjectival ending to match genus). Finally, the significance of *Sweetognathus asymmetricus* and its placement within a distinct lineage was demonstrated using detailed morphometric analysis (Petryshen et al., 2020). It turns out that the original *Sweetognathus whitei* is late Asselian. We have carefully reviewed all previously used material when determining the species-indicator (*Sw. asymmetricus*) for the lower boundary of the Artinskian Stage.

### Conclusions

The main conclusion from our work presented here is that the Uralian Early Artinskian forms are not *Sw. whitei* (Rhodes), but rather *Sw. asymmetricus* Sun and Lai. The main difference between the Uralian forms of *Sw. asymmetricus* and the topotype specimens of *Sw. whitei* from Wyoming is the construction of the carina. In the upper view, nodes exhibit rhomboid outlines, are somewhat flattened and wider in the Uralian forms, and narrower and variably elevated above the platform in typical *Sw. whitei*. The margins of nodes are sloped and the pustulose microornament very irregular in *Sw. whitei*. The steep margins of nodes in *Sw. asymmetricus* confine the microornament to only the top surface of the nodes (or transverse ridges).

The asymmetric construction of the anterior transverse ridges is not an obligatory feature of *Sw. asymmetricus* Sun and Lai as the authors of the species claim. This feature can be noted in the description of the species, as it is observed in some specimens (Plate 1, fig. 6). But as the main feature of the *Sw. asymmetricus*, this feature of the structure of the anterior carinal teeth is not diagnostic of the population. For example, in the depicted specimens found in the upper part of bed 4 and bed 5 in the Dal'ny Tulkas section (Plate 1, figs. 2, 3), the structure of the anterior carinal ridges is symmetrical. The same structure can be seen in specimens of this species from the same section from the clarki Zone (Artinskian stage, Irginian horizon) – as seen in Plate 1 (figs. 4, 5). It would hardly be justified to attribute these specimens to some new species only on the basis of the fact that they have symmetrically constructed anterior carinal ridges.

The typical Early Artinskian forms of the species *Sw. asymmetricus* have one more feature that should be included in the diagnosis – the presence of a fully developed or partially reduced median ridge between the transverse carinal ridges. It consists of single row of pustules closely adjacent to each other and linearly located. In the Early Artinskian forms of the Bursevian Horizon, the median ridge is located on the platform surface, adjacent to the transverse carinal ridges, but does not go over them from above. In the forms of the Irginian horizon, the median ridge can be located both between and above the carinal ridges (Plate 1, figs. 4-6). At the same time, a partial reduction of the carinal ridges is also observed in the Irginian forms. We

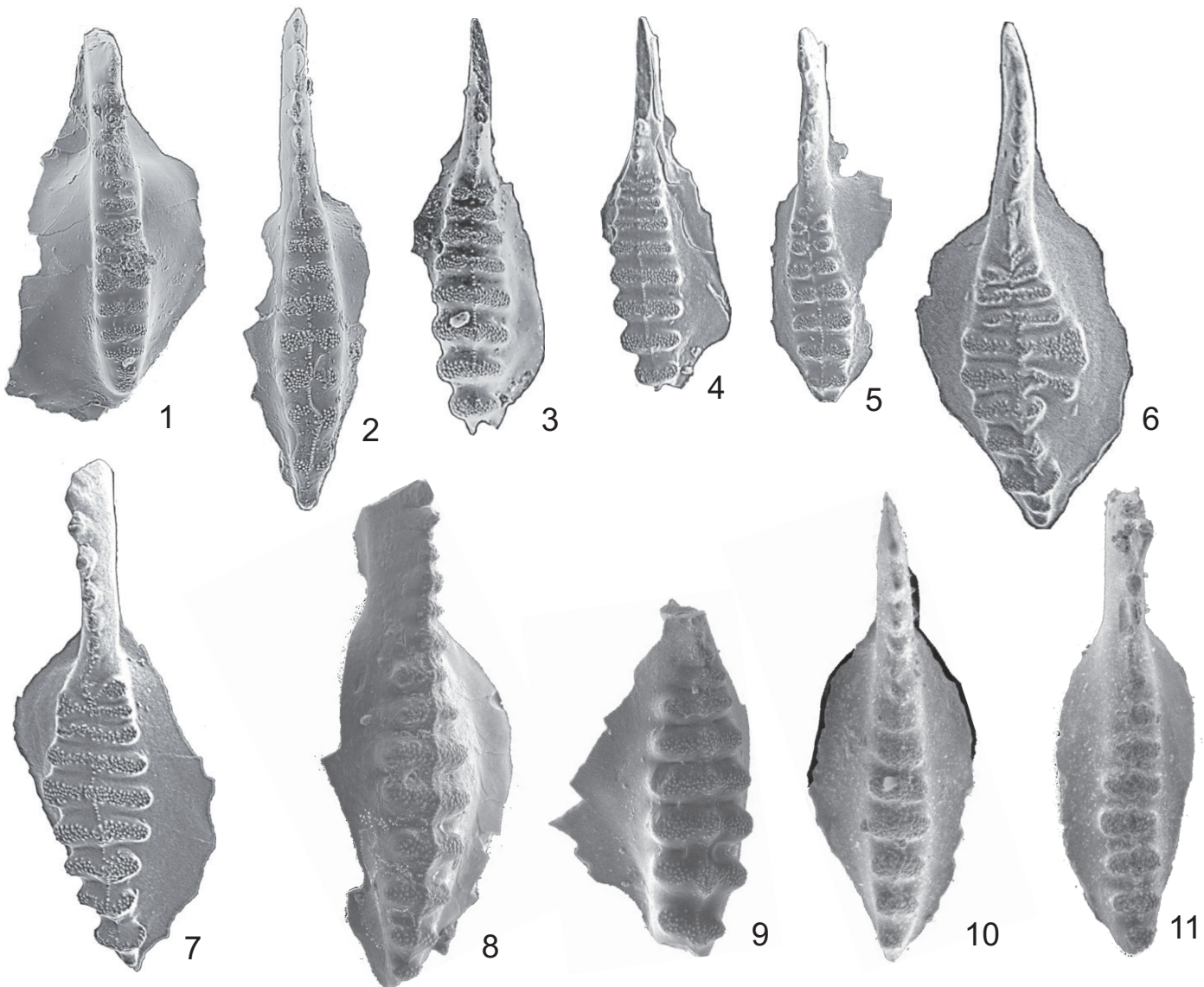


Plate 1. *Sweetognathus asymmetricus* Sun and Lai from deposits of the Artinskian stage of the Dal'ny Tulkas section, from the type locality in south China, and from Carlin Canyon, Nevada. Same magnification with average length of ~1 mm.

1. DT-18a, transitional form from *Sweetognathus anceps* Chernykh to *Sw. asymmetricus* Sun and Lai;
  2. DT-18b, typical specimen with a fully developed median ridge; bed 4b, Bursevian horizon, *asymmetricus* Zone;
  3. T-19-3, specimen with symmetrically built carina, bed 5, Bursevian horizon, *asymmetricus* Zone;
  4. DT40-29, median ridge is located above the upper surface of the carinal ridges;
  5. DT40-17, the median ridge is located below the upper surface of the carinal ridges;
  6. DT40-19, anomalous specimen with relics of the median ridges on carinal denticles and asymmetric posterior carinal denticles; bed 10, Irginian horizon, *clarki* Zone;
  7. DT40-24, partially reduced median ridge, located above the upper surface of the carina; bed 10, Irginian horizon;
  8. Sample 1352-4, lower Buckskin Mt. Fm., Carlin Canyon, NV, USA;
  9. Sample 1352-4, lower Buckskin Mt. Fm., Carlin Canyon, NV, USA.
- 10 – Bed 18 of lower Chihsia Fm. at Tieqiao, provided courtesy of Yadong Sun, referred to as *Sw. whitei*;  
 11 – Bed 18 of lower Chihsia Fm. at Tieqiao, provided courtesy of Yadong Sun, holotype.

do not believe that these variations deserve distinction of two separate species as there are many intermediate forms.

Our conclusions, as described above, regarding the morphologic features of the Uralian Early Artinskian *Sw. asymmetricus*, necessitate a revision of the diagnosis of this species; an initial version of this systematic taxonomy is provided below for *Sw. asymmetricus* Sun and Lai emend Henderson.

The synonymy and list of localities provides a correlation of the Artinskian Stage of the Urals with the sections of the same age in the US midcontinent, Canada, and China.

We hope that this taxonomic agreement eliminates the last obstacle for determination of the base-Artinskian GSSP and recommend that a slightly revised proposal be distributed to voting members for a vote as soon as possible.

## Systematics

### *Sweetognathus asymmetricus* Sun and Lai **emend Henderson**

*Sweetognathus whitei* (Rhodes): Chernykh, 2005, p. 148, plate XXIV, fig. 6, 7, 11; Chernykh, 2006, p. 58, plate XIII, fig. 2, 3, plate XIV, fig. 11, plate XV, fig. 4-7; Ritter, 1986, plate 3, figs. 10, 17, 19, 21 (non figs. 11, 16, 18, 20); Ritter, 1987, plate 23.1, fig. 11 (non fig. 3); Wang et al., 1987, figs. 6.16-6.18; Beauchamp and Henderson, 1994, fig. 20.5; Mei et al., 2002, figs. 10.25, 12.2; Sun et al., 2017, plate 1, figs. 2, ?16.

*Sweetognathus ‘whitei’* (Rhodes): Read and Nestell, 2018, plate 3, figs. 9-12.

*Sweetognathus asymmetricus* Sun and Lai: Sun et al., 2017, plate 1, figs. 1 (holotype), 7, 14, 17; Petryshen et al., 2020, fig. 2e.

**Diagnosis:** A P1 platform element with an elongated rhomboid carina of dumbbell-shaped nodes or transverse ridges with steep margins and pustulose microornament on the upper surface. The transverse ridges are connected by a linear median ridge that consists of a single row of closely spaced and fused pustules. One or two anterior nodes may be asymmetrically distributed with respect to the central pustulose ridge in some specimens, but in other specimens they are symmetric.

**Description:** The P1 platform element has an ovate basal cup that occupies two-thirds of the unit length. The relatively short free blade in mature specimens bears up to 8 denticles that increase in height anteriorly. The blade merges with the carina. The carina usually consists of 7-9 bilobed (dumbbell-shaped) transverse ridges separated by shallow depressions equal in width to the width of the carinal ridges. Transverse carinal ridges are oriented perpendicular to carinal axis. Ridges joined along the midline of the carina by a row of pustulose microornament. Upper surface of carinal denticles paved with blister-like pustulose microornament. The elongated rhomboid low carina forms a planar surface elevated above the basal cup and is widest at the midpoint. The length of the carina is three-four times greater than its width.

**Discussion:** The described species differs from *Sw. whitei* (Rhodes) by the presence of flat elongated rhomboidal carina. *Sw. whitei* (Rhodes) has a narrower carina, the transverse ridges of which are separated by v-shaped transverse troughs. Specimens of *Sweetognathus asymmetricus* are similar in appearance to *Sweetognathus whitei*, but in *Sw. asymmetricus*, the transverse ridge carinal denticles are steep margined, regular in form, and pustules are restricted to the top surface of each ridge. Sun et al. (2017) regarded specimens with more symmetrical anterior nodes within the same samples to be *Sw. whitei*, but we view these as part of a population of *Sw. asymmetricus*. Sun et al. (2017) also indicated that *Sw. asymmetricus* differs from the younger *Sw. subsymmetricus* by having a shorter blade, more expanded basal cavity, wider carinal nodes or transverse ridges, and increased spacing of posterior transverse ridges. More taxonomic descriptions of related taxa can be found in the supplementary material of Petryshen et al. (2020).

**Occurrence and age:** Artinskian Stage, Lower Permian;

the western slope of the South Urals; Riepetown Formation, Moorman Ranch, Nevada; upper Riepe Springs Limestone, Elko County, Nevada; Buckskin Mountain Formation, Carlin Canyon, Nevada; Pequop Formation, Secret Canyon, Nevada; transgressive facies of uppermost Raanes and Great Bear Cape formations, Canadian Arctic (see fig. 10 in Chernykh et al., 2020); lower Ross Creek Formation, southeastern British Columbia, Canada; lower Chihsia Formation (beds 18-23), Tieqiao section, south China.

## References

- Beauchamp, B., and Henderson, C.M., 1994. The Lower Permian Raanes, Great Bear Cape and Trappers Cove formations, Sverdrup Basin, Canadian Arctic: Stratigraphy and Conodont Zonation. Bulletin of Canadian Petroleum Geology, v. 42, no.4, p. 562-597.
- Chuvashov, B.I., Chernykh, V.V., Shen, S.Z. and Henderson, C.M., 2013. Proposal for the Global Stratotype Section and Point (GSSP) for the base-Artinskian Stage (Lower Permian). Permophiles, v. 58, p. 26-34.
- Chernykh V.V., 2005. Zonal method in biostratigraphy, zonal conodont scale of the Lower Permian in the Urals. Institute of Geology and Geochemistry of RAN, Ekaterinburg, 217 pp. (in Russian)
- Chernykh, V.V., 2006. Lower Permian conodonts of the Urals. Institute of Geology and Geochemistry of RAN, Ekaterinburg, 130 pp. (in Russian)
- Chernykh, V.V., Chuvashov, B.I., Shen, S., Henderson, C.M., Yuan, D.X., and Stephenson, M.H., 2020. The Global Stratotype Section and Point (GSSP) for the base-Sakmarian Stage (Cisuralian, Lower Permian). Episodes, v. 43, no. 4, p. 961-979. <https://doi.org/10.18814/epiugs/2020/020059>.
- Henderson, C.M., 2018. Permian conodont biostratigraphy. In Lucas, S.G. and Shen S.Z. (eds). The Permian Timescale. Geological Society, London, Special Publication, v. 450, p. 119-142.
- Henderson, C.M., 2020. Are we ready yet to propose a GSSP for base-Artinskian and base-Kungurian? Permophiles, v. 69, p. 23-26.
- Henderson, C.M., Schmitz, M., Crowley, J., and Davydov, V.I., 2009. Evolution and geochronology of the *Sweetognathus* lineage from Bolivia and the Urals of Russia: Biostratigraphic problems and implications for Global Stratotype Section and Point (GSSP) definition. Permophiles (ICOS Abstracts), 2009 June, v. 53, supplement 1, p. 19.
- Mei, S., Henderson, C.M., and Wardlaw, B.R., 2002. Evolution and distribution of the conodonts *Sweetognathus* and *Iranognathus* and related genera during the Permian and their implications for climate change: Palaeogeography, Palaeoclimatology, Palaeoecology, v. 180, p. 57-91.
- Petryshen, W., Henderson, C.M., de Baets, K., and Jarochowska, E., 2020. Evidence of parallel evolution in the dental elements of *Sweetognathus* conodonts. Proceedings of the Royal Society B, v. 287, p. 20201922. <http://dx.doi.org/10.1098/rspb.2020.1922>
- Read, M.T. and Nestell, M.K., 2018. Cisuralian (Early Permian) Sweetognathid conodonts from the upper part of the

- Riepe Springs Limestone, north Spruce Mountain ridge, Elko County, Nevada. In D. Jeffrey Over and Charles M. Henderson (eds.), Conodont studies dedicated to the careers and contributions of Anita Harris, Glenn Merrill, Carl Rexroad, Walter Sweet, and Bruce Wardlaw. *Bulletins of American Paleontology*, no. 395–396, p. 89–113. <http://doi.10.32857/bap.2018.395.08>.
- Rhodes, F.H.T., 1963. Conodonts from the topmost Tensleep Sandstone of the eastern Big Horn Mountains, Wyoming. *Journal of Paleontology*, v. 37, no. 2, p. 401–408.
- Ritter, S.M., 1986. Taxonomic revision and phylogeny of post-Early Permian crisis *bisselli-whitei* Zone conodonts with comments on late Paleozoic diversity: *Geologica et Palaeontologica*. v. 20, p. 139–165.
- Rittter, S.M., 1987. Biofacies-based refinement of Early Permian conodont biostratigraphy, in central and western USA. In Ronald L. Austin, Conodonts: Investigative Techniques and Applications (eds.), Ellis Horwood Limited for the British Micropalaeontological Society, p. 382–403.
- Sun, Y.D., Liu, X.T., Yan, J.X., Li, B., Chen, B., Bond, D.P.G., Joachimski, M.M., Wignall, P.B., and Lai, X.L., 2017. Permian (Artinskian to Wuchiapingian) conodont biostratigraphy in the Tieqiao section, Laibin area, South China. *Palaeogeography, Palaeoclimatology, Palaeoecology*, v. 465, p. 42–63.
- Wang C.Y., Ritter S.M., and Clark D.L., 1987. The *Sweetognathus* complex in the Permian of China: implications for evolution and homeomorphy. *Journal of Paleontology*. v. 61, no. 5, p. 1047–1057.

## Permian substages

### Spencer G. Lucas

New Mexico Museum of Natural History, 1801 Mountain Road NW, Albuquerque, NM 87104-1375 USA  
Email: [spencer.lucas@state.nm.us](mailto:spencer.lucas@state.nm.us)

### Introduction

The work of the Subcommission on Permian Stratigraphy began in the 1970s and has resulted in current recognition of nine standard Permian stages in three series: Cisuralian Series (Lower Permian)—Asselian, Sakmarian, Artinskian and Kungurian stages; Guadalupian Series (Middle Permian)—Roadian, Wordian and Capitanian stages; and Lopingian (Upper Permian)—Wuchiapingian and Changhsingian stages (Fig. 1). Currently, all but two of these stages (Artinskian and Kungurian) have bases that are defined by GSSPs. Definition of GSSPs for the bases of the Artinskian and Kungurian are close (see the last issue of *Permophiles*), and the SPS is likely a year or less away from having defined a complete Permian chronostratigraphic scale based on the GSSP method.

Realization of this has prompted discussion of what the SPS should focus on in future work. In recent online meetings, the SPS voting and corresponding members have expressed enthusiasm for improving nonmarine Permian chronology and correlations, well exemplified by the work of Schneider et al. (2020). While I fully support this, I also want to advocate another

line of timescale research for the SPS, namely the definition and characterization of substages for the Permian chronostratigraphic scale. Permian substages will provide a much more detailed basis for the subdivision of Permian time than do the nine standard stages.

### Shorter chronostratigraphic units should be a goal

One important facet of chronostratigraphic utility often overlooked is the lengths (durations) of chronostratigraphic units. Shorter units provide a more detailed subdivision of time and more refined correlations than do longer units. Thus, the ideal chronostratigraphic unit is a short one that encompasses one or only a few biostratigraphic zones (Lucas, 2013, 2018).

If we use the latest numerical calibration of the Permian chronostratigraphic scale (Henderson et al., 2020), most of the Permian standard stages (Asselian, Roadian, Wordian, Capitanian and Wuchiapingian) are about 5 million years long. The Sakmarian (~3 million years long) and Changhsingian (~2 million years) are shorter, and the Artinskian (~7 million years) and Kungurian (~9 million years) are the longest Permian stages. Subdividing the Permian standard stages into substages, particularly subdividing the longer stages, will provide better temporal resolution to make correlations more precise, and should be one of the next goals of Permian chronostratigraphic research.

### Lower Permian substages

I do not advocate any particular Permian substages here, but briefly discuss some of the substages already in use by various workers (Fig. 1). In Russia, the Asselian Stage is divided into three horizons—Sjuranian, Uskalykian and Shikhanian—that correspond to fusulinid zones based on species of *Sphaeroschwagerina*. These are sometimes used as substages, or the Sjuranian and Uskalykian are combined into a Kholodnian substage (e.g., Kotlyar, 2000). To my knowledge, no effort has been made to use these substages outside of the Uralian basin.

Sakmarian has long been divided into two substages—Tastubian and Sterlitamakian—sometime treated as stages (e.g., Furnish 1973). Rauser-Chernousova (1940) introduced Tastubian (for Tastuba Mountain on the Ufa Plateau in Bashkiria) for essentially the zone of the fusulinid “*Schwagerina*” (“*Pseudofusulina*”) moelleri and to mark the LOs (lowest occurrences) of the ammonoids *Metalegoceras* and *Uraloceras*. Rauser-Chernousova (1938) had earlier introduced Sterlitamakian, and Ruzhentsev (1951, 1952, 1955) treated it as a substage of the Sakmarian. In the southern Urals, the base of the Sterlitamakian is marked by the LOs of the fusulinid *Pseudofusulina uralense*, the conodont *Sweetognathus primus* and the ammonoid *Sakmarites inflatus*.

The Artinskian has long been divided into two substages (Ruzhentsev, 1956). The lowest, Aktastinian, was introduced by Ruzhentsev (1934) as the Aktastin horizon and later (Ruzhentsev 1955) treated as a substage. It is named for the Aktasty River in western Kazakhstan. Ruzhentsev (1956) introduced the Baigendzhinian substage for the Baigendzhin region on the border of the Aktyubinsk (now Aktobe) and Orenburg districts of the southern Urals. Studies of Baigendzhinian ammonoids go

back to Verneuil (1845) and Karpinsky (1889), and the LOs of ammonoids such as *Pseudoschistoceras*, *Parapronites*, *Sicanites*, *Atsabites*, *Paraceltites* and *Neocrinites* mark the beginning of the Baigendzhinian. Waterhouse (1976, 1978) used Baigendzhinian (consistently mis-spelled as “Baigendzinian”) as a stage instead of Artinskian to refer to what he called the “classic” Artinskian (i.e., the post-Sakmarian Artinskian of Karpinsky), abandoning the Artinskian as a facies term of varied usage.

The traditional Kungurian included two horizons, the Filippovskian (lower) and Irenian (upper). However, because of the lack of biostratigraphically useful fossils in these horizons, Chuvashov (1994) and subsequent workers have moved the base of the Kungurian down to include what had traditionally been the upper horizon of the Artinskian, the Saranian. The Sarana horizon includes conodonts (particularly *Neostreptognathodus pnevi*) by which the Kungurian base could be defined. Saranian, Filippovskian and Irenian are sometimes treated as substages of the Kungurian.

The Russian Stratigraphic Committee moved the top of the Lower Permian (Cisuralian) Series of the Russian Permian chronostratigraphic scale upward to encompass the entire Ufimian regional stage (Russian Interdepartmental Stratigraphic Committee, 2006; Lozovsky et al., 2009). Thus, the Russian concept of Kungurian in Russia now encompasses five regional substages (ascending order): Saranian, Filippovskian, Irenian, Solikamskian and Sheshmian (the latter two comprise the Ufimian), though some workers regard the Sheshmian as of earliest Guadalupian age.

Lower Permian substages have also been proposed in the North American regional chronostratigraphy. Thus, most American fusulinid biostratigraphers have long divided the Wolfcampian into three substages, lower, middle and upper, also termed Newwellian (or Bursumian), Nealian and Lenoxian (e.g., Thompson, 1954; Dunbar et al., 1960; Wilde, 1990, 2002, 2006).

The Leonard Series (Stage) is based on the Hess Formation, the overlying Cathedral Mountain Formation and lateral equivalents in the Glass Mountains of West Texas. These stratigraphic intervals have provided the basis for fusulinid-based substages, the Hessian and Cathedralian (Ross, 1986; Ross and Ross, 1987), also sometimes used as stages. Thus, Furnish (1973) used Leonardian in a restricted sense, dividing the Leonard Series into Aktastinian (= lower Leonard), Leonardian (= upper Leonard) and Roadian (=Road Canyon Formation) stages. Ross (1986) introduced the Cathedralian Stage to replace Furnish’s (1973) restricted Leonardian Stage, and Ross and Ross (1987) proposed the Hessian Stage to replace Aktastinian, though, if used, Hessian and Cathedralian are generally regarded as substages (Fig. 1).

### Middle and Upper Permian substages

The Guadalupian, and its three North American stages (Roadian, Wordian and Capitanian), provide the international chronostratigraphic standard for middle Permian time (Lucas and Shen, 2018). However, to my knowledge no Guadalupian substages have been proposed (Fig. 1). There are substages of the Russian regional chronostratigraphic units correlative to the Guadalupian, the Kazanian and most of the Tatarian, but

they are in nonmarine or evaporitic facies unsuitable for global chronostratigraphic definition.

The base of the Wuchiapingian Stage is defined by the GSSP in the Penglaitan section in southern China that also defines the base of the Lopingian Series. Substages of the Wuchiapingian are Laibinian and Laoshanian, divided by the FAD (first appearance datum) of the conodont *Clarkina leveni* (Jin et al., 1994a, b,

| Series      | Stage         | Substage   |
|-------------|---------------|--|
| Lopingian   | Changhsingian | Meishanian<br>Baoqingian   |
|             | Wuchiapingian | Laoshanian<br>Laibinian  |
|             | Capitanian    |  |
|             | Wordian       |  |
| Guadalupian | Roadian       |  |
|             | Kungurian     | Cathedralian<br>Hessian  |
|             |               | Baigendzhinian   |
| Cisuralian  | Artinskian    | Aktastinian  |
|             | Sakmarian     | Sterlitamakian<br>Tastubian<br>Shikhanian<br>Uskalykian<br>Sjuranian |
|             | Asselian      |  |
|             |               | GSSP   |

Fig. 1. The Permian chronostratigraphic scale showing a possible set of Permian substages. Note that no substages of the Guadalupian have been proposed, and not all substages proposed for the Permian are shown here

1998). Substages of the Changhsingian Stage are the Baoqingian and Meishanian. They are divided by the FAD of the conodont *Clarkina changxingensis* (Jin and Shang, 2000).

### Prospectus

As the GSSPs of the Permian standard stages are completed, chronostratigraphic research should focus on subdividing the nine stages into substages and defining their boundaries. Substages will provide an even more detailed basis for the subdivision of Permian time than do the stages and should be a goal of further work by the SPS. Indeed, the frontier of Permian chronostratigraphy is in the definition and characterization of substages.

## References

- Chuvashov, B. I., 1994. Progress report of Permian Stratotypes Working Group. *Permophiles*, v. 25, p. 7–8.
- Dunbar, C. O., Baker, A. A., Cooper, G. A., King, P. B., McKee, E. D., Miller, A. K., Moore, R. C., Newell, N. D., Romer, A. S., Sellards, E. H., Skinner, J. W., Thomas, H. D. and Wheeler, H. E., 1960. Correlation of the Permian formations of North America. *Geological Society of America Bulletin*, v. 71, p. 1763–1806.
- Furnish, W. M., 1973. Permian stage names. In Logan, A. and Hills, L. V.(eds.), *The Permian and Triassic systems and their mutual boundary*. Society of Petroleum Geology of Canada, Memoir 2, p. 522–548.
- Henderson, C. M., Shen, S. Z., Gradstein, F. M. and Agterberg, F. P., 2020. The Permian Period. In Gradstein, F. M., Ogg, J. G., Schmitz, M. D. and Ogg, G. M.(eds.), *The geologic time scale 2020*. Elsevier, Amsterdam, p. 875–902.
- Jin, Y.G. and Shang, Q.H., 2000. The Permian of China and its interregional correlation. In Yin, H.F., Dickins, J. M., Shi, G.R. and Tong, J.N. (eds.), *Permian-Triassic evolution of Tethys and western circum-Pacific*. Elsevier, Amsterdam, p. 71–98.
- Jin, Y.G., Glenister, B. F., Kotlyar, G. V. and Sheng, J.Z., 1994a. An operational scheme of Permian chronostratigraphy. *Palaeoworld*, v. 4, p. 1–13.
- Jin, Y.G., Mei, S.L., Wang, W., Wang, X.D., Shen, S.Z., Shang, Q.H. and Chen, Z.Q., 1998. On the Lopingian series of the Permian System. *Palaeoworld*, v. 9, p. 1–18.
- Jin, Y.G., Sheng, J.G., Glenister, B. F., Furnish, W. M., Kotlyar, G. V., Wardlaw, B. R., Kozur, H., Ross, C. R. and Spinosa, C., 1994b. Revised operational scheme of Permian chronostratigraphy. *Permophiles*, v. 25, p. 12–15.
- Karpinsky, A. P., 1889. Über die Ammonien der Artinsk-Stufe und einige mit denselben verwandte carbonische Formen. *Memoires de l'Academie Imperiale des Sciences de St.-Petersbourg*, serie 7, v. 37, no. 2, 104p.
- Kotlyar, G. V., 2000. The Permian of Russia and CIS and its interregional correlation. *Permian-Triassic evolution of Tethys and western Circum-Pacific. Developments in Palaeontology and Stratigraphy*, v. 18, p. 17–35.
- Lozovsky, V. R., Minikh, M. G., Grunt, T. A., Kukhtinov, D. A., Ponomarenko, A. G. and Sukacheva, I. D., 2009. The Ufimian Stage of the East European scale: Status, validity, and correlation potential. *Stratigraphy and Geological Correlation*, v. 17, p. 602–614.
- Lucas, S. G., 2013. A new Triassic timescale. *New Mexico Museum of Natural History and Science Bulletin*, v. 61, p. 366–374.
- Lucas, S. G., 2018. The GSSP method of chronostratigraphy: A critical review. *Frontiers in Earth Science*, v. 6 , no. 191, p. 1–18.
- Lucas, S. G. and Shen, S. Z., 2018. The Permian chronostratigraphic scale: History, status and prospectus. In Lucas, S. G. and Shen, S. Z., (eds.), *The Permian timescale*. Geological Society, London, Special Publication, v. 450, p. 21–50.
- Rauser-Chernousova, D. M., 1938. The upper Paleozoic Foraminifera of the Samara Bend and the Trans-Volga region. *Transactions of the Geological Institute of the Academy of Sciences of the USSR*, v. 7, no. 1, p. 69–167 (in Russian).
- Rauser-Chernousova, D. M., 1940. Stratigraphy of the Upper Carboniferous and Artinskian Stage of the west slope of the Urals and data on fusulinacean faunas. *Transactions of the Geological Institute of the Academy of Sciences of the USSR*, v. 7, no. 2, p. 37–101 (in Russian).
- Ross, C. A., 1986. Paleozoic evolution of southern margin of Permian basin. *Geological Society of America Bulletin*, v. 97, p. 536–554.
- Ross, C. A. and Ross, J. P., 1987. Biostratigraphic zonation of late Paleozoic depositional sequences. *Cushman Foundation for Foraminiferal Research Special Publication*, v. 24, p. 151–168.
- Russian Interdepartmental Stratigraphic Committee, 2006. Resolution on the modernization of the upper series of the Permian System of the general (East European) stratigraphic scale. In *Resolutions of the Interdepartmental Stratigraphic Committee and its Regular Commissions 36*. VSEGEI Press, St. Petersburg, p. 14–16 (in Russian).
- Ruzhentsev, V. E., 1934. New data on the stratigraphy of the Artinskian Stage on the west slope of the Urals. *Oil Economy*, v. 6, p. 16–23 (in Russian).
- Ruzhentsev, V. E., 1951. Lower Permian ammonoids of the South Urals. I. Ammonoids of the Sakmarian Stage. *Transactions of the paleontological institute, Academy of Sciences of the USSR*, v. 33, 188p.
- Ruzhentsev, V. E., 1952. Biostratigraphy of the Sakmar Stage in the Aktyubin Region of the Kazakhstan SSR. *Transactions of the Paleontological Institute, Academy of Sciences of the USSR*, v. 42, p. 1–87 (in Russian).
- Ruzhentsev, V.E., 1955. On the family Cyclobidae. *Proceedings of the Academy of Sciences of the USSR*, v. 103, p. 701–703 (in Russian).
- Ruzhentsev, V. E. 1956. Lower Permian ammonites of the southern Urals. II. Ammonites of the Artinskian Stage. *Transactions of the Paleontological Institute, Academy of Sciences of the USSR*, v. 60, 1–274 (in Russian).
- Schneider, J. W., Lucas, S. G., Scholze, F., Voigt, S., Marchetti, L., Klein, H., Opluštil, S., Werneburg, R., Golubev, V. K., Barrick, J. E., Nemyrovska, T., Ronchi, A., Day, M. O., Silantiev, V. V., Rößler, R., Saber, H., Linnemann, U., Zharinov, V. and Shen, S., 2020. Late Paleozoic-early Mesozoic continental biostratigraphy – links to the Standard Global Chronostratigraphic Scale. *Paleoworld*, v. 29, p. 186–238.
- Thompson, M. L., 1954. American Wolfcampian fusulinids. *University of Kansas Paleontological Contributions, Article 5*, p. 1–226.
- Verneuil, E. de, 1845. *Geologie de la Russie d'Europe et des Montagnes de l'Oural* (by Murchison, de Verneuil, and Keyserling). Volume 2, *Paleontologie* by de Verneuil. John Murray, London, 512 p.
- Waterhouse, J. B., 1976. World correlations for Permian marine faunas. *University of Queensland Papers Department of Geology*, v. 7, no. 2, p. 1–232.

Waterhouse, J. B. 1978. Chronostratigraphy for the world Permian. In Cohee, G. V., Glaessner, M. F. and Hedberg, H. D., (eds.), Contributions to the geologic time scale. American Association of Petroleum Geologists Studies in Geology, v. 6, p. 299–322.

Wilde, G. L., 1990. Practical fusulinid zonation—the species concept; with Permian Basin emphasis. West Texas Geological Society Bulletin, v. 29, p. 5–33.

Wilde, G. L., 2002. The Newwellian substage: Rejection of the Bursumian Stage. *Permophiles*, v. 41, p. 53–62

Wilde, G. L., 2006. Pennsylvanian-Permian fusulinaceans of the Big Hatchet Mountains, New Mexico. *New Mexico Museum of Natural History and Science Bulletin*, v. 38, p. 1–321.

## Permian continental trace fossils of Morocco: first record from the Jebilet massif

### Amal Zouicha

Department of Geology, Chouaïb Doukkali University, B.P. 20, El Jadida 24000, Morocco

Email: [amalzouicha456@gmail.com](mailto:amalzouicha456@gmail.com)

### Sebastian Voigt

Urweltmuseum GEOSKOP/Burg Lichtenberg (Pfalz), Burgstr. 19, D-66871 Thallichtenberg, Germany

### Hafid Saber

Department of Geology, Chouaïb Doukkali University, B.P. 20, El Jadida 24000, Morocco

### Lorenzo Marchetti

Museum für Naturkunde Berlin, Leibniz-Institut für Evolutions- und Biodiversitätsforschung, Invalidenstraße 43, 10115 Berlin, Germany

### Abdelkbir Hminna

Laboratory of Geosciences, Environment and Associated Resources (LGERA), Department of Geology, Sidi Mohamed Ben Abdellah University, Faculty of Sciences Dhar El Mahraz, Fès, Morocco

### Ahmed El Attari

Department of Geology, Chouaïb Doukkali University, B.P. 20, El Jadida 24000, Morocco

### Ausonio Ronchi

Department of Earth and Environmental Sciences, University of Pavia, Via Ferrata 1, I-27100 Pavia, Italy

### Joerg W. Schneider

TU Bergakademie Freiberg, Institut für Geologie, Bernhard-von-Cotta-Straße 2, D-09596 Freiberg, Germany

Kazan Federal University, Institute of Geology and Petroleum Technologies, Kremljovskaya street 18, Kazan, Russia

### Introduction

The first trace fossils were discovered in the Jebilet massif of south-central Morocco after extensive fieldwork in spring 2019. Two collection campaigns in autumn of the same year

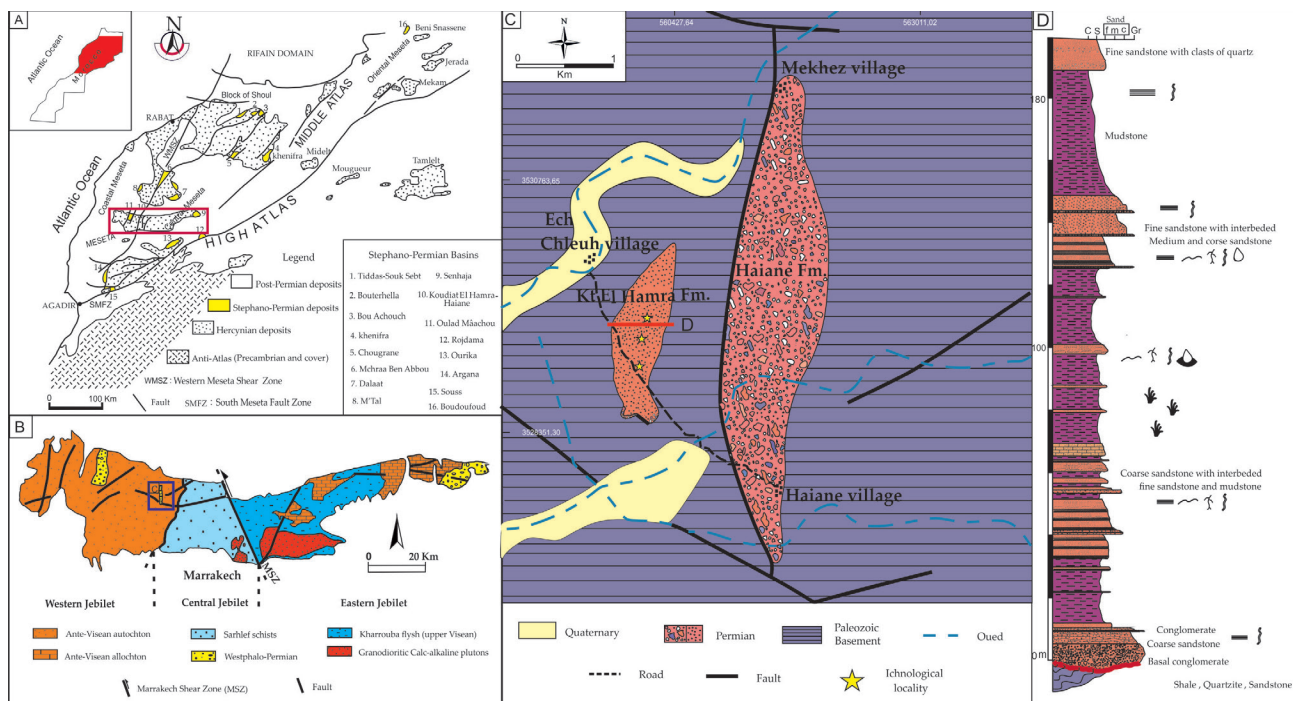


Fig. 1. Geological framework of the Koudiat El Hamra – Haiane Basin. A. position of the study area in south-central Morocco; B. simplified geological map of the Jebilet Massif; C. simplified geological map of the Koudiat El Hamra – Haiane Basin with position of trace fossil localities; D. stratigraphic section of the Koudiat El Hamra Formation.

increased the number of specimens significantly. Our discovery is not only the first record of trace fossils in the Paleozoic of the Koudiat El Hamra-Haiane basin, but also evidence for a Permian age of the fossil-bearing red-beds. This report is intended to shortly highlight the new discovery and its stratigraphic and paleoecological implications for the regional geology (Zouicha et al., 2021, in press). The presented data are another example for the remarkably fast growing record of trace fossils in Paleozoic-Mesozoic continental strata of Morocco since the beginning of systematic exploration on related ichnofossils (Hmich et al., 2006).

### Geological setting and material

The continental Koudiat El Hamra – Haiane Basin is situated about 40 km NW of Marrakech at the easternmost extension of the Western Jbel, south-central Morocco (Fig. 1A, B). The Koudiat El Hamra – Haiane Basin consists of two N-S trending sub-basins, Haiane in the east and Koudiat El Hamra in the west. Both sub-basins are closely adjacent but differ significantly in extent, sedimentary infilling, and bedding orientation (Fig. 1C).

The Koudiat El Hamra sub-basin consists of an almost 300 m-thick succession of interbedded carbonatic sandstones and mudstones with conglomerates and limestone as minor components (Fig. 1D). The trace fossils come from eight localities within the Koudiat El Hamra sub-basin. Since these localities are quite close to each other, we represent them only by three stars (Fig. 1C). Invertebrate and vertebrate trace fossils from fine-grained sediments of the Koudiat El Hamra Formation are associated with ripple marks, raindrops, microbially-induced sedimentary structures, mud-cracks, mud-draped plant remains and root traces.

### Paleoichnology

Invertebrate trace fossils from the study area are assigned to *Helminthoidichnites tenuis* (Fitch, 1850), *Scyenia gracilis* (White, 1929), *Sphaerapus larvalis* (Hitchcock, 1858), cf. *Spongeliomorpha carlsbergi* (Bromley & Asgaard, 1979) (Fig. 2A-C). Penetrative traces are the dominating invertebrate ichnofossils of the Koudiat El Hamra red-beds. Most of them may belong to *Scyenia gracilis* and cf. *Spongeliomorpha carlsbergi*,

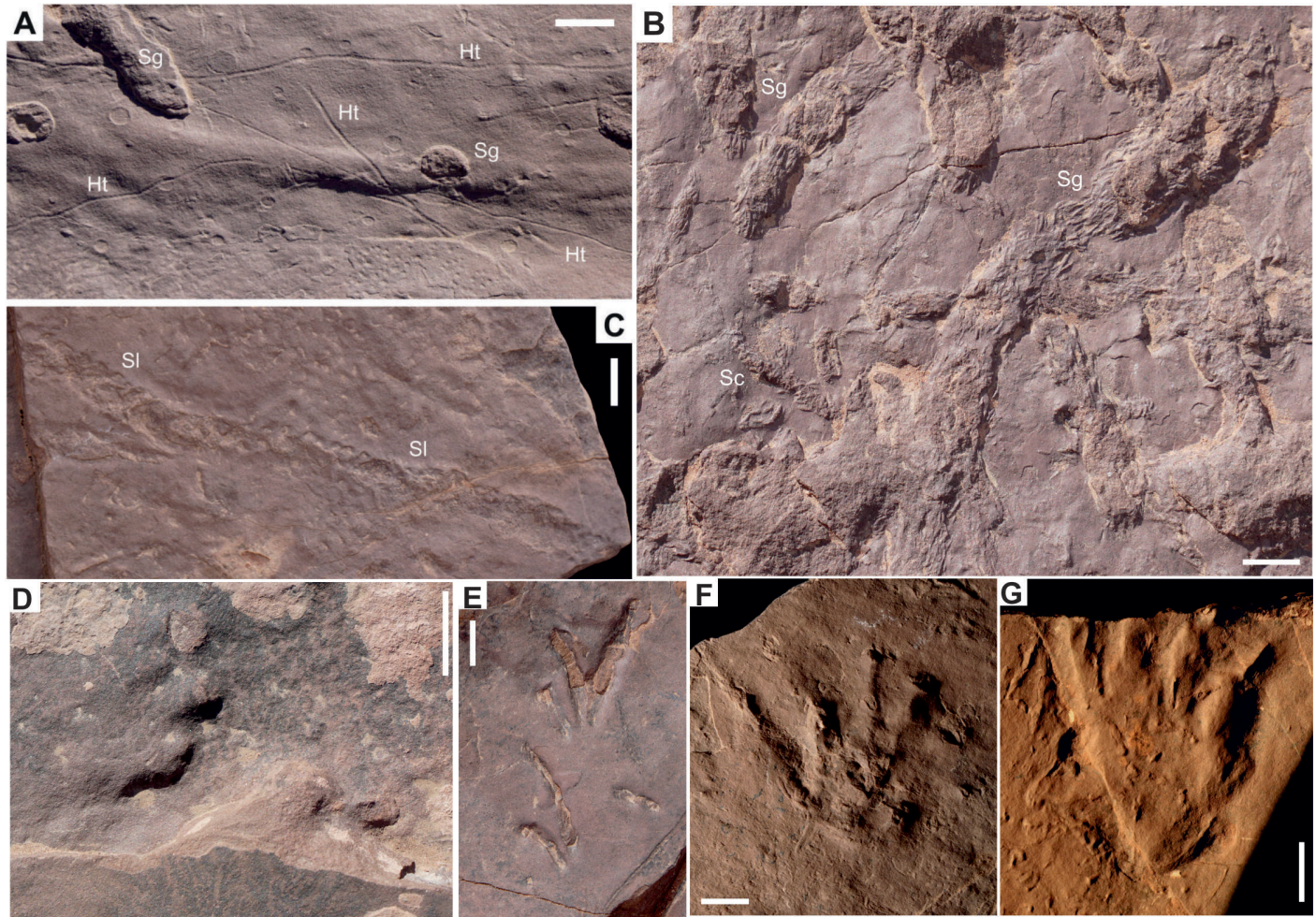


Fig. 2. Trace fossils from the Koudiat El Hamra Formation. A. *Helminthoidichnites tenuis* (Ht), traces preserved beside of scattered raindrop impressions, microbially-induced sediment structures, and burrows of cf. *Scyenia gracilis* (Sg); B. *Scyenia gracilis* (Sg), longitudinally striated burrows of various size and orientation, and a single trace of cf. *Spongeliomorpha carlsbergi* (Sc), short and straight burrow with oblique wall striation; C. *Sphaerapus larvalis* (Sl), single trace preserved in concave hyporelief; D. cf. *Batrachichnus* isp.; E. *Dromopus lacertoides*; F. *Hyloidichnus bifurcatus*; G. cf. *Tambachichnium* isp.

though this cannot be definitely confirmed as ichnotaxonomically significant ornaments are rarely preserved.

Vertebrate traces of the Koudiat El Hamra Formation include tracks assigned to cf. *Batrachichnus* isp. Woodworth, 1900, *Dromopus lacertoides* Geinitz, 1861, *Hyloidichnus bifurcatus* Gilmore, 1927 and cf. *Tambachichnium* isp. Müller, 1954 (Fig. 2D-G). The assemblage is dominated by tracks of *Dromopus* and *Hyloidichnus*, whereas tracks of cf. *Batrachichnus* and cf. *Tambachichnium* are minor components.

### Paleoecology and Biostratigraphy

Sedimentological data from the Koudiat El Hamra-Haiane red-beds suggest deposition in a warm climate. A number of sedimentary structures such as ripple marks, raindrops, microbially-induced sedimentary structures and mud-cracks are evidence of repeated alternation between flooding and subaerial exposure.

The tetrapod ichnoassemblage from the Koudiat El Hamra-Haiane basin constrains the age of the fossil-bearing sediments to the late Early Permian (Artinskian) to middle Permian (Capitanian) interval. This represents progress because the red-beds of the study area were hitherto considered to be of Pennsylvanian-Permian age based on lithostratigraphic data only (Huvelin, 1977). Although invertebrate traces are generally not useful biostratigraphic markers, we note that all known occurrences of *Sphaerapus* are younger than the Sakmarian, since

its first occurrence is from the Hermit Shale of Arizona and the uppermost Abo Formation of New Mexico, both interpreted to be of Artinskian age (Lucas et al., 2013; Marchetti et al., 2020; Fig. 3).

### Acknowledgement

The support of the German Academic Exchange Survey (DAAD) is gratefully acknowledged by H. Saber (study visit grants for joint research work at the TU Bergakademie Freiberg). J.W. Schneider acknowledges the support by the German Research Foundation in the frame of the project on late Palaeozoic and early Mesozoic tetrapod ichnofaunas of Morocco (DFG SCHN 408/17) as well as by a subsidy of the Russian Government allocated to Kazan Federal University by the state assignment no. 5.2192.2017/4.6. This report is a contribution to the tasks of the “Nonmarine–Marine Correlation Working Group” of the Subcommission on Carboniferous Stratigraphy (SCCS), Permian Stratigraphy (SPS), and Triassic Stratigraphy (STS).

### References

- Bromley, R.G. and Asgaard, U., 1979. Triassic freshwater ichnocoenoses from Carlsberg Fjord, East Greenland. *Palaeogeography, Palaeoclimatology, Palaeoecology*, v. 28, p. 39–80.
- Fitch, A., 1850. A historical, topographical and agricultural survey of the Country of Washington: Part 2–5. *Transactions of the New York Agricultural Society*, v. 9, p. 753–944.
- Geinitz, H.B., 1861. *Dyas oder die Zechsteinformation und das Rothliegende—Die animalischen Überreste der Dyas*, Volumen 1, Wilhelm Engelmann, Leipzig, 130 pp.
- Gilmore, G.W., 1927. Fossil footprints from the Grand Canyon. II. *Smithsonian Miscellaneous Collections*, v. 80, p. 1–78.
- Hasiotis, S.T., 2002. Continental Trace Fossils. *SEPM Short Course Notes*, v. 51, p. 1–132.
- Hitchcock, E., 1858. *Ichnology of New England. A Report on the Sandstone of the Connecticut Valley, Especially Its Fossil Footmarks*. W. White, Boston. 220 pp.
- Hmich, D., Schneider, J.W., Saber, H., Voigt, S. and El Wartiti, M., 2006. New continental Carboniferous and Permian faunas of Morocco — implications for biostratigraphy, palaeobiogeography and palaeoclimate. In Lucas, S.G., Cassinis, G., Schneider, J.W. (eds.), *Non-Marine Permian Biostratigraphy and Biochronology*. Geological Society of London, Special Publications, v. 265, no. 1, p. 297–324.
- Hminna, A., Voigt, S., Saber, H., Schneider, J.W. and Hmich, D., 2012. On a moderately diverse continental ichnofauna from the Permian Ikakern Formation (Argana Basin, Western High Atlas, Morocco). *Journal of African Earth Sciences*, v. 68, p. 15–23.
- Huvelin, P., 1977. Etude géologique et géologique du Massif hercynien des Jebilet (Maroc occidental). *Notes et Mémoires du Service Géologique du Maroc*, v. 232, 1–307.
- Lucas, S.G., Voigt, S., Lerner, A.J. and Rainforth, E.C., 2013. *Sphaerapus*, a poorly known invertebrate trace fossil from nonmarine Permian and Jurassic strata of North America. *Ichnos*, v. 20, p. 142–152.
- Marchetti, L., Francischini, H., Lucas, S.G., Voigt, S., Hunt, A.P.,

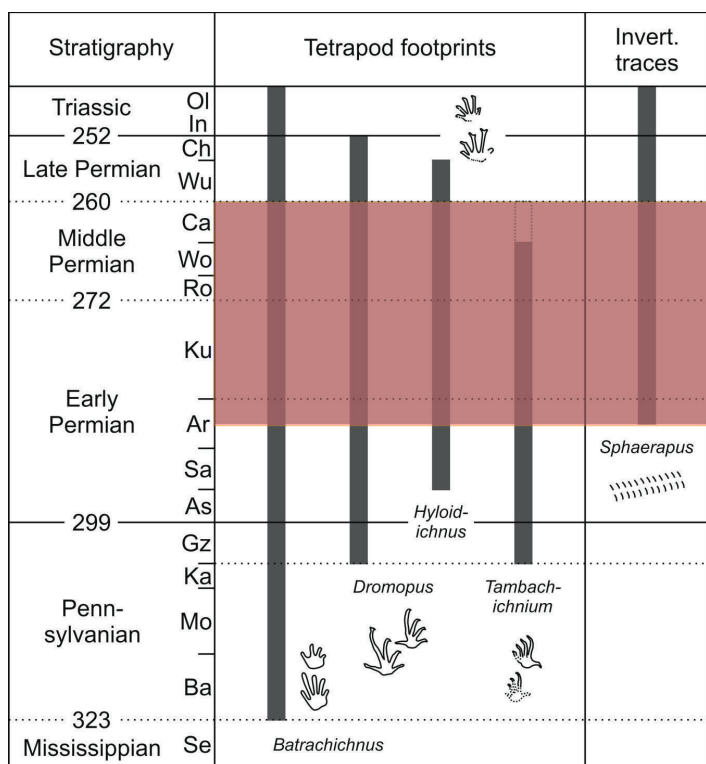


Fig. 3. Global stratigraphic distribution of the ichnotaxa from the Koudiat El Hamra Formation based on Hasiotis (2002), Schlirf (2005), Hminna et al. (2012), Lucas et al. (2013), Voigt and Lucas (2018), Metz (2020), Schneider et al. (2020). The red-colored box refers to the age of the Koudiat El Hamra Formation suggested by the ichnofossils described in this work.

- and Santucci, V.L., 2020. Paleozoic Vertebrate Ichnology of Grand Canyon National Park. In Santucci, V.L. and J.S. Tweet, (eds.), Grand Canyon National Park: Centennial paleontological resource inventory (non-sensitive version). Natural Resource Report NPS/GRCA/NRR—2020/2103. National Park Service, Fort Collins, Colorado, p. 333–379.
- Metz, R., 2020. Trace fossils in fluvial deposits of the uppermost Stockton Formation (Late Triassic), Newark Basin, New Jersey. *Ichnos*, DOI: 10.1080/10420940.2019.1697259.
- Müller, A.H., 1954. Zur Ichnologie und Stratonomie des Oberrotliegenden von Tambach (Thüringen). *Paläontologische Zeitschrift*, v. 28, p. 189–203.
- Schlirf, M., 2005. Revision and description of Keuper (Middle Ladinian to Rhaetian) invertebrate trace fossils from the southern part of the Germanic Basin and studies of related material. Ph.D. thesis, University of Würzburg, 300 pp.
- Schneider, J.W., Lucas, S.G., Scholze, F., Voigt, S., Marchetti, L., Klein, H., Opluštil, S., Werneburg, R., Golubev, V.K., Barrick, J.E., Nemyrovska, T., Ronchi, A., Day, M.O., Silantiev, V.V., Rößler, R., Saber, H., Linnemann, U., Zharinova, V. and Shen, S.Z., 2020. Late Paleozoic–early Mesozoic continental biostratigraphy — Links to the Standard Global Chronostratigraphic Scale. *Palaeoworld*, v. 29, no. 2, p. 186–238.
- Voigt, S. and Lucas, S. G. 2018. Outline of a Permian tetrapod footprint ichnostratigraphy. Geological Society, London, Special Publications, v. 450, no. 1, p. 387–404.
- White, D., 1929. Flora of the Hermit Shale, Grand Canyon, Arizona. Carnegie Institution of Washington Publication, v. 405, p. 1–221.
- Woodworth, J.B., 1900. Vertebrate footprints on Carboniferous shales of Plainville, Massachusetts. *Bulletin of the Geological Society of America*, v. 11, p. 449–454.

## Tectono-sedimentary evolution of the Upper Paleozoic Mulargia-Escalaplano molassic basin (Sardinia, Italy) in the collapsing Variscan chain: matching the pull-a-part model of the W Europe basins

**Luca G. Costamagna**

Dipartimento di Scienze Chimiche e Geologiche, Cittadella Universitaria, Blocco A, 09042 Monserrato (CA)  
Email: [lucakost@unica.it](mailto:lucakost@unica.it)

### Introduction

In Sardinia (Italy) the features of the Mulargia-Escalaplano late to post-Variscan molassic basin have been investigated. After the Variscan orogenesis (Carmignani et al., 1994), in late Pennsylvanian to Permian times, Sardinia was subject to continental sedimentation that took place in scattered basins along major tectonic lines (Carmignani et al., 2001), that possibly were Variscan thrusts surfaces reactivated as transcurrent lines (Ziegler and Stampfli, 2001). These basins (Fig. 1) are related to the collapse of the Variscan chain (Barca et al., 1995;

Carmignani et al., 2001) and have been studied for stratigraphic, sedimentological, and palaeontological aspects (Ronchi et al., 2008, Ronchi et al., 2014, Costamagna, 2019).

### Methods

Geological investigations have been undertaken in all the areas where old and newly found outcrops of the Mulargia – Escalaplano Basin can be traced and examined: reconnaissance surveys were implemented to frame them in the correct stratigraphic order (Fig. 1). The description and interpretation of their sedimentary structures, facies, and lithological associations have been carried out for the setting of a depositional model. Particular consideration has been devoted to the reconstruction of the vertical and lateral evolution of the lithofacies in different sectors, and to the relationships between tectonics and sedimentation.



Fig. 1. Localization of the investigated post-Variscan Mulargia-Escalaplano basin in Sardinia

## Geological framework

The Upper Pennsylvanian-Permian succession of the Mulargia-Escalaplano molassic basin crops out in the Gerrei area of central Sardinia (Barca et al., 1995; Cassinis et al., 2000; Barca and Costamagna, 2005). The stratigraphy is featured by the lower limnic Rio Su Luda Formation (Ronchi and Falorni, 2004) and by the upper red-bed Mulargia Formation (Costamagna, 2019) (Fig. 2). The sedimentary basin consists of two adjacent sectors: to the NW, the Mulargia sector; to the SE, the Escalaplano sector. They are presently separated by a structural Caenozoic high mainly built of Variscan basement rocks. The Mulargia and Escalaplano sectors of the basin were traditionally considered as separated entities, although the close stratigraphic and sedimentological relationship of the Mulargia and Escalaplano Upper Paleozoic successions was evident for long times (Pecorini, 1974) and suggests considering them as a single basin with only consequential differences in the depositional facies. The Upper Paleozoic succession is unconformably sealed by Triassic (Costamagna et al., 2000) or Eocene (Pertusati et al., 2002) deposits.

## Sedimentological and stratigraphic traits

The Rio Su Luda Formation is about 60 m thick and crops out only in the northern area of the NW Mulargia sector: it thins out gradually southeastward until its complete disappearance. It

is formed by usually dark siliciclastic, conglomeratic to pelitic deposits, showing initially a gradually fining-upward trend turning rapidly to a gradually coarsening-upward one. The finest pelitic intermediate deposits are thinly laminated and contain scattered intercalations of graded sandstone beds with erosive base showing groove-casts, tool-casts, and flute casts structures (Fig. 3A). They are also rich in plant remains that support a Stephanian age (Pittau et al., 2008) ("Autuniano sardo" of Ronchi et al., 2008). The top of the unit is featured by meter-thick coarse depositional events referable to subaqueous debris flows (Fig. 3B). The depositional environment of the Rio Su Luda Formation can be referred to as a tectonically active narrow alluvial to palustrine(?) lacustrine basin subject to variable energy in times (Costamagna, 2019) under a wet climate (Pittau et al., 2008).

The coarsest deposits of the Rio Su Luda Formation are followed with erosive, but gradual contact by the Mulargia Formation, a red-bed siliciclastic to volcano-sedimentary unit with scattered carbonate beds. The transition is also marked by a gradual color change from dark grey to red. If there is any significant stratigraphic gap is still unclear. Everywhere but in the northern area of the NW Mulargia sector, the Mulargia Formation rests unconformably over the Variscan metamorphic basement (Fig. 2). At its base, the Mulargia Formation contains pebbles and cobbles deriving from the erosion of the lower Rio Su Luda Formation. The Mulargia Formation thickness varies according to the sector, reaching a maximum of 250 m in the Mulargia sector. Its grain size varies from conglomeratic to pelitic. Also, the Mulargia Formation thins out eastward. It can be subdivided into two fining-upward subcycles, every one of them topped by volcanic deposits of high-K sub-alkaline affinity (Cassinis et al., 2000): they are separated by a weak unconformity marked by a continuous conglomerate level. Radiometric dating reported for this unit an age of about 300 to 295 Ma (Gaggero et al., 2017). Both the Mulargia Formation subcycles show also a directional grain-size fining trend SE-oriented. Sedimentary structures, as cross-bedding and imbrications, support this SE flow direction. The bed shape of the coarsest lithologies changes southeastward from tabular to lenticular (Fig. 3D), as well as their architectural organization, showing growing evidence of lateral accretion in the same direction (Fig. 3C). Thus the fluvial style evolves southeastward from braided towards sinuous channel patterns. Compositional and textural maturity of the siliciclastic deposits grows southeastward likewise. Carbonate deposits, often silicified, are scattered: they are dm-thick beds frequently built of microbialitic mats. Those beds are embedded into reddish pelites: their abundance grows up gradually SE-ward. Here, fossils remain (gastropods, ostracods, Characeae oogons: Pecorini, 1974) are rare. Evaporitic remains are also present in the carbonate beds as quartzose pseudomorphs, as well as streaks and nodules of chert. The age of the Mulargia Formation represents a problem. Despite the reported radiometric age (Gaggero et al., 2017), the presence of Rio Su Luda Formation pebbles into the Mulargia Formation suggests a younger age of this latter unit (Saxonian?). This would agree with the general story of the coeval basins in W Europe. The depositional environment of the Mulargia Formation can be referred to a wider alluvial to playa-lake basin showing evolving lower energy fluvial styles in space

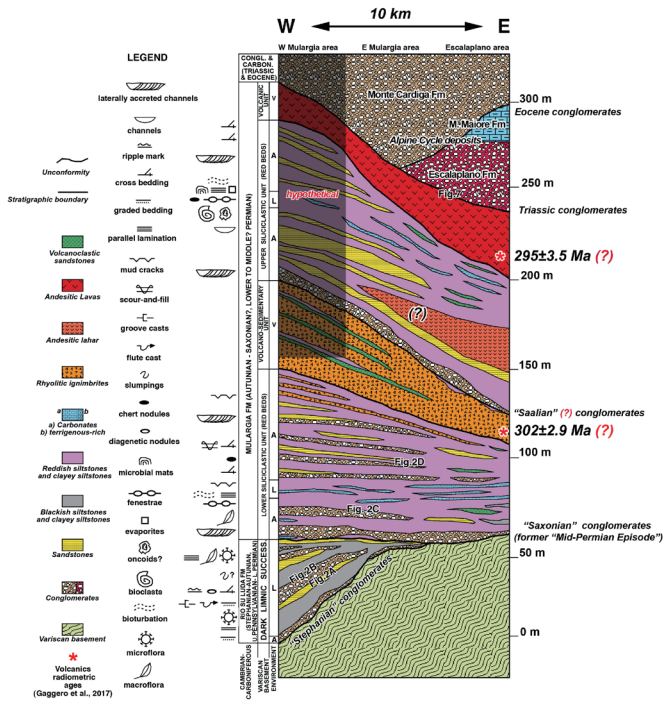


Fig. 2. A 2D - model of the Mulargia-Escalaplano basin showing the NW-SE stratigraphic evolution. Note the E-ward decrease in thickness and mean grain-size of the stratigraphic units, the rapid thinning up to the disappearance of the Rio Su Luda Fm, the growth of carbonate rocks in the same direction, the several unconformities. A: Alluvial environment. L: Lacustrine-palustrine? environment. Radiometric data after Gaggero et al., 2017.

and time, and thus subject to variable energy (Costamagna, 2019) under a dry climate (Pittau et al., 2008): its evolution was punctuated by tectono-magmatic spikes rejuvenating the surrounding landscape.

The coarsest and the finest deposits of both the Rio Su Luda Formation and Mulargia Formation are concentrated close to the NW-most outcrops, as well as the maximum thickness of the investigated stratigraphic units. A gradual decrease of the present dip of the beds from the bottom to the top of the entire succession until a near-horizontal attitude has been detected as well. On the whole, the basin presents a clear NW/SE asymmetry of the filling (Fig. 4).

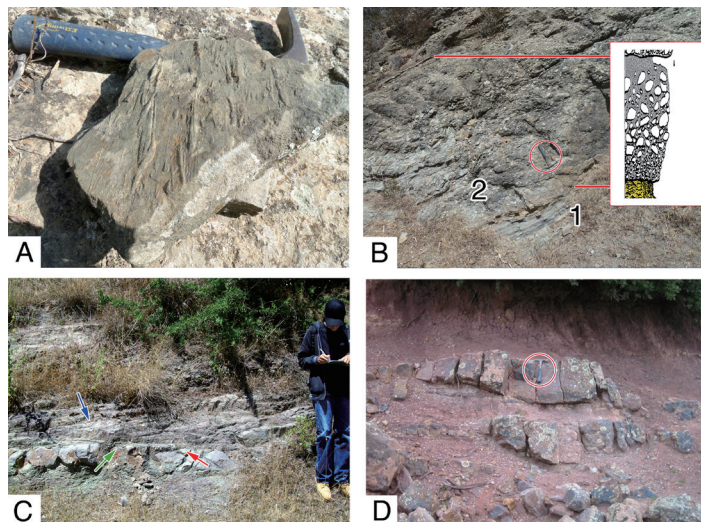


Fig. 3. A. Tool casts and groove casts at the base of a sandstone bed. Hammer = 30 cm. Rio Su Luda Fm, Loc. Genna Ureu; B. Coarse, CU- to FU-graded event (2) over grey sandstones (1). Inset of modeled features of a subaqueous debris flow event from Nemec and Steel, 1984. Rio Su Luda Fm succession, Antoni Cauli N road cut. Hammer = 30 cm. C. Lateral accretion structures (blue arrow) with a thin basal lag (green arrow) over an erosional surface (red arrow) in the. Man height 170 cm. Mulargia Fm, Loc. Su Pitzu de Mataracui. D. Lenticular sandstone bodies with erosive base in the LSU. Hammer 30 cm. Mulargia Fm, Loc. Is Xivas. Stratigraphic location of the pictures in Fig. 2.

#### Tectonics/sedimentation relationships

Previously Barca et al. (1995) suggested that the Mulargia sector of this sedimentary basin was a Variscan tectonically controlled area. By the strongly direction-bound sedimentary data here presented, we confirm that the facies organization of this entire Late Paleozoic basin was ruled by a NW located, NNW/SSE oriented close listric fault area, the Mulargia Fault zone, formerly evidenced as a Variscan main thrust belt (Funedda et al., 2008, and references therein), which reverted its kinematic behavior during the late Pennsylvanian-Permian collapse of the Variscan chain. The Mulargia Fault zone bounds the W-most outcrops of the basin. According to Christie-Blick and Biddle (1985), the telltales of the pull-a-part basins are A) mismatches across basin margins; B) longitudinal and lateral basin asymmetry; C) episodic rapid subsidence; D) abrupt

lateral facies changes and local unconformities; E) marked contrasts in stratigraphy, facies geometry, and unconformities among different basins in the same region (Fig. 4) (Cassinis et al., 2000; Costamagna, 2019). They all are in good accord with the described sedimentary features of the Mulargia-Escalaplano basin, allowing to set it into this frame (Fig. 4). Besides, Nilsen and Sylvester (1995) emphasize the asymmetric distribution of the sediments in the pull-a-part basins, with both the coarsest and the finer-grained and deeper water deposits accumulating subparallel to and next to the most active strike-slip margin: in our case the coarsest deposits (the debris flow events with cobbles of the Rio Su Luda Formation), and the finest and deepest deposits (the dark pelites of the Rio Su Luda Formation) of the Mulargia-Escalaplano succession, are located westward close to the Mulargia Fault zone. The Mulargia Formation facies organization follows closely the same directional trend, with the highest energy deposits located the closest to the Mulargia Fault zone.

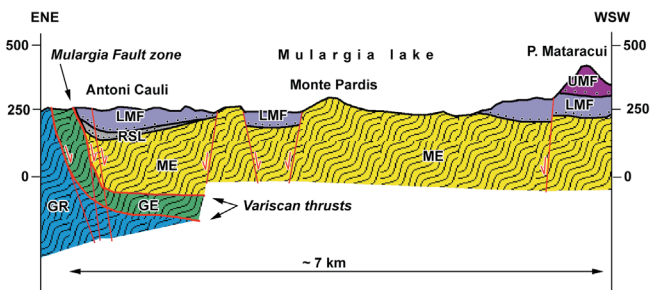


Fig. 4. Interpretative W-E geological sketch of the western-central part of the Mulargia-Escalaplano pull-a-part basin (inspired, redrawn, and modified from Funedda et al., 2008). RSL: Rio Su Luda Fm; LMF: lower Mulargia Fm; UMF: upper Mulargia Fm. Variscan Tectonic Units: GR: Rio Gruppa Tectonic Unit; GE: Gerrei Tectonic Unit; ME: Meana Sardo Tectonic Unit

#### Results

The Mulargia-Escalaplano molassic basin in central Sardinia preserves a thick succession of continental deposits. Alluvial fan-deltas?, braided and sinuous stream to lacustrine-palustrine?/playa sediments were laid down under wet climates evolving to dryer conditions. Sediments are organized in two superposed main depositional cycles punctuated by recurring volcano-tectonic spikes. In the lower limnic cycle and each of the red bed sub-cycles the depositional energy decreases gradually upwards and southeastward until the onset of the following tectonic phase. Thus cycles and sub-cycles represent erosive responses to tectonic climax producing, in the end, the smoothing of the surrounding relieves: high-energy passing to low-energy continental environments develop gradually in times and show a vertical and lateral evolution towards more sedate depositional processes. The investigated depositional basin is a pull-a-part one related to a main NNW/SSE listric master fault: the sedimentary facies and the stratigraphy are organized accordingly, with strong directional control. Both coarsest deposits and finest and deepest deposits of the basin succession are located close to the NW-located Mulargia Fault zone, representing the master fault. The

basin widens progressively in times and its depocenter shifts gradually SE-wards.

Thus the Mulargia-Escalaplano basin outcrops show a well-exposed example of the evolution of a late to post-Variscan sedimentary pull-a-part basin, successfully comparable with its analogs of SW Europe (Provence, Toutin-Mourin and Bonijoli, 1992; Lòdeve, Lopez et al., 2008; Autun, Pellenard et al., 2017; Saar-Nahe, Schäfer, 2011).

## References

- Barca, S., Carmignani, L., Eltrudis, A. and Franceschelli, M., 1995. Origin and evolution of the Permian-Carboniferous basin of Mulargia lake (South-Central Sardinia, Italy) related to the Late-Hercynian extensional tectonics. *Comptes Rendus de l'Académie de Sciences, Paris*, v. 321, p. 171–178.
- Barca, S. and Costamagna, L.G. , 2005. Stratigrafia ed analisi di facies dei depositi permiani del Lago Mulargia (Sardegna sud-orientale): primi risultati. *Geologica Romana*, v. 38, p. 11–17.
- Carmignani, L., Carosi, R., Di Pisa, A., Gattiglio, M., Musumeci, G., Oggiano, G. and Pertusati P.C., 1994. The Hercynian chain in Sardinia. *Geodinamica Acta*, v. 7, p. 31–47.
- Carmignani L., Oggiano G., Barca S., Conti P., Eltrudis A., Funedda A., Pasci S. and Salvadori I., 2001. Geologia della Sardegna: note illustrative della Carta geologica della Sardegna a scala 1:200.000. Istituto poligrafico e Zecca dello Stato, 272 pp.
- Cassinis, G., Cortesogno, L., Gaggero, L., Pittau, P., Ronchi, A. and Sarria, E., 2000. Late Paleozoic continental basins of Sardinia: Field Trip Guidebook. Intern. Field Conference on the continental Permian of the Southern Alps and Sardinia (Italy). Regional reports and general correlations. Brescia, 15–25 September 1999, 116 pp.
- Christie-Blick, N.C. and Biddle, K.T. , 1985. Deformation and basin formation along strike-slip faults. In Biddle, K.T. and Christie, N.C. (eds.), *BlickStrike-Slip Deformation, Basin Formation, and Sedimentation* , SEPM Special Publication, v. 37, p. 1–34.
- Costamagna, L.G., 2019. The Carbonates of the post-Variscan basins of Sardinia: the evolution from Carboniferous-Permian humid-persistent to Permian arid-ephemeral lakes in a morphotectonic frame. *Geological Magazine*, v. 156, p. 1892–1914.
- Costamagna, L.G., Barca, S., Del Rio, M. and Pittau, P. , 2000. Stratigrafia, analisi di facies deposizionale e paleogeografia del Trias del Sarcidano-Gerrei (Sardegna SE). *Bollettino della Società Geologica Italiana*, v. 119, p. 473–496.
- Funedda, A., Carmignani, L., Pertusati, P.C., Uras, V., Pisanu, G. and Murtas, M., 2008. Note Illustrative del F° 540 Mandas. Memorie Descrittive della Carta Geologica d'Italia. APAT Servizio Geologico d'Italia, 208 pp.
- Gaggero, L., Gretter, N., Langone, A. and Ronchi, A., 2017. U-Pb Geochronology and Geochemistry of Late Paleozoic Volcanism in Sardinia (Southern Variscides). *Geoscience Frontiers*, v. 1, p. 1–22.
- Lopez, M., Gand, G., Garric, J., Körner, F. and Schneider, J., 2008. The playa environments of the Lodéve Permian basin (Languedoc-France). *Journal of Iberian Geology*, v. 34, p. 29–56.
- Nemec, W. and Steel, R.J., 1984. Alluvial and coastal conglomerates: their significant features and some comments on gravelly mass-flow deposits. In Koster, E.H. and Steel, R.J. (eds.), *Sedimentology of Gravels and Conglomerates* , Canadian Society of Petroleum Geology, Memories, v. 10, p. 1–31.
- Nilsen, T. H. and Sylvester, A. G., 1995. Strike-slip basins. In Busby, C.J. and Ingersoll, R.V. (eds.), *Tectonics of sedimentary basins*, Blackwell Science, Oxford, p. 425–457.
- Pecorini, G., 1974. Nuove osservazioni sul Permo-Trias di Escalaplano. *Bollettino della Società Geologica Italiana*, v. 93, p. 991–999.
- Pellenard, P., Gand, G., Schmitz, M., Galtier, J., Broutin, B. and Stéyer, J.S., 2017. High-precision U-Pb zircon ages for explosive volcanism calibrating the NW European continental Autunian stratotype. *Gondwana Research*, v. 51, p. 118–136.
- Pertusati, P.C., Sarria, E., Cherchi, G.P., Carmignani, L., Barca, S., Benedetti, M., Chighine, G., Cincotti, F., Oggiano, G., Ulzega, A., Orru, P. and Pintus, C., 2002. F° 541 "Jerzu". Note illustrative della carta geologica d'Italia in scala 1:50.000. APAT-Servizio Geologico d'Italia, Roma, 170 pp.
- Pittau, P., Del Rio, M. and Funedda, A., 2008. Relationships between plant communities characterization and basin formation in the Carboniferous-Permian of Sardinia. *Bollettino della Società Geologica Italiana*, v. 127, p. 637–653.
- Ronchi, A. and Falorni, P., 2004. Formazione di Rio su Luda. *Carta Geologica d'Italia* scala 1:50.000. Catalogo delle Formazioni, Unità validate (a cura della Commissione Italiana di Stratigrafia). Quaderni serie III. 7 (fasc. V), p. 155–159.
- Ronchi, A., Sarria, E. and Broutin, J., 2008. The "Autuniano Sardo": basic features for a correlation through the Western Mediterranean and Paleoeurope. *Bollettino della Società Geologica Italiana*, v. 127, p. 655–681.
- Ronchi, A., Sacchi, E., Romano, M. and Nicosia, U., 2014. A huge caseid pelycosauro from north-western Sardinia and its bearing on European Permian stratigraphy and palaeobiogeography. *Acta Palaeontologica Polonica*, v. 56, p. 723–738.
- Schäfer, A., 2011. Tectonics and sedimentation in the continental strike-slip Saar-Nahe Basin (Carboniferous-Permian, West Germany). *Zeitschrift der Deutschen Gesellschaft für Geowissenschaften*, v. 162, p. 127–155.
- Toutin-Morin, N. and Bonjoly, D., 1992. Structuration des bassins de Provence orientale à la fin de l'ère primaire. *Cuadernos de Geología Iberica*, v. 16, p. 59–74.
- Ziegler, P.A. and Stampfli, G.M., 2001. Late Paleozoic-Early Mesozoic plate boundary reorganization: collapse of the Variscan orogen and opening of the Neotethys. *Natura Bresciana, Annali del Museo Civico, Scienza e Natura Bresciana, Monografia*, v. 25, p. 17–34.

## Latest Carboniferous to Early Permian volcano-stratigraphic evolution in Central Europe: U-Pb CA-ID-TIMS ages of volcanic rocks in the Thuringian Forest Basin (Germany) - summary of the original paper in Int. J. Earth Sci. (Geol. Rundsch.), 2020

Harald Lützner

Institute of Earth Sciences, Friedrich-Schiller-University Jena,  
Burgweg 11, D-07749 Jena, Germany  
Email: [habalue@freenet.de](mailto:habalue@freenet.de)

Marion Tichomirowa, Alexandra Käßner

Institute of Mineralogy, TU Bergakademie Freiberg,  
Brennhausgasse 14, D-09599 Freiberg, Germany  
Email: [tichomir@mineral.tu-freiberg.de](mailto:tichomir@mineral.tu-freiberg.de) (Marion Tichomirowa)

Reinhard Gaupp

Institute of Earth Sciences, Friedrich-Schiller-University Jena,  
Burgweg 11, D-07749 Jena, Germany  
Email: [reinhard.gaupp@uni-jena.de](mailto:reinhard.gaupp@uni-jena.de)

### Introduction

In Thuringia, Germany, Upper Carboniferous to Permian deposits are widespread, the major part, however, occurs at subsurface. Only in the Thuringian Forest outcrops range over a wide area. *Permophiles* repeatedly reported on results from this area. We revisited the Thuringian Forest Basin (TFB) with the intention to sample volcanic rocks for high precision age determinations that could help to correlate the basin fill with the International Chronostratigraphic Chart.

### Regional and lithostratigraphical setting

The Thuringian Forest Basin (TFB) is situated in a central and important geographic position in the Variscan orogenic belt in the Mid-German Crystalline Rise and the Saxothuringian Zone, and located between Saar-Nahe and Kraichgau Basins in the SW and the Saale Basin in the NE (Fig. 1). The TFB formed during the latest Carboniferous and filled with alternating sedimentary and volcanic rocks under continental environments with a thickness of about 2000 m. Lithostratigraphically, the succession is divided into 9 formations (Fig. 2). The oldest two, Möhrenbach und Georgenthal formations, rest unconformably on the Ruhla Crystalline Complex in the NW, on a deeply weathered granite in the middle part of the Thuringian Forest, and in the SE on folded sedimentary rocks of the Thuringian Slate Mountains with a late Proterozoic up to Early Carboniferous age. The Möhrenbach and the Georgenthal formations are thought to be coeval. Thin sedimentary intercalations within the predominating intermediate volcanic rocks have been used for internal correlation of both formations (Lützner et al., 2012, Andreas, 2014). They reflect a first culmination of volcanic activity, including the overlying Ilmenau Formation which consists of local sedimentary beds alternating with volcanic and pyroclastic rocks of bimodal basaltic and rhyolitic composition. Extrusive volcanic rocks

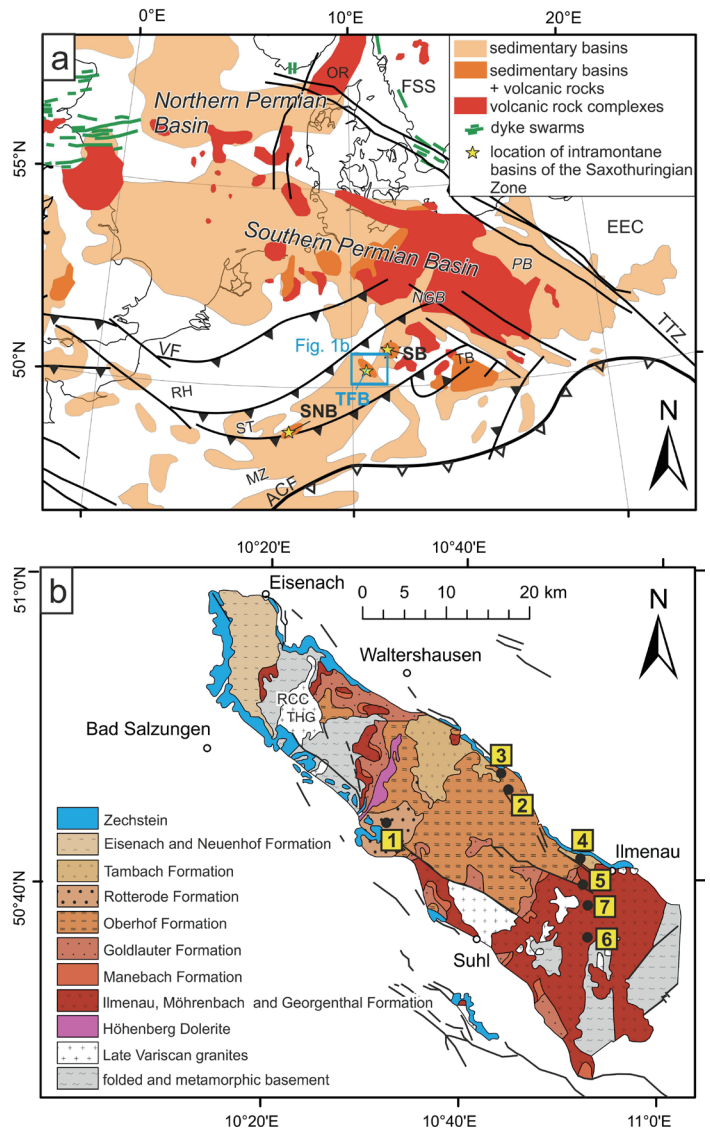


Fig. 1. Simplified geological maps. a) Geological map of the main tectonic elements of Central Europe in relation to the distribution of Upper Carboniferous and Lower Permian sedimentary basins and volcanic rocks (based on McCann et al. 2006 and Mazur et al. 2010). Major tectonic elements are ACF: Alpine-Carpathian front, VF: Variscan deformation front, RH: Rheno-Hercynian Zone, ST: Saxothuringian Zone, MZ: Moldanubian Zone, TB: Tepla-Barrandian Zone, EEC: East European Platform, FSS: Fennoscandian Shield, TTZ: Tornquist-Tisseyre Zone, OR: Oslo Rift. Two sub-basins of the Southern Permian Basin are labelled as NGB: North German Basin, PB: Polish Basin, and the main sedimentary basins of the Saxothuringian Zone are SNB: Saar-Nahe Basin, TFB: Thuringian Forest Basin, SB: Saale Basin. Thick black lines are tectonic elements; thin black lines represent the coastlines of Central Europe. b) Geological Map of the Thuringian Forest Basin. Sample locations for new zircon U-Pb CA-ID-TIMS dating are shown by black circles with sample numbers in yellow boxes. (Lützner et al. 2012, amended). RCC: Ruhla Crystalline Complex, THG – Thüringer Hauptgranit.

are extremely scarce in the subsequent formations, i.e. the coal-bearing Manebach Formation and the fluvial-lacustrine

## Goldlauter Formation.

A second culmination of Rotliegend volcanic activity occurred during the deposition of the following Oberhof Formation with an enormous volume of rhyolitic and rhyodacitic volcanic rocks and associated pyroclastics. Periods of lowered activity permitted the development of limited alluvial and lacustrine sedimentary environments that are rich in fossils or organic matter. The volcanic activity continued during the overlying Rotterode Formation with limited and declining volume of volcanic production at the surface. However, a considerable amount of magma was trapped in a rhyolite intrusion and the finally intruded Höhenberg dolerite during the Rotterode/Oberhof gap or during early Rotterode time. Rotterode sediments exclusively consist of red beds, mainly fluvial sandstones and conglomerates that indicate an uprise of the Ruhla Crystalline Complex.

The Tambach Formation starts with coarse conglomerates that covered an eroded paleolandscape. Locally, deep canyons cut into Oberhof rhyolites filled up with Lower Tambach debris flows (Lützner, 1982) and graded upwards into sandstones and mudstones with the famous Bromacker fossiliferous horizon, well-known for tetrapod footprints and skeletal remains of terrestrial amphibians and reptiles.

The Eisenach Formation occurs at the West flank of the Ruhla Crystalline Complex. Marginal alluvial fans interfingered with sandy mudstones which can be traced to the west below the Zechstein and Triassic by numerous boreholes. The partly haloturbidic mudstones are devoid of fossils.

The Neuenhof Formation is the uppermost Permian formation still with the appearance of Rotliegend red beds. It consists of a 5-10 m thick alternation with fine gravels, sandstones and siltstones of mainly fluvial environment. Magnetostratigraphically, the Neuenhof Formation belongs to the Permian-Triassic Mixed Superchron, whereas all Permian formations mentioned before are part of the Kiaman Reversed superchron (Menning et al., 1986).

Outstanding fossiliferous horizons in the TFB, which are important for basic research in paleontology and biostratigraphy, are marked in Fig. 2 by the letters A to J. Fundamental progress has been obtained during the last decades in paleontology in respect to define biozones of selected fossil assemblages, to trace phylogenetic lineages and finally to correlate timelines through separated basins. Schneider et al. (2020) recently summarized the state of art in biostratigraphic correlation of the Upper Carboniferous and Permian continental basins.

One or two samples were collected from each formation that contain volcanic rocks (for details cp. original paper). We preferred to sample acidic rocks with medium- to large-sized phenocrysts of quartz and feldspar because these rocks generally yielded sufficient zircon crystals.

## High-precision U-Pb CA-ID-TIMS method

Recent development in ID-TIMS dating substantially reduced the analytical error of zircon dating, especially through the application of chemical abrasion (CA) on single zircon grains prior to their analysis. In addition, due to efforts of the EARTHTIME initiative (<http://www.earthtimetestsite.com/>), the inter-laboratory bias of zircon ages has been reduced to

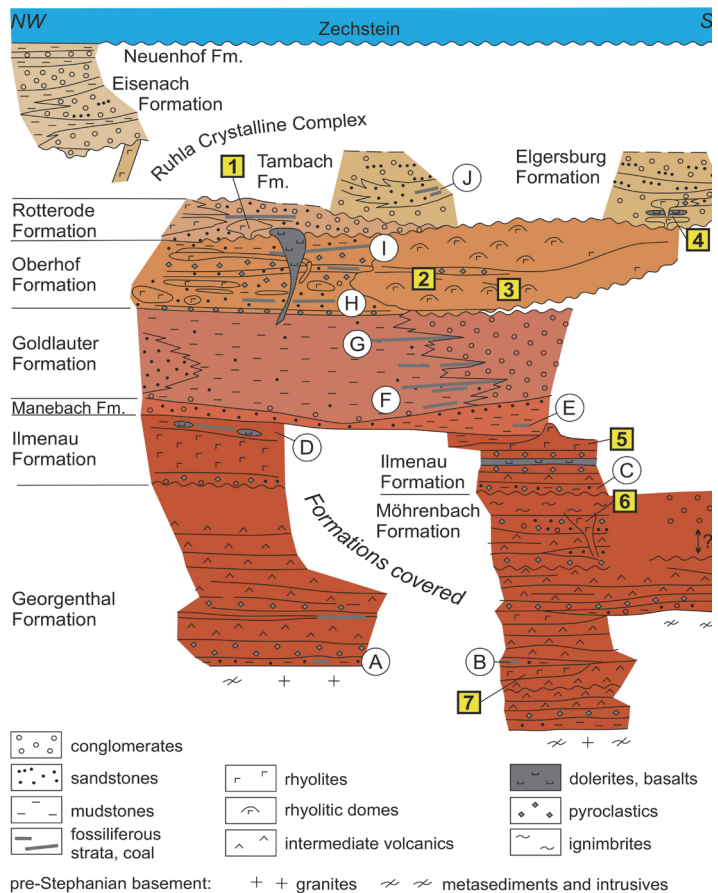


Fig. 2. Lithostratigraphic subdivision of the Carboniferous-Permian sediments of the Thuringian Forest Basin, presented as a schematic NW-SE cross-section. Circled letters label biostratigraphically important fossiliferous horizons: A. Öhrenkammer Horizon (Georgenthal Fm.), B. Ilmtal Horizon (Möhrenbach Fm.), C. Lindenberg Horizon (base of Ilmenau Fm.), D. Sembachtal Horizon (top of Ilmenau Fm.), E. Manebach fossiliferous horizons (Manebach Fm.), F. Sperbersbach Horizon (lower Goldlauter Fm.), G. Gottlob Horizon (upper Goldlauter Fm.), H. Lochbrunnen Horizon (lower Oberhof Fm.), I. Wintersbrunn Horizon (upper Oberhof Fm.), J. Bromacker Horizon (Tambach Fm.). Numbers in yellow boxes represent new sample locations for zircon U-Pb CA-ID-TIMS dating.

0.1% through the use of precisely and accurately calibrated tracers (Condon et al., 2015) and the standardization of raw data correction by the development and supply of open source programs (McLean et al., 2015). As a result, the accuracy and external reproducibility of zircon ages from participating laboratories can be  $\leq 0.1\%$  and can be proved by their reported international zircon standard ages. U-Pb CA-ID-TIMS dating was performed in the TIMS lab at the TU Bergakademie Freiberg (Germany). In the original paper (<https://doi.org/10.1007/s00531-020-01957-y>) we provide our ages for the international standards 91500 and Temora 2. We use the error expressed as  $z$  that also includes the error in tracer calibration and that of the decay constant. This allows us to compare our ages to those obtained with other tracers and other dating systems.

## Results and discussion

Samples 7 and 6 yielded identical (within errors)  $^{206}\text{Pb}/^{238}\text{U}$  mean ages ( $299.7 \pm 0.4$  Ma vs.  $300.0 \pm 0.5$  Ma) representing the age of the Möhrenbach Formation. Consequently, the Möhrenbach Formation was deposited during the latest Carboniferous, i.e., the Gzhelian (Standard Global Chronostratigraphic Scale) or Stephanian (West European regional scale). Our new age of the Ilmenau Formation (sample 5) is the first precise depositional age for this unit. The sample dates the Kickelhahn Rhyolite near Manebach to  $299.3 \pm 0.3$  Ma. This age overlaps with the recorded age of the Carboniferous–Permian boundary ( $298.90 \pm 0.15$  Ma; International Chronostratigraphic Chart 2019/05; the age was obtained by the same U–Pb CA-ID-TIMS method using the 535 spike; Ramezani et al., 2007). Thus, the age of the Kickelhahn Rhyolite provides important information for the stratigraphic position of the C–P boundary in the Thuringian Forest Basin, which has long been discussed as not exactly known.

The Kickelhahn Rhyolite (near Manebach village) is only covered by 10–15 m of tuffaceous conglomerates, above which the Manebach Formation begins with grey fluviatile sandstones. Considering the low thickness of post-rhyolitic volcanoclastic sedimentation, we estimate that the C–P boundary should be positioned approximately at the boundary between the Ilmenau and Manebach formations (cp. Fig. 3).

Our new data suggest an age difference of about 2.5 Myr between sample 5 and sample 3. During this time, the Manebach and Goldlauter formations filled a pull-apart basin with paludal, lacustrine, fluvial, and alluvial sediments. The maximum thickness of both formations is nearly 1000 m, i.e., the rate of subsidence (uncorrected) corresponds to about 400 m/Myr.

Samples 3 and 2 (Oberhof Formation) reflect the culmination of the second volcanic phase within the TFB, which occurred in the range between 296 and 297 Ma. The age of the Komberg Rhyolite intrusion is provided by sample 1 and dates the red beds of the Rotterode Formation. As this formation clearly overlies the Oberhof Formation, the youngest zircon age of this sample ( $295.8 \pm 0.4$  Ma) is in agreement with the stratigraphy.

Sample 4 (Wolfstein Rhyolite) was dated with the idea of determining a representative age for the Elgersburg Formation. However, the obtained age is much older than expected, similar to that of the Möhrenbach Formation. The Wolfstein Rhyolite is directly bordered by the Schöffenhaus fault that dislocates the Elgersburg Formation against members of the Ilmenau Formation and the Oberhof or (in question) Rotterode formations. Thus, we suggest that the Wolfstein Rhyolite could be interpreted as a small, tectonically uplifted block.

The new zircon data for the profile of Carboniferous–Permian volcanic rocks in the TFB show older ages compared to the previously published age data (Fig. 3). This reflects the fact that the pre-treatment of the dated zircons by CA removed those components that suffered severe Pb loss.

In general, the new zircon ages (single zircon ages as well as mean sample ages) show less age scatter than those of earlier publications. Consequently, the total duration of the volcanic activity in the TFB was considerably shorter. Whereas previously an age interval between 295 and 275 Ma was expected for the interval between the Möhrenbach Formation and the Elgersburg

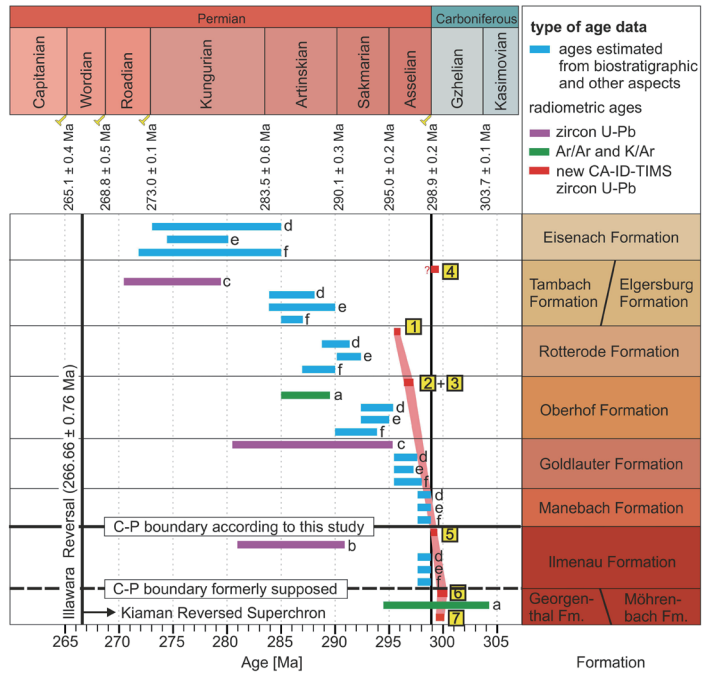


Fig. 3. Compilation of age data from the Rotliegend section of the Thuringian Forest. Radiometric age data are from a: Goll and Lippolt (2001), b: Zeh and Brätz (2000), c: Lützner et al. (2007). The blue bars show the tentative assessment of the Thuringian Forest formations to the International Stratigraphic Chart 2019 after d: Schneider and Werneburg (2012), e: Menning et al. (2016; explanatory notes in Gebhardt et al. 2018) and f: Schneider et al. (2020). Our new CA-ID-TIMS ages are shown in red. Numbers in yellow boxes are sample numbers for new zircon U-Pb CA-ID-TIMS dating. Most of the previous age data and assessments are remarkably younger than the new zircon ages.

Formation (Lützner et al., 2007), our new data suggest a range between ca. 300 Ma for the Möhrenbach Formation and ca. 296 Ma for the Rotterode Formation. Even if the age of the youngest rhyolite (Elgersburg) has not yet been determined, the total duration of volcanic activity has to be reduced from ca. 20 Myr to ca. 4 Myr. The sedimentary gap up to the Illawarra Reversal (ca. 265 Ma after Isozaki, 2009;  $266.66 \pm 0.76$  Ma after Hounslow and Balabanov, 2018) therefore has to be extended to > 25 Myr. This result requires a new view on the early evolution of the Thuringian Forest Basin. The sedimentary hiatus, which can extend locally to 30 Myr in Northern Germany (e.g., between Permian volcanics and the Wustrow Member as the oldest Permian sediment), is at least partially caused by volcano-topographic features (morphology) besides intrabasinal tectonics according to Geißler et al. (2008). Further work is required to evaluate this hiatus in sedimentation for the TFB region as well.

The modern state of biostratigraphy in the continental basins of Pangea has been summarized by Schneider et al. (2020). In the TFB, biostratigraphy is well investigated in the sedimentary record, particularly since Schneider and Werneburg (2012 and papers cited therein) started their work on biostratigraphic zoning in this region. The correlation of zircon ages and biostratigraphic data in continental Carboniferous and Permian basins is partially problematic (e.g., Schneider et al., 2020).

Comparison of Schneider et al. (2020; their Figure 2) with our new age data for the formations near the Carboniferous–Permian boundary (Möhrenbach Fm. plus Ilmenau Fm. = Gehren subgroup) indicates that both datasets are compatible. However, contradictory interpretations are obtained for the Oberhof and Rotterode formations: according to our new ages, both formations originated during the Asselian Stage while Schneider et al. (2020) placed the Oberhof Formation in the Sakmarian and the Rotterode Formation in the Artinskian Stage.

An important amphibian biozone occurs in the uppermost part of the Oberhof Formation (amphibian zone 7 in Schneider et al., 2020) termed the *Melanerpeton pusillum*–*Melanerpeton gracile* assemblage zone, found in the Wintersbrunn fossiliferous horizon [syn. Upper Protriton Horizon (letter I in Fig. 2)]. The evidence of this biozone is widespread. It is reported from the Niederhäslich Formation (Döhlen Basin, Saxony), the Schöneck Formation (Hessian Basins), the Humberg Horizon (top of Meisenheim Formation, Saar–Nahe Basin), from several French basins and from the Olevčín Member (Broumov Formation, Intrasudetic Basin) as well. In the Intrasudetic Basin, this biozone is found in the Ruprechtice limestone horizon in the middle part of the Olevčín Member. Below, at the top of the Nowaruda Member, there occurs the Vraní hory Rhyolite, which is dated by the CA-ID–TIMS U–Pb method at  $297.1 \pm 0.3$  Ma (Opluštíl et al. 2016). This is in good agreement with samples 2 and 3 from the Oberhof Formation and sample 1 from the Rotterode Formation of the TFB. Approximately, 70 m of clastic deposits were accumulated between the Vraní hory Rhyolite and the Ruprechtice Horizon. The amphibian zone 7 is situated in an intermediate position between the uppermost Older Rhyolite of the Oberhof Formation, represented by samples 2 and 3 and the Komberg Rhyolite of the Rotterode Formation (sample 1). Hence, the age of this biozone can be estimated at about 296 Ma from our data.

## Conclusions

We report the first investigation by the U–Pb CA–ID–TIMS method of a Stephanian to Lower Permian (lower Rotliegend) profile in the Thuringian Forest Basin. We draw the following conclusions.

1. First, the results fulfill the expectation that the ages change in the same order as the lithostratigraphic sequence.

2. New geochronological results for the Ilmenau Formation (sample 5) and the Oberhof Formation (samples 2 and 3) indicate an age difference of 2.5 Myr between both formations, indicating a ca. 2.5 Myr nearly quiescent magmatic period for the predominantly sedimentary Manebach and Goldlauter formations. This is in accordance with different biostratigraphic zones. However, still-existing discrepancies between biostratigraphy and geochronology have to be resolved by further geochronological dating and additional paleobiological data.

3. The zircon ages of sample 5 (Kickelhahn Rhyolite, Ilmenau Formation) and the two rhyolite samples (samples 6 and 7, Möhrenbach Formation) are very close to the internationally valid chronostratigraphic Carboniferous–Permian boundary (International Chronostratigraphic Chart 2019) at  $298.90 \pm 0.15$  Ma. Based on the new Kickelhahn Rhyolite zircon age, we assume that the position of the C–P boundary should be located

at the base of the Manebach Formation. Thus, the position of the C–P boundary in the TFB can be established more precisely compared to previous estimates.

4. Compared to earlier concepts, the new zircon ages indicate that the total duration of the volcanic activity in the TFB was considerably shorter. Whereas previously an age interval between 295 and 275 Ma was expected for the whole volcanic period in the TFB, now the range is reduced to a period from ca. 300 Ma (Möhrenbach Formation) to ca. 296 Ma (Rotterode Formation). The total duration of volcanic activity is shortened from ca. 20 Myr to ca. 4 Myr.

5. Consequently, the possible time span from the early Permian volcanic rocks (top Rotterode Formation) up to the Illawarra Reversal has to be extended to ca. 30 Myr. This stratigraphic interval can cover 25–30 Myr in parts of the external Variscides.

6. Our newly obtained ages of the dated TFB formations that contain important biostratigraphic fossils can be used as time marks for certain biostratigraphic zones in other continental Late Carboniferous–Early Permian basins.

7. In the future, the chronostratigraphic sequence in the Thuringian Forest could be even more precisely defined by dating the Inselsberg and/or Heuberg Rhyolite as a mark for the base of the Oberhof Formation, and the Elgersburg Rhyolite as a mark for the youngest rhyolite. In addition, new age data from the other continental basins are urgently needed, in particular from the Saar–Nahe Basin, the Saale Basin near Halle and the Chemnitz Basin. Such new data will allow the definition of volcanic–subvolcanic–plutonic complexes as cogenetic systems and the assessment of their geochemical signatures, thermal history, and magmatic–hydrothermal evolution in an integrated way.

## References

- Andreas, D., 2014. Der Thüringer Wald im Zeitraum der Stefan-Unterperm-Entwicklung—ein Abschnitt der Zentraleuropäischen N-S Riftzone innerhalb des Mitteleuropäischen Großschollenscharniers. Freiberger Forschungshefte, Volume C 547, 181p.
- Condon, D.J., Schoene, B., McLean, N.M., Bowring, S.A. and Parrish, R.R., 2015. Metrology and traceability of U–Pb isotope dilution geochronology (EARTHTIME Tracer Calibration Part I). Geochimica et Cosmochimica Acta, v. 164, p. 464–480.
- Gebhardt, U., Lützner, H., Ehling, B.C., Schneider, J.W., Voigt, S. and Walther, H., 2018. Comments on the Stratigraphical Table of Germany 2016 – Rotliegend Version B. Zeitschrift Deutsche Gesellschaft Geowissenschaften, v.169, no.2, p.129–137.
- Geißler, M., Breitkreuz, C. and Kiersnowski, H., 2008. Permian Basin (NE Germany, W Poland): facies distribution and volcano-topographic hiatus. International Journal of Earth Sciences (Geologische Rundschau), v. 97, p. 973–989.
- Goll, M. and Lippolt, H.J., 2001. Biotit-Geochronologie (40Ar/40K, 40Ar/39Ar, 87Sr/87Rb) spätvariszischer Magmatite des Thüringer Waldes. Neues Jahrbuch Geologische Abhandlungen, v. 222, p. 353–405.
- Hounslow, M.W. and Balabanov, Y.P., 2018. A geomagnetic polarity timescale for the Permian, calibrated to stage

- boundaries. Geological Society, London, Permian GPTS. International Chronostratigraphic Chart 2019. www.stratigraphy.org. International Commission on Stratigraphy. 2019-05.
- Isozaki, Y., 2009. Illawarra reversal: the fingerprint of a superplume that triggered Pangean breakup and the end-Guadalupian (Permian) mass extinction. *Gondwana Research*, v. 15, p. 421–432.
- Lützner, H., Littmann, S., Mädler, S., Romer, R.L. and Schneider, J.W., 2007. Radiometric and biostratigraphic data of the continental Permocarboniferous reference-section Thüringer Wald, Germany. In Wong, Th. E.,(ed.), Proceeding of the 15th International Congress on Carboniferous and Permian Stratigraphy, Utrecht, the Netherlands, 10–16, August 2003, p. 161–174.
- Lützner, H., Andreas, D., Schneider, J.W., Voigt, S. and Werneburg, R., 2012. Stefan und Rotliegend im Thüringer Wald und seiner Umgebung. In Deutsche Stratigraphische Kommission (Hrsg, Koordination und Redaktion: Lützner, H., Kowalczyk, G. für die Subkommission Perm-Trias): *Stratigraphie von Deutschland X. Rotliegend. Teil I: Innervariscische Becken*. Schriftenr. Deutsche Gesellschaft Geowissenschaften, v. 61, p. 418–487.
- McLean, N.M., Condon, D.J., Schoene, B. and Bowring, S.A., 2015. Evaluating uncertainties in the calibration of isotopic reference materials and multi-element isotopic tracers (EARTHTIME Tracer Calibration Part II). *Geochimica et Cosmochimica Acta*, v. 164, p. 481–501.
- Menning, M. and Hendrich, A., Deutsche Stratigraphische Kommission, 2016. *Stratigraphische Tabelle von Deutschland 2016 (STD 2016)*.
- Opuštil, S., Schmitz, M., Kachlík, V. and Štamberg, S., 2016. Re-assessment of lithostratigraphy, biostratigraphy, and volcanic activity of the Late Paleozoic Intra-Sudetic, Krkonoše-Piedmont and Mnichovo Hradiště basins (Czech Republic) based on new U–Pb CA-IDTIMS ages. *Bulletin Geosciences*, v. 91, no. 2, p. 399–432.
- Ramezani, J., Schmitz, M.D., Davydov, V.I., Bowring, S.A., Snyder, W.S. and Northrup, C.J., 2007. High-precision U–Pb zircon age constraints on the Carboniferous–Permian boundary in the southern Urals stratotype. *Earth Planetary Science Letters*, v. 256, p. 244–257.
- Schneider, J.W. and Werneburg, R., 2012. Biostratigraphie des Rotliegend mit Insekten und Amphibien. In Deutsche Stratigraphische Kommission (Hrsg.; Koordination und Redaktion: H. Lützner und G. Kowalczyk für die Subkommission Perm-Trias): *Stratigraphie von Deutschland X. Rotliegend. Teil I: Innervariscische Becken*. Schriftenreihe Deutsche Gesellschaft Geowissenschaften, Heft 61, p. 110–142.
- Schneider, J.W., Spencer, G.L., Scholze, F., Voigt, S., Marchetti, L., Klein, H., Opuštil, S., Werneburg, R., Golubev, V.K., Barrick, J.E., Nemyrovska, T., Ronchi, A., Day, M.O., Silantiev, V.V., Rößler, R., Saber, H., Linnemann, U., Zharinova, V. and Shen, S.Z. 2020. Late Paleozoic—early Mesozoic continental biostratigraphy—links to the Standard Global Chronostratigraphic Scale. *Palaeoworld*, v. 29, p. 186–238.
- Zeh, A. and Brätz, H., 2000. Radiometrische und morphologische Untersuchungen an Zirkonen aus Granitporphyren, Rhyolithen und Granitgerölle des nordwestlichen Thüringer Waldes. *Zeitschrift Deutsche Geologische Gesellschaft*, v. 151, p. 187–206.
- 
- ## Guadalupian and Lopingian transgression of the Khuff Formation carbonate sea in the Middle East and Levant
- Michael H. Stephenson**  
British Geological Survey, Keyworth, Nottingham, NG12 5GG, United Kingdom.  
Email: [mhste@bgs.ac.uk](mailto:mhste@bgs.ac.uk)
- Dorit Korngreen**  
Geological Survey of Israel, 32 Yesha'yahu Leibowitz St., Givat Ram, Jerusalem 9692100, Israel
- Recent work on the palynology of the Permian rocks of the Saad and Arqov formations in boreholes in the Negev desert of Israel and the Umm Irna Formation of Jordan (in preparation; Stephenson and Korngreen, 2020), and the sedimentological character of these deposits, has allowed close comparison with the Permian elsewhere in the Middle East, for example the Arabian Peninsula. These comparisons allow a possible subdivision of the Oman and Saudi Arabia Palynological Zone 6 (OSPZ6) using the first uphole appearance of the distinctive multi-taeniate bisaccate pollen *Protohaploxylinus uttingii*, and the tri-sulcate pollen *Pretricolpipollenites bharadwajii*. The comparison also establishes many similarities between the Lopingian tectono-sedimentary evolution of the successions of the Levant and Arabian Peninsula. Amongst other findings, this confirms that the major marine transgression that formed the Khuff Formation and which brought widespread carbonate depositional conditions across the northern Gondwana Tethys margin, was markedly diachronous.
- The Guadalupian to Lower Triassic Khuff Formation represents a major transgressive-regressive cycle deposited along the northern Gondwanan margin across the Arabian Peninsula, Iran (where it is known as the Dalan Formation), and Iraq (Chia Zairi Formation). Palynomorphs are rarely recovered from the Khuff Formation itself in core or outcrops, due to inimical preservation conditions in limestone, and modern desert weathering. However, the basal Khuff Formation siliciclastic beds (BKS), part of the genetic package of the Khuff Formation (Osterloff et al., 2004) yield palynomorphs from both the subsurface and at outcrop. The beds are known across the Arabian Peninsula for their unusually well-preserved plant fossils, for example in Oman the ‘Gharif Palaeoflora’ (Broutin et al., 1995), and in Saudi Arabia the ‘Unayzah Plant Beds’ (El-Khayal and Wagner, 1985). The Jordanian Umm Irna Plant Beds (Kerp et al., 2006) are considered taxonomically, taphonomically and palaeoenvironmentally to be related to the ‘Gharif Palaeoflora’ and ‘Unayzah Plant Beds’.
- Stephenson and Powell (2013) considered that the Umm Irna

Formation showed closely similar fluvial and paralic depositional environments to those described for the upper Gharif Formation alluvial plain ‘Type Environment P2’ in the subsurface in Oman (Osterloff et al., 2004) and the basal Khuff Formation siliciclastic beds at outcrop and in the subsurface in Central Saudi Arabia, and also remarked on their lithological similarity with the Arqov and Umm Irna formations. However, evidence from the palynology of the Umm Irna Formation, Avdat-1 borehole and now the Makhtesh Qatan-2, Ramon-1 and Boquer-1 boreholes (paper in preparation) indicate markedly younger taxa characterise possible BKSB-equivalent beds in the Levant (Fig. 1).

The diachronous onset of the basal Khuff Formation siliciclastic beds which have similar lithological, sedimentological and taphonomic characteristics, but apparently progressively younger palynomorph taxa, appears to occur northwest through the Arabian Plate (Fig. 1) over an extended period of around 15 my, from the early Wordian (base ~269 My) to the Changhsingian (base ~254 My). The BKSB may indicate a period of humid high runoff producing river systems draining previously drier hinterlands, that heralded the transgression that brought on the main Khuff Formation carbonate sedimentation that in parts of the Middle East persisted for 20 My.

Angiolini et al. (2003) interpreted the Khuff Formation

to record a major transgression of Neotethyan waters in the Wordian, at a stage of full oceanization and tectonic quiescence, when thermal subsidence caused final drowning of rift shoulders and deposition of marine carbonates onto vast portions of stable Arabia.. They concluded that similar transgressive trends took place during the Wordian in the Himalayas, Tunisia, and the Salt Range of Pakistan. However, our preliminary findings relating to diachronism northwest along the Neotethys shore may indicate either slower thermal subsidence or less thermal subsidence in central Arabia and the Levant since this was transgressed later. It may also indicate the influence of persistent ‘Hercynian’ structures/highs such as the central Arabian arch, or in the Levant, the Helez Geanticline (Gvirtzman and Weissbrod, 1984), or the influence of the Arabian Nubian Shield.

Further studies are required to understand the reason for the strongly diachronous base of the Khuff Formation and its equivalents. Comparison with similar tectono-stratigraphic events elsewhere in the Phanerozoic may also provide insights.

## References

- Angiolini, L., Balini, M., Garzanti, E., Nicora, A., Tintori, A., Crasquin, S. and Muttoni, G., 2003. Permian climatic and paleogeographic changes in Northern Gondwana:

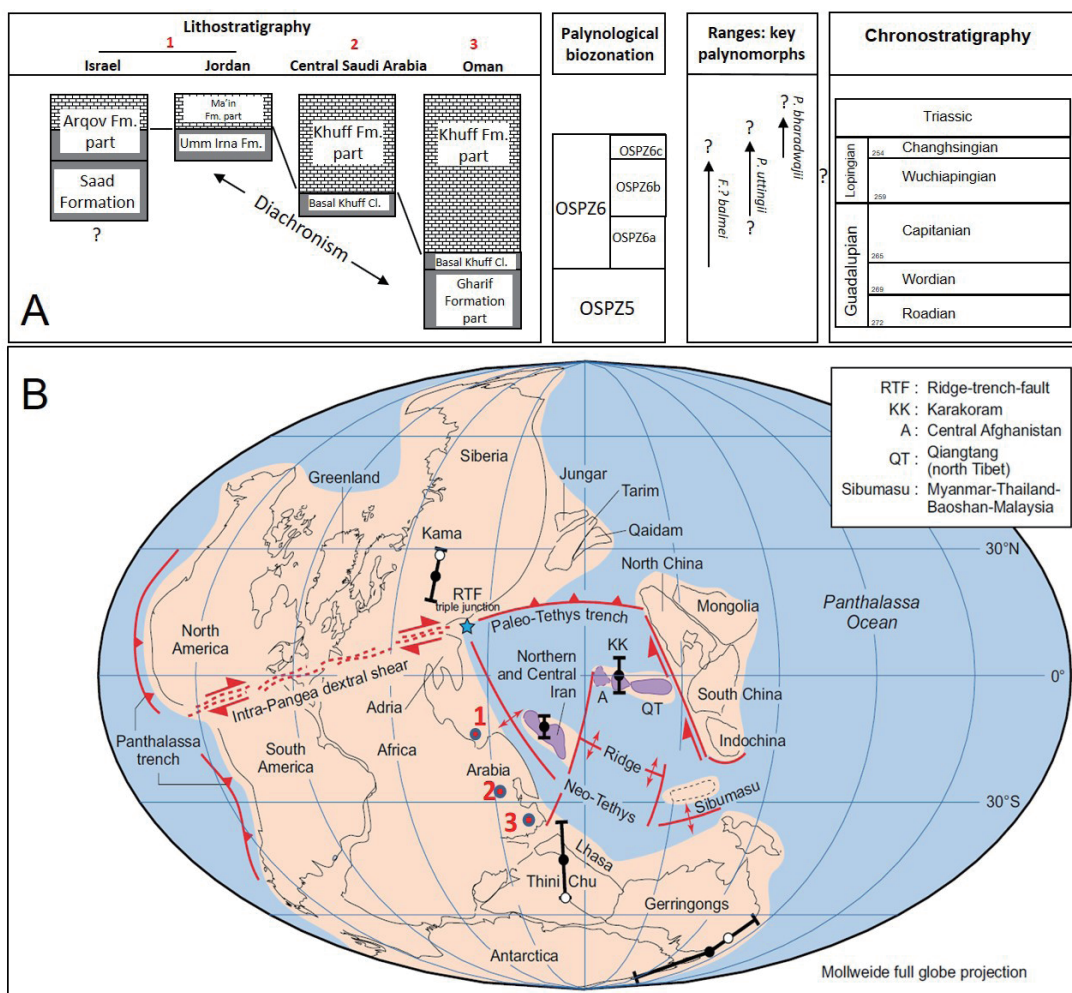


Fig. 1. (A) Stratigraphic distribution of OSPZ5 and proposed subdivisions of OSPZ6 (a, b, and c). (B) Middle Permian continental configuration. 1. Jordan/Israel ; 2. Saudi Arabia; 3. Oman. (map modified after Muttoni et al. 2009)

- the Khuff Formation of Interior Oman, Palaeogeography, Palaeoclimatology, Palaeoecology, v. 191, p. 269–300.
- Broutin, J., Roger, J. Platel, J.P. Angiolini, L. Baud, A. Bucher, H. Marcoux J. and Al Hasmi H., 1995. The Permian Pangea. Phylogenetic implications of new palaeontological discoveries in Oman (Arabian Peninsula). Compte Rendus de l'Academie des Sciences de Paris, Series IIa, v. 321, p. 1069–1086.
- El-Khayal, A.A., and Wagner, R.H., 1985. Upper Permian stratigraphy and megafloras of Saudi Arabia: Palaeogeographic and climatic implications. Dixième Congrès International de Stratigraphie et de Géologie Carbonifère, Madrid, 1983. Compte Rendu, v. 3, p.17–26.
- Gvirtzman, G. and Weissbrod, T., 1984 The Hercynian Geanticline of Helez and the Late Palaeozoic history of the Levant. Geological Society, London, Special Publications, v. 17, p. 177–186.
- Kerp, H., Abu Hamad, A., Vörding, B., and Bandel, K., 2006. Typical Triassic Gondwana floral elements in the Upper Permian of the paleotropics. Geology v. 34, p. 265–268.
- Muttoni G., Gaetani M., Kent D V, Sciunnach D., Angiolini L., Berra F., Garzanti E., Mattei M. and Zanchi A. 2009. Opening of the Neo-Tethys Ocean and the Pangea B to Pangea A transformation during the Permian. GeoArabia, v. 14, p. 17–48
- Osterloff, P., Al-Harthy, A., Penney, R., Spaak, P., Williams G., Al-Zadjali, F., Knox, R., Stephenson, M., Oliver G. and Al-Husseini, M., 2004. Depositional sequence of the Gharif and Khuff formations, subsurface Interior Oman. In Al-Husseini, M.I. (ed.). Carboniferous, Permian and Early Triassic Arabian Stratigraphy. GeoArabia Special Publication 3, Bahrain, Gulf PetroLink, p. 83–147.
- Stephenson M. H., Korngreen, D., 2020. Palynological correlation of the Arqov and Saad formations of the Negev, Israel, with the Umm Irna Formation of the eastern Dead Sea, Jordan, Review of Palaeobotany and Palynology, v. 274, 104153.
- Stephenson, M. H. and Powell, J. H., 2013. Palynology and alluvial architecture in the Permian Umm Irna Formation, Dead Sea, Jordan. GeoArabia, v. 18, p. 17–60.
- 

## One step closer to understanding the Permian-Triassic mass extinction

**Hana Jurikova**

School of Earth and Environmental Sciences, University of St Andrews, St Andrews, UK  
Email: [hj43@st-andrews.ac.uk](mailto:hj43@st-andrews.ac.uk)

Last October Jurikova et al. (2020) published a new paper that illuminates the causes and consequences of the events that resulted in Earth's largest mass extinction. Here, I summarise the key findings and discuss their implications.

The last few decades have seen many exciting developments in palaeontology, geology, geochemistry, and geochronology which have significantly progressed our understanding of the

Permian-Triassic mass extinction (and much of Earth's intriguing history). New evidence emerged suggesting factors as dramatic increase in sea surface temperatures, widespread anoxia and even euxinia, or ocean acidification to have played an important role in the extinction. But how do these different environmental stressors come together in a bigger picture, and fundamentally, what was their underlaying trigger?

Naturally, magmatism from the large igneous province Siberian Traps lends itself as the most likely trigger candidate due to being contemporaneous with the extinction, and the fact that we actually do have a direct evidence for it (unlike gas hydrates or bolide impact). Mantle as a source of isotopically light carbon (considering a value of about –6 ‰) in principle could qualify as a potential cause of the well-known global negative carbon isotope excursion characteristic of the extinction, at least unless latest chronologies are considered. Assuming that the duration of the extinction was on the order of few thousands to ten thousands of years (Burgess et al., 2014), then the mass balance falls out with geologic evidence. In other words, there is no reasonable way a mantle source could explain the sharp carbon isotope excursion; we would need a much larger province or a much lighter source (and this is where gas hydrates which isotopic composition is around –30‰ for biogenic to –60‰ for thermogenic methane offer a convenient hypothesis). So how can we reconcile this issue?

We set out to explore these questions using a novel geochemical approach – the boron isotope pH-proxy. The knowledge of seawater pH on its own is a critical parameter; it is of great relevance to marine life, but most importantly because ocean pH and atmospheric CO<sub>2</sub> are closely coupled, it allows for the reconstruction of the latter. The pre-requisite for a robust pH and CO<sub>2</sub> reconstruction from boron isotopes is a well-preserved and well-calibrated “archive”, specifically a skeletal component of a marine calcifying organism (for obvious reasons this makes boron-based reconstructions over mass extinction intervals rather challenging). Using brachiopods from the Southern Alps in Italy and few specimens for comparison from South China, we reconstructed seawater pH over the onset of the extinction (I am indebted to Lucia Angiolini, Renato Posenato and Uwe Brand who entrusted a starting PhD their precious brachiopod fossils for what was at the beginning a rather experimental adventure). We paired our pH data with global carbon isotope records, and assimilated it into an innovative geochemical modelling framework that simulated the carbon cycle as well as redox-resolving biogeochemistry and nitrogen isotope turnover in the oceans.

In the first place, we quantified the source and volume of CO<sub>2</sub> emissions required to match the carbon isotope and pH constraints. Our results showed that a large pulse of CO<sub>2</sub> was released into the atmosphere reflecting the metamorphic degassing of organic carbon during volcanic intrusions into coal basin sediments. Our estimated total emissions amounted to approximately 106,000 Pg C or 388,000 Pg CO<sub>2</sub> over the duration of the extinction (with carbon isotope composition of predominantly –18‰). To put it in perspective, this is more than 40 times the amount of carbon available in modern fossil fuel reserves, including that already burned since the industrial

revolution, and likely the biggest single event of carbon release during the Phanerozoic. The volcanism lasted for millions of years; it was however first when the intruded magma heated the organic-rich sediments that resulted in the sudden and steep CO<sub>2</sub> release that triggered the extinction!

In the second place, we studied the impact of the CO<sub>2</sub> release on the marine environment and global biogeochemical cycles (Fig. 1). Running numerous sensitivity and model tests to envelope the boundary conditions, we created a scenario that effectively combined available geochemical, geological and palaeontological records to explain the course of the extinction. Our results showed that the large CO<sub>2</sub> pulse led to a strong greenhouse effect on the environment, causing severe heating and acidification of the ocean, which would have provoked the preferential early disappearance of shallow-water and reef-building taxa. An important consequence of the high atmospheric CO<sub>2</sub> levels and hot temperatures in our model was a dramatic increase in chemical weathering rates on land, which led to an elevated flux of nutrients to the ocean affecting the marine biological pump. Warm temperatures and new nutrients supported elevated primary production, which on one hand side aided the drawdown of atmospheric CO<sub>2</sub>, but on the other resulted in greater respiration at depth. This led to the decline of oxygen and accumulation of dissolved sulphide in the waters, and would have contributed to the later disappearance of many deeper-dwelling species and remaining benthos. Deoxygenation of the oceans also

holds the key for the persistence of the marine crisis throughout much of Early Triassic. Under low oxygen conditions, ammonium, phosphate and iron were released from seabed sediments and supported the rise in export production and respiration in a strong positive feedback loop, delaying the recovery of the marine redox state.

I dare not to say that this provides the ultimate answer for the mass extinction, quite the opposite, I think it raises interesting questions which I hope will inspire future research and contribute new ideas (indeed this seems to have been the case and I gratefully acknowledge the many comments and interesting debates that followed the publication of the article), but in the meantime I believe it offers a compelling scenario that brings together many pieces of the Permian-Triassic mass extinction puzzle.

I have dedicated a large part of my work over the past years to improving our understanding of brachiopod geochemistry and biomineralisation (Jurikova et al., 2019; 2020), and more recently in particular to pushing the boundaries of trace element and boron isotope analyses; we can now go smaller (sub-mg calcite sample size for most cases), more precise (<0.2 ‰ for δ<sup>11</sup>B) and most importantly reach higher sample throughput than ever before. While this has greatly reduced what has traditionally been the biggest bottleneck to geochemical proxy-based palaeoenvironmental and palaeo-climatic reconstructions, paradoxically, it has also created a new one. I am now constantly on the



Figure 1. Artist's reconstruction of the onset of the Permian-Triassic mass extinction based on Jurikova et al. 2020. Illustrated by Dawid Adam Iurino (PaleoFactory, Sapienza University of Rome).

search of new well-preserved Permian-Triassic (but not only) brachiopods and would warmly welcome new collaborations and opportunities to access and/or collect new material.

This work would not have been possible without the incessant support of all the co-authors and the funding from European Union's Horizon 2020 programme (grant agreement no. 643084, "BASELiNE-Earth").

## References

- Jurikova H., Gutjahr M., Wallmann K., Flögel S., Liebetrau V., Posenato R., Angiolini L., Garbelli C., Brand U., Wiedenbeck M., and Eisenhauer A., 2020. Permian-Triassic mass extinction pulses driven by major marine carbon cycle perturbations. *Nat. Geosci.*, v. 13, p. 745–750, <https://doi.org/10.1038/s41561-020-00646-4>.
- Burgess S. D., Bowring S., and Shen S.-Z., 2014. High-precision timeline for Earth's most severe extinction. *Proc. Natl Acad. Sci. USA*, v. 111, p. 3316–332, <https://doi.org/10.1073/pnas.1317692111>.
- Jurikova H., Liebetrau V., Gutjahr M., Rollion-Bard C., Hu M.Y., Krause S., Henkel D., Hiebenthal C., Schmidt M., Laudien J., and Eisenhauer A., 2019. Boron isotope systematics of cultured brachiopods: response to acidification, vital effects and implications for palaeo-pH reconstruction. *Geochim. Cosmochim. Acta*, v. 248, p. 370–386, <https://doi.org/10.1016/j.gca.2019.01.015>.
- Jurikova H., Ippach M., Liebetrau V., Gutjahr M., Krause S., Büssé S., Gorb S.N., Henkel D., Hiebenthal C., Schmidt M., Leipe L., Laudien J., and Eisenhauer A., 2020. Incorporation of minor and trace elements into cultured brachiopods: implications for proxy application with new insights from a biomineralisation model. *Geochim. Cosmochim. Acta*, v. 286, p. 418–440, <https://doi.org/10.1016/j.gca.2020.07.026>.

## Report of fieldtrip to northern Tibet: Permian successions in blocks of the Qingshai-Tibet Plateau

**Yichun Zhang, Hua Zhang, Quanfeng Zheng, Mao Luo, Wenkun Qie, Dongxun Yuan, Feng Qiao, Qi Ju, Biao Gao**

State Key Laboratory of Palaeobiology and Stratigraphy, Nanjing Institute of Geology and Palaeontology, Chinese Academy of Sciences, 39 East Beijing Road, Nanjing, 210008, China  
Center for Excellence in Life and Paleoenvironment, Chinese Academy of Sciences, Nanjing 210008, China  
Email: qiju@nigpas.ac.cn(Qi Ju)

**Haipeng Xu**

State Key Laboratory for Mineral Deposits Research, School of Earth Sciences and Engineering, Nanjing University, Nanjing 210023, China

## Introduction

It has been widely acknowledged that the Qingshai-Tibet Plateau played an important role in the process of rifting of the Cimmerian continents during the Permian Period. The strata

together with pronounced marine paleobiogeography during the Permian are significant in reconstruction of the paleogeography.

Supported by the Second Tibetan Plateau Scientific Expedition and Research Programme and other programs, a team of 25 people (including researchers, reporters, drivers and chef) conducted a 29-day field expedition to several localities in northern Tibet from 9th September to 3rd October, 2020 (Fig. 1). The goals of this fieldtrip include: (1) to explore the origin of exotic limestone blocks within the Bangong-Nujiang suture zone; (2) to understand the transition from Permian to Triassic in the North Qiangtang Block; (3) to explore the composition of the accretionary complex within the Longmu Co-Shuanghu suture zone and (4) to study the depositional processes of glacio-marine siliciclastic deposits and warm-water carbonates in the Lhasa Block. Here, we will report the preliminary findings of the fieldwork.

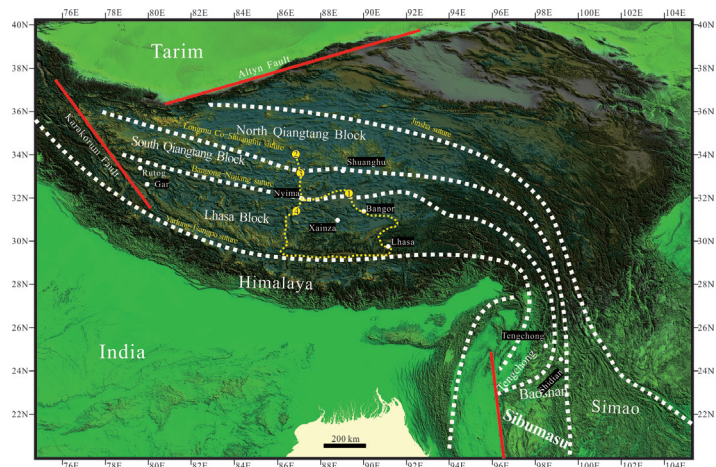


Fig. 1. The field route and study sites in the northern Tibet.  
① Duomar area; ② Raggorycaka area; ③ Rongma area; ④ Wenbu area

## First locality: Duomar Town, Shuanghu County

The opening mechanism of the Neotethys Ocean is a key scientific problem that has not been resolved. Some scholars argued that the southward subduction of the Mesotethys (Bangong-Nujiang) Ocean triggered the formation of the Neotethys Ocean to the south of the Lhasa Block (e.g., Zhu et al., 2013). However, so far there is not enough evidence to support a southward subduction. Within the Bangong-Nujiang suture zone, there is a set of Mesozoic accretionary complexes, namely the Mugagangri Group (Wen, 1979). Numerous detrital zircon studies have proved that this group originated from the South Qiangtang Block in the north (Sun et al., 2019; Ma et al., 2020). Interestingly, there are numerous Permian exotic limestone blocks within the accretionary complex (Fig. 2A). The purpose of our fieldwork in this region was to explore the origin of the Permian limestone blocks. If the limestone blocks came from the Lhasa Block, we can suggest that the Bangong-Nujiang Ocean subducted toward north rather than south.

We found that most limestone blocks had been subjected to strong recrystallization, which hampered the preservation of fossils. The most common fossils found in the limestones are sponges and calcareous algae (Fig. 2B). Fortunately, we found a limestone block with relatively weaker recrystallization to the

south of Duoma Town. Within this limestone block, we found diverse fusulines. The fusulines are now being processed in the laboratory.



Fig. 2. Field views in the Duoma area, Shuanghu County  
A, Permian limestone blocks within the Mugagangri Group; B, Permian limestone with sponges and calcareous algae

#### Second locality: Raggyorcaka area, Nyima County

The Raggyorcaka area belongs to the North Qiangtang Block based on the typical warm-water biota across the Carboniferous-Permian transition (Zhang et al., 2016). The Permian and Triassic strata are widely exposed in this region. Previously, the Permian strata were named as the Raggyorcaka Formation, which is characterized by mudstones and shales with sandstone and limestone interbeds (Wen et al., 1979). Abundant fusulines such as *Palaeofusulina nana*, *P. sinensis*, and *P. fusiformis* were discovered in the limestone, suggesting a Changhsingian Age (Wang et al., 1981). In our fieldwork, we found a thick succession of limestones about 100 meters below the Raggyorcaka Formation (Fig. 3A). This unit has been named the Xueyuanhe Formation by the Institute of Geological Survey of Jilin University (2005). According to the original definition, the age of the Xueyuanhe Formation was assigned to the Middle Permian. However, in the fieldwork, we preliminary confirmed the presence of the foraminifera *Colaniella*, suggesting a Late Permian age for this limestone interval. Consequently, the transition from the limestones of the Xueyuanhe Formation to the siliciclastic successions of the Raggyorcaka Formation represents a regression event. The sea-level variations continued in the Raggyorcaka Formation and resulted in the frequent occurrence of many limestone interlayers within the mudstones. Abundant fusulines such as *Palaeofusulina* and the brachiopod *Leptodus* were found in the limestone interlayers (Fig. 3B). In the upper part of the Raggyorcaka Formation, with the ultimate diminishment and demise of the limestone interbeds, the strata are dominated by several layers of coals with abundant plant fossils (Fig. 3C). The Permian-Triassic boundary is tentatively considered here to be correlate to the formation boundary between the Raggyorcaka Formation and the overlying Kanglu Formation based on lithofacies and biofacies data (Fig. 3D). As has been proposed by Zhang et al. (2019), the eustatic variation of the Raggyorcaka Formation is similar to that in the Qamdo region more than 1000 km in the east. More study is required to study their paleogeographic relationships.

#### Third locality: Rongma Town, Nyima County

This region is very close to the Longmu Co-Shuanghu suture zone. There are many ophiolites and blueschists preserved in this region. The Permian strata are widely distributed, which were

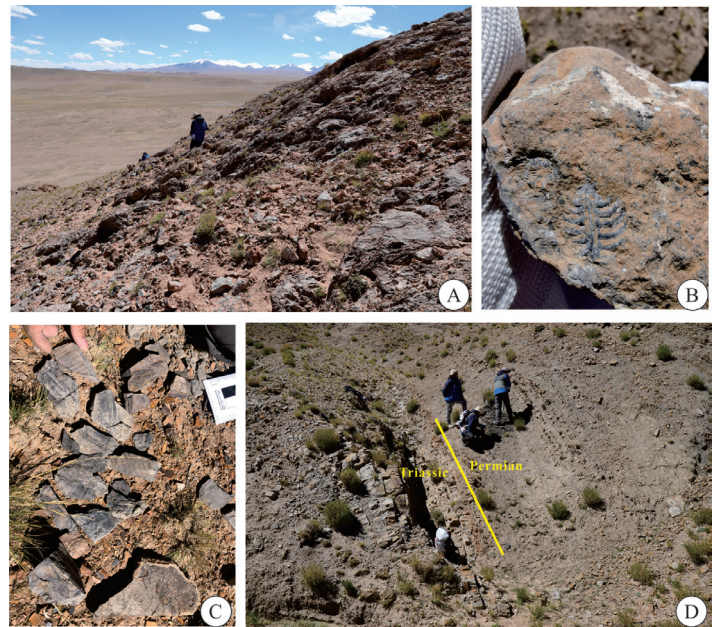


Fig. 3. Permian and PTB strata and biotas in the Raggyorcaka area. A. the limestone of the Xueyuanhe Formation; B. *Leptodus* (brachiopod) in the Raggyorcaka Formation; C. plant fossils in the upper part of the Raggyorcaka Formation; D. probable Permian-Triassic boundary in the Raggyorcaka area

assigned to the Cameng and Zhanjin formations (Institute of Geological Survey of Jilin University, 2005). Due to the strong tectonic deformation in the convergence zone, fossils are not reported in both formations previously. Thus, we didn't check them during the fieldwork.

During the fieldwork, we investigated outcrops in a deep valley to the south of Jiaomuri Hill. The outcrops there are represented by an accretionary complex with different tectonic units (Fig. 4). These units include well-bedded reddish limestone (Fig. 4A), thin-bedded siltstones with sandstone olistostromes (Fig. 4B), well-bedded grey limestones (Fig. 4C) and thin-bedded cherts (Fig. 4D). The ages of these units are not known. However, it is clear that they are accretionary complex related to the subduction of the Paleotethys Ocean beneath the North Qiangtang Block, judging from their field occurrences.

#### Fourth locality: Wenbu Town, Nyima County

This area is located at Wenbu Town, south of Nyima County. Tectonically, it belongs to the Lhasa Block. The Permian strata in this region consist of the Yunzhub, Largar, Angjie and Xiala formations, in ascending order. We measured two sections. The first one preserves a perfect transition from glaciomarine deposits to marine carbonates (Fig. 5A). The lowermost part of the section is characterized the Largar Formation, which is composed of thick-bedded sandstones, and massive siltstones with common dropstones (Fig. 5B). The dropstones are dominated by quartzite and granites, indicating an exotic glacial origin. The Angjie Formation conformably overlies the Largar Formation. Interestingly, many brachiopod shells were found in the base of the Angjie Formation (Fig. 5C). They occurred directly above or within the conglomerate, suggesting sea-level rise during the



Fig. 4. Permian strata in the Rongma area.

A. accretionary complex in the Longmu Co-Shuanghu suture zone; B. thin-bedded siltstones with sandstone olistostromes; C. Permian thin- to middle-bedded limestone beds; D. cherts beds at a steep angle

initial deglaciation. In the upper part of the Angie Formation, grey thin-bedded siltstones dominated. In the top of the section, the reddish limestone of the Xiala Formation conformably overlies the Angie Formation.

The middle part of the Xiala Formation outcrops in the west of the famous Tangra Yumco Salt Lake, where the sequence is dominated by carbonates with chert nodules (Fig. 5D). Diverse fossils, such as colonial corals, brachiopods and fusulines were collected in the section. Both the coral and fusuline indicate a Guadalupian age for the limestone.

In conclusion, the Permian strata in the Wenbu area represent a transition from glaciomarine deposits (cold climate) to marine carbonate deposits (warm climate). This transition is similar to that in other regions in the Lhasa Block such as in the Xainza, Tsochen and Lhunzhub areas. It suggests that the Lhasa Block was very stable during the Permian.

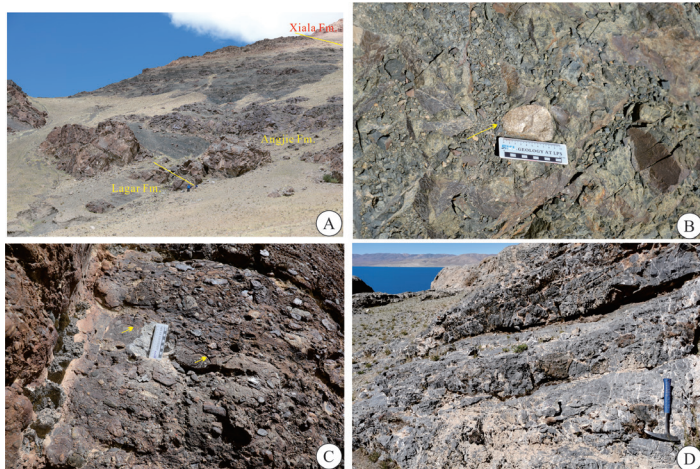


Fig. 5. Permian strata from the Wenbu area, Lhasa Block.

A. Permian section in the north of the Wenbu village; B. dropstones in the Largar Formation; C. brachiopods from the lower part of the Angie Formation; D. Middle Permian limestone beds of the Xiala Formation.

In total, we investigated more than twenty sections in different blocks in the Qinghai-Tibet Plateau. The Permian sequences and faunas in these blocks are quite different, which is of great significance in the reconstruction of the paleogeography.

### Acknowledgement

The fieldwork is financially supported by the Second Tibetan Plateau Scientific Expedition and Research (2019QZKK0706), the National Science Foundation of China (91855205) and Strategic Priority Research Program (B) of the Chinese Academy of Sciences (XDB26000000, XDB18000000).

### References

- Institute of Geological Survey of Jilin University, 2005. 1:250000 Mayer Kangri Sheet in Xizang. Sedimentary Geology and Tethyan Geology, v. 25, p. 51–56 (in Chinese with English abstract).
- Ma, A.L., Hu, X.M., Kapp, P., BouDagher-Fadel, M., Lai, W., 2020. Pre-Oxfordian (>163Ma) ophiolite obduction in Central Tibet. Geophysical Research Letters, v. 47, p. e2019GL086650.
- Sun, G.Y., Hu, X.M., Xu, Y.W., BouDagher-Fadel, M. K., 2019. Discovery of Middle Jurassic trench deposits in the Bangong-Nujiang suture zone: Implications for the timing of Lhasa-Qiangtang initial collision. Tectonophysics, v. 750, p. 344–358.
- Wang Y.J., Sheng J.Z., Zhang L.X., 1981. Fusulinids from Xizang of China. In Nanjing Institute of Geology and palaeontology (ed.), Palaeontology of Xizang, Book 3. Science Press, Beijing, pp. 1–80 (in Chinese with English abstract).
- Wen S.X., 1979. New stratigraphic materials from Northern Tibet. Acta Stratigraphic Sinica, v. 3, p. 150–156 (in Chinese with English abstract).
- Zhang Y.C., Shen S.Z., Zhang Y.J., Zhu T.X., An X.Y., 2016. Middle Permian non-fusuline foraminifers from the middle part of the Xiala Formation in Xainza County, Lhasa Block, Tibet. Journal of Foraminiferal Research, v. 46, p. 99–114.
- Zhang Y.C., Shen, S.Z., Xu, H.P., Qiao, F., Yuan, D.X., Ju, Q., 2020. Recent progress and future perspectives in the application of Permian palaeobiogeography in the reconstruction of the palaeogeography of the Qinghai-Tibet plateau and adjacent regions. Permophiles, v. 68, p. 19–23.
- Zhu D. C., Zhao Z.D., Niu Y.L., Dilek Y., Hou Z.Q., Mo X.X., 2013. The origin and pre-Cenozoic evolution of the Tibetan Plateau. Gondwana Research, v. 23, p. 1429–1454.

**Comment to Chen et al., 2020: Abrupt warming in the latest Permian detected using high-resolution in situ oxygen isotopes of conodont apatite from Abadeh, central Iran. Importance of correct stratigraphic correlation, reporting of existing data and their scientific interpretation**

### Micha Horacek

Department of Lithospheric Research, University of Vienna, Althanstr. 14, 1090 Vienna, Austria

### Leopold Krystyn

Department for Palaeontology, University of Vienna, Austria

## Aymon Baud

Institute of Earth Sciences, University of Lausanne, Switzerland

This comment was intended to be published in Palaeo3, where the paper we are discussing has been released. However, its editor decided not to consider our contribution without giving any reason. We regard the Abadeh section as one of the most important PTB sections in the world, evidenced by numerous investigations carried out there, therefore an exact and unequivocal high-resolution stratigraphy must be ensured, which we hope to support by this contribution.

We have enjoyed reading the outcome of Chen et al. with its impressive sea surface water temperature curve across the PTB in Iran. However, we are very surprised and concerned about the biostratigraphy applied to the Abadeh section for this so important and sensitive time interval by disregarding major published work. Based on intense research, there is a broad agreement on the position of the PTB interval at Abadeh when following the results of three independent research groups: the first investigation by the Iranian-Japanese-Research Group (IJRG: Taraz et al., 1981) showed the PTB (FO of *Hindeodus parvus*) at the top of the boundary clay, ca. 30 cm above the top of the *Paratirolites* Limestone at the base of the microbialite interval (Fig. 1). This position was subsequently confirmed by Gallet et al. (2000), Horacek et al. (2007) and Richoz et al. (2010) (the latter two part of the same research group), and adopted by Kershaw et al. (2012), Shen et al. (2013), Liu et al. (2013) and Dudas et al. (2017) (all henceforth called GROUP 1, Fig. 1). However, one research group (here called GROUP 2) including Korte et al. (2004, 2010) and Kozur (2004, 2005, 2007) drew the PTB distinctly (ca. 1.4 metres) above the top of the *Paratirolites* Limestone, thereby moving the boundary above their microbialite interval. Shen and Mei (2010) adopted this position, though, as Ghaderi et al. (2014) pointed out, without any own observations or data from this interval. Thereby they artificially extended the range of the Late Permian and pre-extinction conodont *C. hauschkei* across their non-investigated interval until their first data point significantly above the PTB sensu GROUP 1. This completely confuses the PTB interval in Abadeh, because, between the *Clarkina* (*C.*) *hauschkei* and *Hindeodus* (*H.*) *parvus* zones, now there is either no conodont zone [Shen and Mei (2010), adopted by Liu et al. (2013)], or one [*C. meishanensis* – *H. praeparvus* zone (z.) in Korte et al. (2004) and Richoz et al. (2010)] or two conodont zones. [*C. meishanensis* – *H. preparvus* and *Merillina* (*M.*) *ultima* – *Stepanovites?* (S.?) *mostleri* z. (Kozur, 2005, 2007; Korte, 2010)]. The base of the latter zone approximates to the FO of *H. parvus* in Taraz et al. (1981), Gallet et al. (2000), Horacek et al. (2007) and Richoz et al. (2010) (GROUP 1). Chen et al. adopted the low-resolution stratigraphy of Shen and Mei (2010) and thus the higher stratigraphic base of the Triassic of GROUP 2 for reasons we can only speculate (see below).

The PTB-interval represents a period of profound and quick environmental changes, for which a detailed chronology with exact and correct assignment of the boundary is indispensable. Therefore, the decision by Chen et al. to apply a low-resolution and incorrect stratigraphy, is very problematic, resulting in confusion and incorrect conclusions. Specifically we criticize the

following points:

## Problems with biochronology and lithostratigraphy

Firstly, by following Mei and Shen (2010), the authors ignore the existence of one [*C. meishanensis*-*H. praeparvus*, Korte et al.(2004), Richoz et al.(2010)], or two latest Permian conodont zones [*C. meishanensis*-*H. praeparvus* and *M. ultima*-*S.?* *mostleri*: Kozur (2005, 2007)] above the *C. hauschkei* zone. Instead, they enlarge this rather short-lived conodont zone, which in the Abadeh section is strongly reduced (just up to 14 cm in the uppermost pre-extinction *Paratirolites* beds) – see Korte et al. (2004), Kozur (2005, 2007) – to an interval of ca. 140 cm across the entire boundary interval.

Secondly, their placement of the PTB in Abadeh is done in a way that seems to us unsound and non-scientific. In Abadeh, GROUP 1 has identified the first occurrence of *Hindeodus parvus* at ca. 30 cm above the top of the *Paratirolites* beds and GROUP 2 at ca. 1 metre higher. The conodonts are well described and displayed in Kozur (2004) and Richoz et al. (2010, pl. 2), with respect to GROUP 2 and GROUP 1. Chen et al. do neither evaluate these documentations nor the ambiguity between the two groups, and do not draw the logic conclusion that GROUP 1, representing three teams, must have correctly identified the boundary, which GROUP 2 (representing one team) has missed. Also, they did not document their own conodont material, which might have added further valuable detailed information. Instead, they claim not having had sufficient material to determine the *Hindeodus* lineage and thus the boundary in the section. This is rather curious, as they obviously had collected enough material to perform the oxygen isotope analysis – assumingly they analysed all material before a proper conodont determination. Inacceptable, however, is Chen's et al. justification of their PTB definition by wrongly quoting Kershaw et al. (2012), that “the biostratigraphic boundary is most likely close to the top of the microbialite bed”. Kershaw et al. (2012), showed in their fig. 9C the PTB in Abadeh at ca. 30 cm above the top of the *Paratirolites* limestone, thus following GROUP 1. Nonetheless, Chen et al. locate the PTB in Abadeh close to the top of the microbialites by adopting the boundary position of GROUP 2 as the correct one.

Thirdly, if Chen et al. (2020) would do follow the claim of Kershaw et al. (2012), they would need to draw the boundary even further up, to 190 cm above the *Paratirolites* beds, as Baud and Richoz (2007, fig. 3a), Richoz et al. (2010, fig. 5), and Kershaw et al. (2012, fig. 9C) show the top of the microbialites at this level.

Fourthly, Chen et al. (2020) failed to show both published PTB levels that have been identified in the section in their figures (nor do they mention them in the captions), but exclusively note the *H. parvus* datum of GROUP 2, persuading a non-in-depth reader that this is the undisputed PTB at Abadeh section. As this is not the case, Chen et al. produce confusion and uncertainty in the stratigraphy of the Abadeh section instead of aiming for clarification and solution of this question.

## Consequences

The criticized points in the Chen et al. paper lead to significant errors and problems:

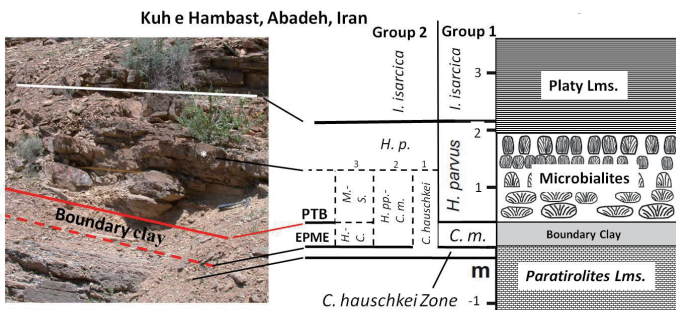


Fig. 1. PTB at Abadeh showing the biostratigraphy of the different research groups and publications. BS: boundary shale, Lms.: Limestone, C.: *Clarkina*, C.m.: *Clarkina meishanensis*, H. p.: *Hindeodus parvus*, H. pp.: *Hindeodus praeparvus*, H.-C.: *Hindeodus praeparvus-Clarkina meishanensis*, I.: *Isarcicella*, M.-S.: *Merillina ultima* – *Stepanovites? Mostleri*. EPME: End Permian Mass Extinction, PTB: Permian-Triassic Boundary. 1: Shen and Mei, 2010; Chen et al., 2020. 2: Korte et al., 2004. 3: Kozur 2005, 2007; Korte et al., 2010. White star in photo: PTB according to GROUP 2. Length of hammer in photo is 35 cm.

Problem 1: By enlarging the *C. hauschkei* zone beyond the entire boundary interval and thus significantly beyond the end-Permian mass extinction event (EPME) – and the quick and strong increase in seawater temperature following the EPME , Chen et al. suggest that *C. hauschkei* might have thrived in the P-T post-extinction hot-water environment of Abadeh. However, this has not been documented in any equatorial Tethyan section so far and appears rather unlikely, as *Clarkina* is a LPL cool-water genus (e.g. Kozur 2007) and usually a decline (or total disappearance) is reported after the EPME (Richoz et al., 2010); this is also evidenced by its absence above the EPME in Chen's et al. dataset.

Problem 2: If the PTB-definition of GROUP 1 (PTB at ca. 30cm above top of the *Paratirolites* limestone) is used, the isotopic results of Chen et al. indicate that the warming trend of the ocean water continues into the basal Lower Triassic at Abadeh. We hypothesize that one reason for their opposing "... conservative option..." in placing the PTB higher up might have been the urge to find an agreement with the recently published seawater-temperature curve of Joachimski et al. (2019). There the increase in seawater-temperature is also restricted to the Late Permian [Interestingly the PTB position in Joachimski et al. (2019) is disputed, too and will be discussed elsewhere]

## Conclusions

Theoretically, the placement of the PTB in Abadeh should be straight forward, as three independent working groups [Taraz et al. (1981), Gallet et al. (2000), Horacek et al. (2007), Richoz et al. (2010)] identically determined the boundary and just one research group published diverging results [Korte et al. (2004, 2010), and all further publications by Kozur are based on the same material]. The study by Chen et al. would have been an excellent opportunity to solve and refine the question concerning the exact position of the PTB in Abadeh as a useful by-product of their main aim. Sadly, the authors have failed in this point and

have instead added confusion concerning the PTB position in Abadeh and the range of *C. hauschkei*. Following our correction, the data of Chen et al. of a temperature change from the EPME into the earliest Triassic do agree with those from Meishan, China (Chen et al., 2016; Wang et al., 2020).

## Acknowledgments

This is a contribution to IGCP-projects 630 and 710.

## References

- Baud, A., Richoz, S., and Pruss, S., 2007. The lower Triassic anachronistic carbonate facies in space and time. *Global and Planetary Change*, v. 55, p. 81–89. doi.org/10.1016/j.gloplacha.2006.06.008.
- Chen, J., Shen, S.Z., Li, X.H., Joachimski, M.M., Bowring, S.A., Erwin, D.E., Yuan, D.X., Chen, B., Zhang, H., Wang, Y., Cao, C.Q., Zheng, Q.F. and Mu, L., 2016, High-resolution SIMS oxygen isotope analysis on conodont apatite from South China and implications for the end-Permian mass extinction. *Palaeogeography, Palaeoclimatology, Palaeoecology*, v. 448, p. 26–38.
- Chen, J., Shen, S.Z., Zhang, Y.C., Angiolini, L., Gorgij, M., N., Crippa, G., Wang, W., Zhang, H., Yuan, D.X., Li, X.H. and Xu, Y.G., 2020. Abrupt warming in the latest Permian detected using high-resolution *in situ* oxygen isotopes of conodont apatite from Abadeh, central Iran. *Palaeogeography, Palaeoclimatology, Palaeoecology*, v. 560, https://doi.org/10.1016/j.palaeo.2020.109973
- Dudás, F. Ö., Yuan, D.X., Shen, S.Z. and Bowring, S. A., 2017. A conodont-based revision of the  $^{87}\text{Sr}/^{86}\text{Sr}$  seawater curve across the Permian-Triassic boundary. *Palaeogeography, Palaeoclimatology, Palaeoecology*, v. 470, p. 40–53. http://dx.doi.org/10.1016/j.palaeo.2017.01.007
- Gallet, Y., Krystyn, L., Besse, J. and Ricou, L.E., 2000. New constraints on the Upper Permian and Lower Triassic geomagnetic polarity timescale from the Abadeh section (central Iran). *Journal of Geophysical Research*, v. 105/ B2, p. 2805–2815.
- Ghaderi, A., Leda, L., Schobben, M., Korn, D. and Ashouri, A.R., 2014. High-resolution stratigraphy of the Changhsingian (Late Permian) successions of NW Iran and the Transcaucasus based on lithological features, conodonts and ammonoids. *Fossil Record*, v. 17, p. 41–57.
- Horacek, M., Richoz, S., Brandner, R., Krystyn, L. and Spötl, C., 2007. Evidence for recurrent changes in Lower Triassic oceanic circulation of the Tethys: The  $\delta^{13}\text{C}$  record from marine sections in Iran. *Palaeogeography, Palaeoclimatology, Palaeoecology*, v. 252, p. 355–369.
- Joachimski, M.M., Alekseev, A.S., Grigoryan, A. and Gatovsky, Y.A., 2020. Siberian Trap volcanism, global warming and the Permian-Triassic mass extinction: New insights from Armenian Permian-Triassic sections. *Geological Society of America Bulletin*, v. 132, p. 427–443.
- Kershaw, S., Crasquin, S., Li, Y., Collin, P.Y., Forel, M.B., Mu, X., Baud, A., Wang, Y., Xie, S., Maurer, F. and Guo, L., 2012. Microbialites and global environmental change across the Permian-Triassic boundary: a synthesis. *Geobiology*, v. 10, p.

- 25–47.
- Korte, C., Kozur, H.W., Joachimski, M.M., Strauss, H., Veizer, J. and Schwark, L., 2004. Carbon, sulfur, oxygen and strontium isotope records, organic geochemistry and biostratigraphy across the Permian/Triassic boundary in Abadeh, Iran. *International Journal of Earth Sciences*, v. 93, p. 565–581.
- Korte, C., Pande, P., Kalia, P., Kozur, H.W., Joachimski, M.M. and Oberhänsli, H., 2010. Massive volcanism at the Permian-Triassic boundary and its impact on the isotopic composition of the ocean and atmosphere. *Journal of Asian Earth Sciences*, v. 37, p. 293–311. doi.org/10.1016/j.jseas.2009.08.012.
- Kozur, H.W., 2004. Pelagic uppermost Permian and the Permian-Triassic boundary conodonts of Iran. Part I: Taxonomy. *Hallesches Jahrbuch für Geowissenschaften B Beiheft* 18, 39–68.
- Kozur, H.W., 2005. Pelagic uppermost Permian and the Permian-Triassic boundary conodonts of Iran. Part II: investigated sections and evaluation of the conodont faunas. *Hallesches Jahrbuch für Geowissenschaften B Beiheft*, v. 19, p. 49–86.
- Kozur, H.W., 2007. Biostratigraphy and event stratigraphy in Iran around the Permian-Triassic Boundary (PTB): Implications for the causes of the PTB biotic crisis. *Global and Planetary Change*, v. 55, p. 155–176.
- Liu, X.C., Wang, W., Shen, S.Z., Gorgij, M.N., Ye, F.C., Zhang, Y.C., Furuyama, S., Kano, A. and Chen, X.Z., 2013. Late Guadalupian to Lopingian (Permian) carbon and strontium isotopic chemostratigraphy in the Abadeh section, central Iran. *Gondwana Research*, v. 24, p. 222–232.
- Richoz, S., Krystyn, L., Baud, A., Brandner, R., Horacek, M. and Mohtat-Aghai, P., 2010. Permian-Triassic boundary interval in the Middle East (Iran and N. Oman): Progressive environmental change from detailed carbonate carbon isotope marine curve and sedimentary evolution. *Journal of Asian Earth Sciences*, v. 39, p. 236–253.
- Shen, S.Z. and Mei, S.L., 2010. Lopingian (Late Permian) high-resolution conodont biostratigraphy in Iran with comparison to South China zonation. *Geological Journal*, v. 45, p. 135–161.
- Shen, S.Z., Cao, C.Q., Zhang, H., Bowring, S.A., Henderson, C.M., Payne, J.L., Davydov, V.I., Chen, B., Yuan, D.X., Zhang, Y.C., Wang, W. and Zheng, Q.F., 2013. High-resolution  $\delta^{13}\text{C}_{\text{carb}}$  chemostratigraphy from latest Guadalupian through earliest Triassic in South China and Iran. *Earth and Planetary Science Letters*, v. 375, p. 156–165.
- Taraz, H., Golshani, F., Nakazawa, K., Shimura, D., Bando, Y., Ishii, K.I., Maurata, M., Okimura, Y., Sakamura, S., Nakamura, K. and Tokuoka, T., 1981. The Permian and the Lower Triassic Systems in Abadeh Region, Central Iran. *Memoirs of the Faculty of Science, Kyoto University, Series of Geology and Mineralogy*, v. 47, p. 62–133.
- Wang, W. Q., Garbelli, C., Zhang, F. F., Zheng, Q. F., Zhang, Y. C., Yuan, D. X., Shi, Y.K., Chen, B. and Shen, S. Z., 2020. A high-resolution Middle to Late Permian paleotemperature curve reconstructed using oxygen isotopes of well-preserved brachiopod shells. *Earth and Planetary Science Letters*, v. 540, p. 116245.
- Compilation of selected papers published on Permian topics in 2020**
- ### Stratigraphy
- Bagherpour, B., Bucher, H., Vennemann, T., Schneebeli-Hermann, E., Yuan, D.X., Leu, M., Shen, S.Z. (2020). Are Late Permian carbon isotope excursions of local or of global significance? *Geological Society of America Bulletin*, 132(3-4), 521–544. https://doi.org/10.1130/B31996.1
- Botha, J., Huttenlocker, A.K., Smith, R.M.H., Prevec, R., Viglietti, P., Modesto, S.P. (2020). New geochemical and palaeontological data from the Permian-Triassic boundary in the south African Karoo basin test the synchronicity of terrestrial and marine extinctions. *Palaeogeography Palaeoclimatology Palaeoecology*, 540, 109467. https://doi.org/10.1016/j.palaeo.2019.109467
- Chernykh, V.V., Chuvashov, B.I., Shen, S.Z., Henderson, C.M., Yuan, D.X., Stephenson, M.H. (2020). The Global Stratotype Section and Point (GSSP) for the base-Sakmarian stage (Cisuralian, Lower Permian). *Episodes*, 43(4), 961–979. https://doi.org/10.18814/epiugs/2020/020059
- Chernykh, V.V., Kotlyar, G.V., Chuvashov, B.I., Kutygin, R.V., Filimonova, T.V., Sungatullina, G.M., Batalin, G.A. (2020). Multidisciplinary study of the Mechetlino quarry section (Southern Urals, Russia) - the GSSP candidate for the base of the Kungurian stage (Lower Permian). *Palaeoworld*, 29(2), 325–352. https://doi.org/10.1016/j.palwor.2019.05.012
- Davydov V.I., Arefiev M.P., Golubev V.K., Karasev E.V., Naumcheva M.A., Schmitz M.D., Silantiev V.V., Zharinova V.V. (2020). Radioisotopic and biostratigraphic constraints on the classical Middle-Upper Permian succession and tetrapod fauna of the Moscow synecline, Russia. *Geology* 48, 742–747. https://doi.org/10.1130/G47172.1
- Ellwood, B.B., Nestell, G.P., Lan, L.T.P., Nestell, M.K., Tomkin, J.H., Ratcliffe, K.T., Dang, T.H. (2020). The Permian-Triassic boundary Lung Cam expanded section, Vietnam, as a high-resolution proxy for the GSSP at Meishan, China. *Geological Magazine*, 157(1), 65–79. https://doi.org/10.1017/S0016756819000566
- Li Y., Shao L., Fielding C.R., Wang D., Mu G., Luo H., (2020). Sequence stratigraphic analysis of thick coal seams in paralic environments - A case study from the Early Permian Shanxi Formation in the Anhe coalfield, Henan Province, North China. *International Journal of Coal Geology* 222, 103451, https://doi.org/10.1016/j.coal.2020.103451
- Rampino, M.R., Eshet-Alkalai, Y., Koutavas, A., Rodriguez, S. (2020). End-Permian stratigraphic timeline applied to the timing of marine and non-marine extinctions. *Palaeoworld*, 29(3), 577–589. https://doi.org/10.1016/j.palwor.2019.10.002
- Pan L., Shen A., Zhao J.X., Hu A., Hao Y., Liang F., Feng Y., Wang X., Jiang L., (2020). LA-ICP-MS U-Pb geochronology and clumped isotope constraints on the Formation and evolution of an ancient dolomite reservoir: The Middle Permian of northwest Sichuan Basin (SW China). *Sedimentary Geology* 407, 105728. https://doi.org/10.1016/

- j.sedgeo.2020.105728  
 Pfeifer L.S., Hinnov L., Zeeden C., Rolf C., Laag C., Soreghan G.S., (2020). Rock Magnetic Cyclostratigraphy of Permian Loess in Eastern Equatorial Pangea (Salagou Formation, South-Central France). *Frontiers in Earth Science* 8, 241. <https://doi.org/10.3389/feart.2020.00241>
- Schmitz, M.D., Pfefferkorn, H.W., Shen, S.Z., Wang, J., (2020). A volcanic tuff near the Carboniferous–Permian boundary, Taiyuan Formation, North China: Radioisotopic dating and global correlation. *Review of Palaeobotany and Palynology*, 104244, <https://doi.org/10.1016/j.revpalbo.2020.104244>.
- Shen, S. Z., Yuan, D. X., Henderson, C. M., Wu, Q., Zhang, Y. C., Zhang, H., Wang, T. T. (2020). Progress, problems and prospects: An overview of the Guadalupian series of South China and North America. *Earth-Science Reviews*, 211. <https://doi.org/10.1016/j.earscirev.2020.103412>
- Wu, Q., Ramezani, J., Zhang, H., Yuan, D.X., Erwin, D.H., Henderson, C.M., Shen, S.Z. (2020). High-precision U-Pb zircon age constraints on the Guadalupian in West Texas, USA. *Palaeogeography Palaeoclimatology Palaeoecology*, 548. <https://doi.org/10.1016/j.palaeo.2020.109668>
- Zhong, Y.T., Mundil, R., Chen, J., Yuan, D.X., Denyszyn, S.W., Jost, A.B., Xu, Y.G. (2020). Geochemical, biostratigraphic, and high-resolution geochronological constraints on the waning stage of Emeishan Large Igneous Province. *Geological Society of America Bulletin*, 132(9-10), 1969-1986. <https://doi.org/10.1130/B35464.1>
- Geochemical proxies and paleoclimate**
- Abedini A., Mongelli G., Khosravi M., Sinisi R. (2020). Geochemistry and secular trends in the Middle-Late Permian karst bauxite deposits, northwestern Iran. *Ore Geology Reviews* 124, 103660. <https://doi.org/10.1016/j.oregeorev.2020.103660>
- Brookfield M.E., Williams J., Stebbins A.G., (2020). Geochemistry of the new Permian-Triassic boundary section at Sitarićka Glavica, Jadran block, Serbia. *Chemical Geology* 550, 119696. <https://doi.org/10.1016/j.chemgeo.2020.119696>
- Di Michele W.A., Bashforth A.R., Falcon-Lang H.J., Lucas S.G., (2020). Uplands, lowlands, and climate: Taphonomic megabiases and the apparent rise of a xeromorphic, drought-tolerant flora during the Pennsylvanian-Permian transition. *Palaeogeography, Palaeoclimatology, Palaeoecology* 559, 109965. <https://doi.org/10.1016/j.palaeo.2020.109965>
- Chen J., Shen S.Z., Zhang Y.C., Angiolini L., Gorgij M.N., Crippa G., Wang W., Zhang H., Yuan D.X., Li X.H., Xu Y.G., (2020). Abrupt warming in the latest Permian detected using high-resolution *in situ* oxygen isotopes of conodont apatite from Abadeh, central Iran. *Palaeogeography, Palaeoclimatology, Palaeoecology* 560, 109973. <https://doi.org/10.1016/j.palaeo.2020.109973>
- Grasby S.E., Liu X., Yin R., Ernst R.E., Chen Z. (2020). Toxic mercury pulses into Late Permian terrestrial and marine environments. *Geology*, v. 48, p. 830-833. <https://doi.org/10.1130/G47295.1>
- Huang H., Gao Y., Jones M.M., Tao H., Carroll A.R., Ibarra D.E., Wu H., Wang C., (2020). Astronomical forcing of Middle Permian terrestrial climate recorded in a large paleolake in northwestern China. *Palaeogeography, Palaeoclimatology, Palaeoecology* 550, 109735. <https://doi.org/10.1016/j.palaeo.2020.109735>
- Jurikova H., Gutjahr M., Wallmann K., Flögel S., Liebetrau V., Posenato R., Angiolini L., Garbelli C., Brand U., Wiedenbeck M., Eisenhauer A. (2020). Permian-Triassic mass extinction pulses driven by major marine carbon cycle perturbations. *Nature Geoscience* 13, 745-750. <https://doi.org/10.1038/s41561-020-00646-4>
- Li, Q., Azmy, K., Yang, S., Xu, S.L., Yang D., Zhang, X.H., Chen, H.D., (2020). Early-Middle Permian strontium isotope stratigraphy of marine carbonates from the northern marginal areas of South China: Controlling factors and implications. *Geological Journal*. <https://doi.org/10.1002/gj.4010>
- Li, L., Liao, Z., Lei, L., Lash, G.G., Chen, A., Tan, X., (2020). On the negative carbon isotope excursion across the Wuchiapingian–Changhsingian transition: A regional event in the lower Yangtze region, South China? *Palaeogeography, Palaeoclimatology, Palaeoecology*, 540, 109501. <https://doi.org/10.1016/j.palaeo.2019.109501>.
- Liao Z., Hu W., Cao J., Wang X., Fu X. (2020). Oceanic anoxia through the Late Permian Changhsingian Stage in the Lower Yangtze region, South China: Evidence from sulfur isotopes and trace elements. *Chemical Geology*, 532, 119371. <https://doi.org/10.1016/j.chemgeo.2019.119371>
- Liu Z., Selby D., Zhang H., Shen S., (2020). Evidence for volcanism and weathering during the Permian-Triassic mass extinction from Meishan (South China) osmium isotope record. *Palaeogeography, Palaeoclimatology, Palaeoecology* 553, 109790. <https://doi.org/10.1016/j.palaeo.2020.109790>
- Lu J., Zhang P., Yang M., Shao L., Hilton J. (2020). Continental records of organic carbon isotopic composition ( $\delta^{13}\text{C}_{\text{org}}$ ), weathering, paleoclimate and wildfire linked to the End-Permian Mass Extinction. *Chemical Geology* 558, 119764. <https://doi.org/10.1016/j.chemgeo.2020.119764>
- Pettigrew R.P., Priddy C., Clarke S.M., Warke M.R., Stueken E.E., Claire M.W., (2020). Sedimentology and isotope geochemistry of transitional evaporitic environments within arid continental settings: From erg to saline lakes. *Sedimentology*. <https://doi.org/10.1111/sed.12816>
- Rampino M.R., Baransky E., Rodriguez S., (2020). Proxy evidence from the Gartnerkofel-1 core (Carnic Alps, Austria) for hypoxic conditions in the western Tethys during the end-Permian mass-extinction event. *Chemical Geology* 533, 119434. <https://doi.org/10.1016/j.chemgeo.2019.119434>
- Schobben M., Foster W.J., Sleveland A.R.N., Zuchuat V., Svensen H.H., Planke S., Bond D.P.G., Marcelis F., Newton R.J., Wignall P.B., Poulton S. W. (2020). A nutrient control on marine anoxia during the end-Permian mass extinction. *Nature Geoscience* 13, 640-646. <https://doi.org/10.1038/s41561-020-0622-1>
- Seo, I., Lee Y.I., Ampaiwan T., Kwon H., Kim M.G. (2020). Geochemistry and Nd isotopic composition of the Permian Ko Sire Formation, Phuket Island, Thailand: Implications for

- palaeoclimate and palaeogeographical configuration of the Sibumasu Terrane. *Journal of the Geological Society*, 177(4), 866-881. <https://doi.org/10.1144/jgs2019-170>
- Sial A.N., Chen J., Lacerda L.D., Korte C., Spangenberg J.E., Silva-Tamayo J.C., Gaucher C., Ferreira V.P., Barbosa J.A., Pereira N.S., Benigno A.P. Globally enhanced Hg deposition and Hg isotopes in sections straddling the Permian-Triassic boundary: Link to volcanism. *Palaeogeography, Palaeoclimatology, Palaeoecology* 540, 109537, (2020). <https://doi.org/10.1016/j.palaeo.2019.109537>
- Shen J., Chen J., Algeo T.J., Feng Q., Yu J.; Xu Y.G., Xu G., Lei Y.; Planavsky N.J., Xie S. (2020). Mercury fluxes record regional volcanism in the South China craton prior to the end-Permian mass extinction. *Geology*. <https://doi.org/10.1130/G48501.1>
- Wang W.Q., Garbelli C., Zhang F.F., Zheng Q.F., Zhang Y.C., Yuan D.X., Shi Y.K., Chen B., Shen S.Z., (2020). A high-resolution Middle to Late Permian paleotemperature curve reconstructed using oxygen isotopes of well-preserved brachiopod shells. *Earth and Planetary Science Letters* 540, 116245. <https://doi.org/10.1016/j.epsl.2020.116245>
- Wei H., Geng Z., Zhang X. Guadalupian (Middle Permian) δ<sub>13</sub>C<sub>org</sub> changes in the Lower Yangtze, South China. *Acta Geochim.* 39, 988-1001. <https://doi.org/10.1007/s11631-020-00417-3>
- Xiang L., Zhang H., Schoepfer S.D., Cao C.Q., Zheng Q.F., Yuan D.X., Cai Y.F., Shen S.Z., (2020). Oceanic redox evolution around the end-Permian mass extinction at Meishan, South China. *Palaeogeography, Palaeoclimatology, Palaeoecology* 544, 109626. <https://doi.org/10.1016/j.palaeo.2020.109626>
- Xu Z., Hamilton S.K., Rodrigues S., Baublys K.A., Esterle J.S., Liu Q. Golding S.D., (2020) Palaeoenvironment and palaeoclimate during the late Carboniferous-early Permian in northern China from carbon and nitrogen isotopes of coals. *Palaeogeography, Palaeoclimatology, Palaeoecology* 539, 109490. <https://doi.org/10.1016/j.palaeo.2019.109490>
- Zhang F.F., Shen S.Z., Cui Y., Lenton T.M., Dahl T.W., Zhang H., Anbar A.D., (2020). Two distinct episodes of marine anoxia during the Permian-Triassic crisis evidenced by uranium isotopes in marine dolostones. *Geochimica Et Cosmochimica Acta*, 287, 165-179. <https://doi.org/10.1016/j.gca.2020.01.032>
- Zhang, J., Cao, J., Xia, L., Xiang, B., Li, E., (2020). Investigating biological nitrogen cycling in lacustrine systems by FT-ICR-MS analysis of nitrogen-containing compounds in petroleum. *Palaeogeography, Palaeoclimatology, Palaeoecology*, 556, 109887. <https://doi.org/10.1016/j.palaeo.2020.109887>.
- Zhang B., Yao S., Mills B.J.W., Wignall P.B., Hu W., Liu B., Ren Y., Li L., Shi G., (2020). Middle Permian organic carbon isotope stratigraphy and the origin of the Kamura Event. *Gondwana Research* 79, 217-232. <https://doi.org/10.1016/j.gr.2019.09.013>
- Zheng X., Dai S., Nechaev V., Sun R. (2020). Environmental perturbations during the latest Permian: Evidence from organic carbon and mercury isotopes of a coal-bearing section in Yunnan Province, southwestern China. *Chemical Geology* 549, 119680. <https://doi.org/10.1016/j.chemgeo.2020.119680>
- ## Paleoecology and paleoenvironments
- Candido M., Cagliari J., Lavina E.L. (2020). Tidal circulation in an Early Permian epicontinental sea: Evidence of an amphidromic system. *Palaeogeography, Palaeoclimatology, Palaeoecology* 546, 109671. <https://doi.org/10.1016/j.palaeo.2020.109671>
- Cribb A.T., Bottjer D.J. (2020). Complex marine bioturbation ecosystem engineering behaviors persisted in the wake of the end-Permian mass extinction. *Scientific Reports* 10, 203. <https://doi.org/10.1038/s41598-019-56740-0>
- Dong, Y., Xu, S., Wen, L., Chen, H., Fu, S., Zhong, Y., Wang, J., Zhu, P., Cui, Y., (2020). Tectonic control of Guadalupian-Lopingian cherts in northwestern Sichuan Basin, South China. *Palaeogeography, Palaeoclimatology, Palaeoecology*, 557, 109915. <https://doi.org/10.1016/j.palaeo.2020.109915>.
- Feng Z., Wei H.B., Guo Y., He X.Y., Sui Q., hou Y., Liu H.Y., Gou X.D., Lv Y. (2020). From rainforest to hermland: New insights into land plant responses to the end-Permian mass extinction. *Earth-Science Reviews* 204, 103153. <https://doi.org/10.1016/j.earscirev.2020.103153>
- Gao P., He Z., Lash G.G., Li S., Xiao X., Han Y., Zhang R., (2020). Mixed seawater and hydrothermal sources of nodular chert in Middle Permian limestone on the eastern Paleo-Tethys margin (South China). *Palaeogeography, Palaeoclimatology, Palaeoecology* 551, 109740. <https://doi.org/10.1016/j.palaeo.2020.109740>
- Gulbranson E.L., Cornamusini G., Ryberg P.E., Corti V. (2020). When does large woody debris influence ancient rivers? Dendrochronology applications in the Permian and Triassic, Antarctica. *Palaeogeography, Palaeoclimatology, Palaeoecology* 541, 109544. <https://doi.org/10.1016/j.palaeo.2019.109544>
- Luo M., Shi G.R., Lee S. (2020). Stacked Parahaentzschelinia ichnofabrics from the Lower Permian of the southern Sydney Basin, southeastern Australia: Palaeoecologic and palaeoenvironmental significance. *Palaeogeography, Palaeoclimatology, Palaeoecology* 541, 109538. <https://doi.org/10.1016/j.palaeo.2019.109538>
- Luo, M., Shi, G.R., Buatois, L.A., Chen, Z.Q., (2020). Trace fossils as proxy for biotic recovery after the end-Permian mass extinction: A critical review' *Earth-Science Reviews*, Volume 203,103059. <https://doi.org/10.1016/j.earscirev.2019.103059>.
- Matheson E.J., Frank T.D. (2020). An epeiric glass ramp: Permian low-latitude neritic siliceous sponge colonization and its novel preservation (Phosphoria Rock Complex). *Sedimentary Geology* 399, 105568. <https://doi.org/10.1016/j.sedgeo.2019.105568>
- Matheson, E.J., Frank, T.D. (2020). Phosphorites, glass ramps and carbonate factories: The evolution of an epicontinental sea and a Late Palaeozoic upwelling system (phosphoria rock complex). *Sedimentology*, 67(6), 3003-3041. <https://doi.org/10.1111/sed.12731>
- McLoughlin S., Mays C., Vajda V., Bocking M., Frank T.D., Fielding C.R. (2020). Dwelling in the dead zone - vertebrate burrows immediately succeeding the End-Permian Extinction

- event in Australia 35, 342-357. <https://doi.org/10.2110/palo.2020.007>
- Pan Y., Huang Z., Li T., Guo X., Xu X., Chen X. (2020). Environmental response to volcanic activity and its effect on organic matter enrichment in the Permian Lucaogou Formation of the Malang Sag, Santanghu Basin, Northwest China. *Palaeogeography, Palaeoclimatology, Palaeoecology* 560, 110024. <https://doi.org/10.1016/j.palaeo.2020.110024>
- Shan X., Yu X.H., Jin L., Li Y.L., Tan C.P., Li S.L., Wang J.H. (2020). Bed type and flow mechanism of deep water sub-lacustrine fan fringe facies: an example from the Middle Permian Lucaogou Formation in Southern Junggar Basin of NW China. *Petroleum Science* <https://doi.org/10.1007/s12182-020-00534-x>
- Sun F., Hu W., Wang X., Cao J., Fu B., Wu H., Yang S. (2020). Methanogen microfossils and methanogenesis in Permian lake deposits. *Geology*, 49 (1): 13–18. <https://doi.org/10.1130/G47857.1>
- Vajda V., McLoughlin S., Mays C., Frank T.D., Fielding C.R., Tevyaw A., Lehsten V., Bocking M., Nicoll R.S. (2020). End-Permian (252 Mya) deforestation, wildfires and flooding—An ancient biotic crisis with lessons for the present. *Earth and Planetary Science Letters* 529, 115875. <https://doi.org/10.1016/j.epsl.2019.115875>
- Wang W., Jiang Z., Xie X., Guo J., Yang Y. (2020). Sedimentary characteristics and interactions among volcanic, terrigenous and marine processes in the Late Permian Kuishan Member, Eastern Block of the North China Craton. *Sedimentary Geology* 407, 105741. <https://doi.org/10.1016/j.sedgeo.2020.105741>
- Yan Z., Liu J., Jin X., Shi Y., Tian K., Wang H. (2020). Evolution pattern of Early Permian carbonate buildups: With reference to the carbonate mounds in eastern Inner Mongolia, North China. *Sedimentary Geology*, 409, 105775. <https://doi.org/10.1016/j.sedgeo.2020.105775>
- Zhang L.J., Fan R.Y., Dang Z.Y., Gong Y.M. (2020). The youngest known Dictyodora from the Late Permian (Lopingian) deep sea in West Qinling, central China. *Palaeogeography, Palaeoclimatology, Palaeoecology* 558, 109948. <https://doi.org/10.1016/j.palaeo.2020.109948>
- Zhang X.Y., Zheng Q.F., Li Y., Yang H.Q., Zhang H., Wang W.Q., Shen S.Z., (2020). Polybessurus-like fossils as key contributors to Permian-Triassic boundary microbialites in South China. *Palaeogeography, Palaeoclimatology, Palaeoecology* 552, 109770. <https://doi.org/10.1016/j.palaeo.2020.109770>
- Zuchuat V., Sleveland A.R.N., Twitchett R.J., Svensen H.H., Turner H., Augland L.E., Jones M.T., Hammer Ø., Hauksson B.T., Haflidason H., Midtkandal I., Planke S., (2020). A new high-resolution stratigraphic and palaeoenvironmental record spanning the End-Permian Mass Extinction and its aftermath in central Spitsbergen, Svalbard. *Palaeogeography, Palaeoclimatology, Palaeoecology* 554, 109732. <https://doi.org/10.1016/j.palaeo.2020.109732>
- Campbell M.J., Rosenbaum G., Allen C.M., Mortimer N. (2020). Origin of dispersed Permian-Triassic fore-arc basin terranes in New Zealand: Insights from zircon petrochronology. *Gondwana Research* 78, 210-227. <https://doi.org/10.1016/j.gr.2019.08.010>
- Hou Z.S., Fan J.X., Henderson C.M., Yuan D.X., Shen B.H., Wu J., Wang Y., Zheng Q.F., Zhang Y.C., Wu Q., Shen S.Z. (2020). Dynamic palaeogeographic reconstructions of the Wuchiapingian Stage (Lopingian, Late Permian) for the South China Block. *Palaeogeography, Palaeoclimatology, Palaeoecology* 546, 109667. <https://doi.org/10.1016/j.palaeo.2020.109667>
- Huang, H., Gao, Y., Jones, M.M., Tao, H., Carroll, A.R., Ibarra, D.E., Wu, H., Wang, C., (2020). Astronomical forcing of Middle Permian terrestrial climate recorded in a large paleolake in northwestern China. *Palaeogeography, Palaeoclimatology, Palaeoecology*, 550,109735, <https://doi.org/10.1016/j.palaeo.2020.109735>.
- Kent, D.V., Muttoni, G., Pangea B and the Late Paleozoic Ice Age. *Palaeogeography, Palaeoclimatology, Palaeoecology*. 553,109753. [https://doi.org/10.1016/j.palaeo.2020.109753.](https://doi.org/10.1016/j.palaeo.2020.109753)
- Tang W., Zhang Y., Pe-Piper G., Piper D.J.W., Guo Z., Li W. (2020). Soft-sediment deformation structures in alkaline lake deposits of Lower Permian Fengcheng Formation, Junggar Basin, NW China: Implications for syn-sedimentary tectonic activity. *Sedimentary Geology* 406, 105719. <https://doi.org/10.1016/j.sedgeo.2020.105719>
- Wang X., Shao L., Eriksson K.A., Yan Z., Wang J., Li H., Zhou R., Lu J. (2020). Evolution of a plume-influenced source-to-sink system: An example from the coupled central Emeishan Large Igneous Province and adjacent western Yangtze cratonic basin in the Late Permian, SW China. *Earth-Science Reviews* 207, 103224. <https://doi.org/10.1016/j.earscirev.2020.103224>

## Vertebrate paleontology (excluding conodonts)

- Agliano, A., Sander, P.M., Wintrich, T. (2020). Bone histology and microanatomy of *Edaphosaurus* and *Dimetrodon* (Amniota, Synapsida) vertebrae from the Lower Permian of Texas. *Anatomical Record-Advances in Integrative Anatomy and Evolutionary Biology*. <https://doi.org/10.1002/ar.24468>
- Alves, Y.M., Gama, J.M., Cupello, C. (2020). Palaeoniscoid remains from the Lower Permian Pedra De Fogo Formation (Parnaiba basin): Insights from general morphology and histology. *Historical Biology*. <https://doi.org/10.1080/08912963.2020.1754815>
- Bakaev, A., Kogan, I. (2020). A new species of *Burguklia* (Pisces, Actinopterygii) from the Middle Permian of the Volga Region (European Russia). *Palz*, 94(1), 93-106. <https://doi.org/10.1007/s12542-019-00487-6>
- Bakaev, A.S. (2020). A new morphotype of fish teeth of the order Eurynotoidiformes (Actinopterygii) from the Upper Permian deposits of European Russia. *Paleontological Journal*, 54(2), 171-179. <https://doi.org/10.1134/S0031030120020033>
- Bakaev, A.S., Kogan, I., Yankevich, D.I. (2020). On the validity of names of some Permian Actinopterygians from European

## Paleogeography and tectonics

- Russia. Neues Jahrbuch Fur Geologie Und Palaontologie-Abhandlungen, 296(3), 305-316. <https://doi.org/10.1127/njgpa/2020/0907>
- Francischini, H., Lucas, S.G., Voigt, S., Marchetti, L., Santucci, V. L., Knight, C. L., Schultz, C. L. (2020). On the presence of *Ichniotherium* in the Coconino Sandstone (Cisuralian) of the Grand Canyon and remarks on the occupation of deserts by non-amniote tetrapods. *Palz*, 94(1), 207-225. <https://doi.org/10.1007/s12542-019-00450-5>
- Gastaldo, R. A., Neveling, J. (2020). Discussion of "Permian-Triassic vertebrate footprints from south Africa: Ichnotaxonomy, producers and biostratigraphy through two major faunal crises" By Marchetti, L., Klein, H., Buchwitz, M., Ronchi, A., Smith, R.M.H., Deklerk, W.J., Sciscio, L., and Groenewald, G.H. (2019). *Gondwana Research*, 78, 375-378. <https://doi.org/10.1016/j.gr.2019.08.003>
- Gastaldo, R.A., Kus, K., Tabor, N., Neveling, J. (2020). Calcic Vertisols in the upper *Daptocephalus* Assemblage Zone, Balfour Formation, Karoo Basin, South Africa: Implications for Late Permian Climate. *Journal of Sedimentary Research* 90, 609-628. <https://doi.org/10.2110/jsr.2020.32>
- Gastaldo, R.A., Kamo, S.L., Neveling, J., Gastaldo, R.A., Kamo, S.L., Neveling J., Geissman, J.W., Looy, C.V., Martini A.M. (2020). The base of the *Lystrosaurus* Assemblage Zone, Karoo Basin, predates the end-Permian marine extinction. *Nat. Commun.* 11, 1428. <https://doi.org/10.1038/s41467-020-15243-7>
- Huttenlocker, A.K., Shelton, C.D. (2020). Bone histology of varanopids (Synapsida) from Richards Spur, Oklahoma, sheds light on growth patterns and lifestyle in early terrestrial colonizers. *Philosophical Transactions of the Royal Society B-Biological Sciences*, 375(1793). <https://doi.org/10.1098/rstb.2019.0142>
- Huttenlocker, A.K., Sidor, C.A. (2020). A basal non-mammaliaform Cynodont from the Permian of Zambia and the Origins of Mammalian Endocranial and Postcranial Anatomy. *Journal of Vertebrate Paleontology*. <https://doi.org/10.1080/02724634.2020.1827413>
- Ivanov, A.O., Nestell, M.K., Nestell, G.P., Bell, G.L. (2020). New fish assemblages from the Middle Permian from the Guadalupe Mountains, West Texas, USA. *Palaeoworld*, 29(2), 239-256. <https://doi.org/10.1016/j.palwor.2018.10.003>
- Kato, K.M., Rega, E.A., Sidor, C.A., Huttenlocker, A.K. (2020). Investigation of a bone lesion in a gorgonopsian (Synapsida) from the Permian of Zambia and periosteal reactions in fossil non-mammalian tetrapods. *Philosophical Transactions of the Royal Society B-Biological Sciences*, 375(1793). <https://doi.org/10.1098/rstb.2019.0144>
- Liu, J., Abdala, F. (2020). The tetrapod fauna of the Upper Permian Naobaogou Formation of China: 5. *Caodeyao liuyufengi* gen. et sp. nov., a new peculiar therocephalian. *PeerJ*, 8. <https://doi.org/10.7717/peerj.9160>
- Marchetti, L., Klein, H., Buchwitz, M., Ronchi, A., Smith, R.M.H., De Klerk, W.J., Groenewald, G.H. (2020). Reply to discussion of "Permian-Triassic vertebrate footprints from south Africa: Ichnotaxonomy, producers and biostratigraphy through two major faunal crises" By Marchetti, L., Klein, H., Buchwitz, M., Ronchi, A., Smith, R.M.H., Deklerk, W.J., Sciscio, L., Groenewald, G.H., (2019). *Gondwana Research*, 78, 379-383. <https://doi.org/10.1016/j.gr.2019.08.002>
- Marchetti, L., Voigt, S., Mujal, E., Lucas, S.G., Francischini, H., Fortuny, J., Santucci, V.L. (2020). Extending the footprint record of Pareiasauromorpha to the Cisuralian: Earlier appearance and wider palaeobiogeography of the group. *Papers in Palaeontology*. <https://doi.org/10.5061/dryad.h9w0vt4g3>
- Sennikov, A.G., Bulanov, V.V., Scholze, F. (2020). Coprolite with Conchostracans from the Terminal Permian of Central Russia-Paleobiological and Stratigraphic Significance. *Paleontological Journal*, 54(1), 6-13. <https://doi.org/10.1134/S0031030120010098>
- Stamberg, S. (2020). Teeth of actinopterygians from the Permo-Carboniferous of the Bohemian Massif with special reference to the teeth of Aeduellidae and Amblypteridae. *Bulletin of Geosciences*, 95(4), 369-389. <https://doi.org/10.3140/bull.geosci.1799>
- Rey K., Day M.O., Amiot R., Fourel F., Luyt J., Lécuyer C. (2020). Rubidge B.S. Stable isotopes ( $\delta^{18}\text{O}$  and  $\delta^{13}\text{C}$ ) give new perspective on the ecology and diet of *Endothiodon bathystoma* (Therapsida, Dicynodontia) from the Late Permian of the South African Karoo Basin. *Palaeogeography, Palaeoclimatology, Palaeoecology* 556, 109882. <https://doi.org/10.1016/j.palaeo.2020.109882>
- Rey, K., Day, M.O., Amiot, R., Fourel, F., Luyt, J., Van den Brandt, M.J., Lécuyer, C., Rubidge, B.S. (2020). Oxygen isotopes and ecological inferences of Permian (Guadalupian) tetrapods from the main Karoo Basin of South Africa. *Palaeogeography, Palaeoclimatology, Palaeoecology*, 538, 109485. <https://doi.org/10.1016/j.palaeo.2019.109485>
- Mujal E., Marchetti L. (2020). *Ichniotherium* tracks from the Permian of France, and their implications for understanding the locomotion and palaeobiogeography of large diadectomorphs. *Palaeogeography, Palaeoclimatology, Palaeoecology* 547, 109698. <https://doi.org/10.1016/j.palaeo.2020.109698>

## Conodonts

- Golding, M.L., McMillan, R. (2020). The impacts of diagenesis on the geochemical characteristics and color alteration index of conodonts. *Palaeobiodiversity and Palaeoenvironments*. <https://doi.org/10.1007/s12549-020-00447-y>
- Lara-Pena, R.A., Navas-Parejo, P., Amaya-Martinez, R. (2020). New conodont data related to the western Ouachita-Marathon-Sonora orogen: Age of the autochthonous Laurentian deformation. *Journal of South American Earth Sciences*, 103. <https://doi.org/10.1016/j.jsames.2020.102763>
- Metcalf, I., Crowley, J.L. (2020). Upper Permian and Lower Triassic conodonts, high-precision U-Pb zircon ages and the Permian-Triassic boundary in the Malay Peninsula. *Journal of Asian Earth Sciences*, 199. <https://doi.org/10.1016/j.jseas.2020.104403>
- Petryshen, W., Henderson, C.M., De Baets, K., Jarochowska,

- E. (2020). Evidence of parallel evolution in the dental elements of *Sweetognathus* conodonts. Proceedings of the Royal Society B-Biological Sciences, 287(1939). <https://doi.org/10.1098/rspb.2020.1922>
- Ritter, S.M. (2020). Improved conodont biostratigraphic constraint of the Carboniferous/Permian boundary in South-Central New Mexico, USA. Stratigraphy, 17(1), 39-56. <https://doi.org/10.29041/strat.17.1.39-56>
- Sun, Z.Y., Liu, S., Ji, C., Jiang, D.Y., Zhou, M. (2020). Synchrotron-aided reconstruction of the prioniodinid multielement conodont apparatus (*Hadrodontina*) from the Lower Triassic of China. Palaeogeography Palaeoclimatology Palaeoecology, 560. <https://doi.org/10.1016/j.palaeo.2020.109913>
- Yuan D.X., Aung K.P., Henderson C.M., Zhang Y.C., Zaw T., Cai F., Ding L., Shen S.Z. (2020). First records of Early Permian conodonts from eastern Myanmar and implications of paleobiogeographic links to the Lhasa Block and northwestern Australia. Palaeogeography, Palaeoclimatology, Palaeoecology 549, 109363. <https://doi.org/10.1016/j.palaeo.2019.109363>

## Foraminifera and algae

- Arefifard, S., Payne, J. L. (2020). End-Guadalupian extinction of larger fusulinids in Central Iran and implications for the global biotic crisis. Palaeogeography Palaeoclimatology Palaeoecology, 550. <https://doi.org/10.1016/j.palaeo.2020.109743>
- Chen, W.H., Wang, Y.B., Huang, Y.F., Wang, T., Yi, Z.X., Kiessling, W. (2020). Reef-building red algae from an uppermost Permian reef complex as a fossil analogue of modern coralline algal ridges. Facies, 66(4). <https://doi.org/10.1007/s10347-020-00606-9>
- Fassihi, S., Vachard, D., Esfahani, F.S. (2020). Taxonomic composition of the latest Carboniferous-earliest Permian smaller foraminifers in the Sanandaj-Sirjan Zone, Iran: New insights about palaeobiogeography, palaeoclimate and paleoecology of the northern margin of the Palaeotethys. Journal of Asian Earth Sciences, 193. <https://doi.org/10.1016/j.jseas.2020.104310>
- Feng, Y., Song, H.J., Bond, D.P.G. (2020). Size variations in foraminifers from the Early Permian to the Late Triassic: Implications for the Guadalupian-Lopingian and the Permian-Triassic mass extinctions. Paleobiology, 46(4), 511-532. <https://doi.org/10.1017/pab.2020.37>
- Grigoryan, G., Danelian, T., Vachard, D., Tsourou, T., Zambetakis-Lekkas, A. (2020). Calcareous algae and foraminifera from the Upper Capitanian/Lower Wuchiapingian (Middle/Upper Permian) transitional carbonates of the Chios Island (Greece). Biostratigraphic and paleogeographic implications. Revue De Micropaleontologie, 68. <https://doi.org/10.1016/j.revmic.2020.100409>
- Haghigat, N., Hashemi, H., Tavakoli, V., Nestell, G.P., (2020). Permian-Triassic extinction pattern revealed by foraminifers and geochemical records in the central Persian Gulf, southern Iran. Palaeogeography, Palaeoclimatology, Palaeoecology, 543, <https://doi.org/10.1016/j.palaeo.2020.109588>.
- Huang, H., Jin, X.C., Shi, Y.K. (2020). Permian fusulinid *Rugososchwagerina* (*Xiaoxinzhaiella*) from the Shan Plateau, Myanmar: Systematics and paleogeography. Journal of Foraminiferal Research, 50(1), 11-24. <https://doi.org/10.2113/gsjfr.50.1.11>
- Huang, H., Jin, X.C., Shi, Y.K., Wang, H.F., Zheng, J.B., Zong, P. (2020). Fusulinid-bearing oolites from the Tengchong Block in Western Yunnan, SW China: Early Permian warming signal in the eastern peri-gondwana. Journal of Asian Earth Sciences, 193. <https://doi.org/10.1016/j.jseas.2020.104307>
- Ketwetsuriya, C., Nose, M., Charoentitirat, T., Nutzel, A. (2020). Microbial-, fusulinid limestones with large gastropods and calcareous algae: An unusual facies from the early Permian Khao Khad Formation of Central Thailand. Facies, 66(4). <https://doi.org/10.1007/s10347-020-00605-w>
- Kulagina, E.I., Filimonova, T.V. (2020). Taxonomy and evolution of Visean-Roadian (Late Mississippian-Guadalupian) Lasiodiscidae. Journal of Foraminiferal Research, 50(2), 141-173. <https://doi.org/10.2113/gsjfr.50.2.141>
- Leven, E.J., Yarahmadzahi, H. (2020). Fusulinids from the Lower Permian Emarat Formation, Gaduk section, Central Alborz, Iran. Stratigraphy and Geological Correlation, 28(2), 167-176. <https://doi.org/10.1134/S0869593820020033>
- Liu X., Song H., Bond D.P.G., Tong J., Benton M.J. (2020). Migration controls extinction and survival patterns of foraminifers during the Permian-Triassic crisis in South China. Earth-Science Reviews 209, 103329. <https://doi.org/10.1016/j.earscirev.2020.103329>
- Okuyucu, C., Tekin, U. K., Bedi, Y., Sayit, K. (2020). Biostratigraphy of Lower Permian foraminiferal assemblages from platform-slope carbonate blocks within the Mersin Melange, Southern Turkey: Paleogeographical implications. Geobios, 59, 61-77. <https://doi.org/10.1016/j.geobios.2020.02.001>
- Shahinfar, S., Yeganeh, B. Y., Arefifard, S., Vachard, D., Payne, J.L. (2020). Refined foraminiferal biostratigraphy of upper Wordian, Capitanian, and Wuchiapingian strata in Hambast Valley, Abadeh Region (Iran), and paleobiogeographic implications. Geological Journal, 55(9), <https://doi.org/10.1002/gj.3798>
- Wahlman, G.P., Vaughan, G., Nestell, M. (2020). Fusulinids from slope debris flow beds in The word Formation (Guadalupian, Middle Permian), Gilleland Canyon, Northwestern Glass Mountains, West Texas. Micropaleontology, 66(6), 469-490. <https://doi.org/10.47894/mpal.66.6.01>
- Zhang, Y.C., Aung, K.P., Shen, S.Z., Zhang, H., Zaw, T., Ding, L., Cai, F.L., Sein, K., (2020). Middle Permian fusulines from the Thitsipin Formation of Shan State, Myanmar and their palaeobiogeographical and palaeogeographical implications. Papers in Palaeontology, 6(2), 293-327. <https://doi.org/10.1002/spp2.1298>

## Brachiopods, bivalve and other invertebrates

- Garcia-Ramos, D.A., Coric, S., Joachimski, M.M., Zuschin, M., (2020). The environmental factors limiting the distribution of shallow-water terebratulid brachiopods. Paleobiology, 46(2),

- 193-217. <https://doi.org/10.1017/pab.2020.11>
- Hernandez, J.A.R. (2020). *Linnaeocaninella* nomen novum for the Middle Permian fossil Caninella Liang, 1990 (Brachiopoda: Productida: Richthofenidae), preoccupied by Caninella Gorsky, 1938 (Cnidaria: Anthozoa: Bothrophyllidae). *Zootaxa*, 4732(2), 335-336. <https://doi.org/10.11646/zootaxa.4732.2.9>
- Makoshin, V.I., Kutygin, R.V. (2020). Asselian-Sakmarian (Lower Permian) brachiopod zonation of the Verkhoyansk Region, Northeast Russia. *Stratigraphy and Geological Correlation*, 28(7), 716-744. 10.1134/s0869593820040061
- Samira, T.N., Payman, R., Reza, M.H., Mohammad, K., (2020). Shell concentrations analysis in the Lower Permian carbonate rocks (Khan Formation) in Central Iran (Kalmard Area). *Historical Biology*, 32(6), 789-802. <https://doi.org/10.1080/08912963.2018.1539969>
- Saravia, P.D., Gonzalez, C.R., (2020). New Pennsylvanian Bivalvia (Mollusca), the Early Permian glaciation and the Carboniferous-Permian boundary in Western Argentina. *Palz*, 94(4), 675-695. <https://doi.org/10.1007/s12542-020-00517-8>
- Shi, G.R., Waterhouse, J.B., Lee, S.M., (2020). Early Permian brachiopods from the Pebby Beach Formation, southern Sydney Basin, Southeastern Australia. *Alcheringa*, 44(3), 411-429. <https://doi.org/10.1080/03115518.2020.1810773>
- Song, J.J., Qie, W.K., Luo, M., Guo, W., Gong, Y.M., (2020). Evolution of the genus *Cribroconcha* Cooper, 1941 (Ostracoda, Crustacea) in relationship to palaeoecological changes during the late Palaeozoic. *Palaeogeography, Palaeoclimatology, Palaeoecology*, 560, 110028. <https://doi.org/10.1016/j.palaeo.2020.110028>.
- Wu, H.T., Zhang, Y., Stubbs, T.L., Liu, J.Q., Sun, Y.L. (2020). A new Changhsingian (Lopingian) brachiopod fauna of the shallow-water clastic shelf facies from Fujian province, South-Eastern China. *Papers in Palaeontology*. <https://doi.org/10.1002/spp.2.1318>
- Wu, H.T., Zhang, Y., Stubbs, T.L., Sun, Y.L. (2020). Changhsingian brachiopod communities along a marine depth gradient in South China and their ecological significance in the end-Permian mass extinction. *Lethaia*, 53(4), 515-532. <https://doi.org/10.1111/let.12373>
- ## Palaeobotany and Palynology
- Blomenkemper, P., Kerp, H., Abu Hamad, A., Bomfleur, B. (2020). Contributions towards whole-plant reconstructions of *Dicroidium* plants (Umkomasiaceae) from the Permian of Jordan. *Review of Palaeobotany and Palynology*, 278. <https://doi.org/10.1016/j.revpalbo.2020.104210>
- da Conceição, D.M., Crisafulli, A., Iannuzzi, R., Neregato, R., Cisneros, J.C., de Andrade, L.Z., (2020). New petrified gymnosperms from the Permian of Maranhão (Pedra de Fogo Formation), Brazil: Novaiorquepitys and Yvyrapitys. *Review of Palaeobotany and Palynology*, 276, 104177. <https://doi.org/10.1016/j.revpalbo.2020.104177>
- Feng, Z., Wang, J., Zhou, W.M., Wan, M.L., Pšenička, J., (2020). Plant-insect interactions in the early Permian Wuda Tuff Flora, North China. *Review of Palaeobotany and Palynology*. <https://doi.org/10.1016/j.revpalbo.2020.104269>.
- Gibson, M.E., Taylor, W.A., Wellman, C.H. (2020). Wall ultrastructure of the Permian pollen grain *Lueckisporites virkkiae* Potonié et Klaus 1954 emend. Clarke 1965: Evidence for botanical affinity. *Review of Palaeobotany and Palynology*, 275. <https://doi.org/10.1016/j.revpalbo.2020.104169>
- Guo, Y., Zhou, Y., Pšenička, J., Bek, J., Yang, S.L., Feng, Z., (2020). Reinvestigation of the marattialean *Zhutheca densata* (Gu et Zhi) Liu, Li et Hilton from the Lopingian of Southwest China, and its evolutionary implications. *Review of Palaeobotany and Palynology*, 282, 104310. <https://doi.org/10.1016/j.revpalbo.2020.104310>.
- He, X. Y., Spencer, A. R. T., Wang, S. J., Hilton, J. Hydrasperm pteridosperm ovules from the Permian of China: palaeoecological and palaeobiogeographic implications. *Historical Biology*. <https://doi.org/10.1080/08912963.2020.1867125>
- He, X., Zhou, W., Li, D., Wang, S., Hilton, J., Wang, J., (2020). A 298-million-year-old gleicheniaceous fern from China, *Review of Palaeobotany and Palynology*. <https://doi.org/10.1016/j.revpalbo.2020.104355>.
- Liu, F., Peng, H. P., Bomfleur, B., Kerp, H., Zhu, H.C., Shen, S.Z. (2020). Palynology and vegetation dynamics across the Permian-Triassic boundary in southern Tibet. *Earth-Science Reviews*, 209. <https://doi.org/10.1016/j.earscirev.2020.103278>
- Liu, L., Pšenička, J., Bek, J., Wan, M., Pfefferkorn, H.W., Wang, J., (2020). A whole calamitacean plant *Palaeostachya guanglongii* from the Asselian (Permian) Taiyuan Formation in the Wuda Coalfield, Inner Mongolia, China, *Review of Palaeobotany and Palynology*. <https://doi.org/10.1016/j.revpalbo.2020.104245>.
- Murthy, S., Aggarwal, N., Saxena, A. (2020). Early Permian floral diversity and paleoenvironment of the West Bokaro Coalfield, Damodar basin, India. *Journal of the Palaeontological Society of India*, 65(1), 1-14. <https://doi.org/10.1007/s12549-019-00375-6>
- Opluštil, S., Wang, J., Pfefferkorn, H.W., Pšenička, J., Bek, J., Libertín, M., Wang, J., Wan, M., He, X., Yan, M., Wei, H., Frojdová, J.V., (2020). Early Permian coal-forest preserved in situ in volcanic ash bed in the Wuda Coalfield, Inner Mongolia, China. *Review of Palaeobotany and Palynology*. <https://doi.org/10.1016/j.revpalbo.2020.104347>.
- Saxena, A., Murthy, S., Singh, K.J. (2020). Floral diversity and environment during the Early Permian: a case study from Jarangdih Colliery, East Bokaro Coalfield, Damodar Basin, India. *Palaeobiodiversity and Palaeoenvironments*, 100(1), 33-50. <https://doi.org/10.1007/s12549-019-00375-6>
- Stephenson, M.H., Korggreen, D., (2020). Palynological correlation of the Arqov and Saad formations of the Negev, Israel, with the Umm Irna Formation of the eastern Dead Sea, Jordan, *Review of Palaeobotany and Palynology*, Volume 274. DOI: 10.1016/j.revpalbo.2019.104153
- Wan, M. Shi, G.R., Luo M., Lee, S., Wang, J., (2020). First record of a petrified gymnospermous wood from the Kungurian (late Early Permian) of the southern Sydney Basin, southeastern

Australia, and its paleoclimatic implications. Review of Palaeobotany and Palynology, 276, 104202. <https://doi.org/10.1016/j.revpalbo.2020.104202>

Zavialova, N., Blomenkemper, P., Kerp, H., Abu Hamad, A., Bomfleur, B.A Lyginopterid pollen organ from the upper Permian of the Dead Sea region. *Grana*. <https://doi.org/10.1080/00173134.2020.1772360>

## Resources

Busch, B., Hilgers, C., Adelmann, D. (2020). Reservoir quality controls on Rotliegend fluvio-aeolian wells in Germany and the Netherlands, Southern Permian Basin - Impact of grain coatings and cements. *Marine and Petroleum Geology* 112, 104075. <https://doi.org/10.1016/j.marpetgeo.2019.104075>

Cai L., Guo X., Zhang X., Zenga Z., Xiao G., Pang Y., Wang S. (2020). Pore-throat structures of the Permian Longtan Formation tight sandstones in the South Yellow Sea Basin, China: A case study from borehole CSDP-2. *Journal of Petroleum Science and Engineering* 186, 106733. <https://doi.org/10.1016/j.petrol.2019.106733>

Kotarba, M.J., Bilkiewicz E., Kosakowski P. (2020). Origin of hydrocarbon and non-hydrocarbon (H<sub>2</sub>S, CO<sub>2</sub> and N<sub>2</sub>) components of natural gas accumulated in the Zechstein Main Dolomite carbonate reservoir of the western part of the Polish sector of the Southern Permian Basin. *Chemical Geology* 554, 119807. <https://doi.org/10.1016/j.chemgeo.2020.119807>

Latyshev, A.V., Rad'ko, V.A., Veselovskiy, R.V., Fetisova A.M., Pavlov, V.E. (2020). Correlation of the Permian-Triassic Ore-

Bearing Intrusions of the Norilsk Region with the Volcanic Sequence of the Siberian Traps Based on the Paleomagnetic Data. *Economic Geology* 115, 1173-1193. <https://doi.org/10.5382/econgeo.4746>

Liu B., Song Y., Zhu K., Su P., Ye X., Zhao W. (2020). Mineralogy and element geochemistry of salinized lacustrine organic-rich shale in the Middle Permian Santanghu Basin: Implications for paleoenvironment, provenance, tectonic setting and shale oil potential. *Marine and Petroleum Geology* 120, 104569. <https://doi.org/10.1016/j.marpetgeo.2020.104569>

Sahlström, F., Chang, Z., Arribas, A., Dirks, P., Johnson, C.A., Huizenga, J.M., Corral I. (2020). Reconstruction of an Early Permian Sublacustrine Magmatic-Hydrothermal System: Mount Carlton Epithermal Au-Ag-Cu Deposit, Northeastern Australia. *Economic Geology* 115, 129-152. <https://doi.org/10.5382/econgeo.4696>

Sośnicka, M., Lüders, V. (2020). Fluid inclusion evidence for low-temperature thermochemical sulfate reduction (TSR) of dry coal gas in Upper Permian carbonate reservoirs (Zechstein, Ca2) in the North German Basin. *Chemical Geology* 534, 119453. <https://doi.org/10.1016/j.chemgeo.2019.119453>

Xiao D., Cao J., Luo B., Zhang Y., Xie C., Chen S., Gao G., Tan X. (2020). Mechanism of ultra-deep gas accumulation at thrust fronts in the Longmenshan Mountains, Lower Permian Sichuan Basin, China. *Journal of Natural Gas Science and Engineering* 83, 103533. <https://doi.org/10.1016/j.jngse.2020.103533>

---

## SUBMISSION GUIDELINES FOR ISSUE 71

It is best to submit manuscripts as attachments to E-mail messages. Please send messages and manuscripts to Yichun Zhang's E-mail address. Hard copies by regular mail do not need to be sent unless requested. To format the manuscript, please follow the TEMPLATE that you can find on the SPS webpage at <http://permian.stratigraphy.org/>.

Please submit figures files at high resolution (600dpi) separately from text one. Please provide your E-mail addresses in your affiliation. All manuscripts will be edited for consistent use of English only.

Prof. Yichun Zhang (SPS secretary)

Nanjing Institute of Geology and Palaeontology, Chinese Academy of Sciences, Nanjing, Jiangsu, 210008, P.R.China, Email: [yczhang@nigpas.ac.cn](mailto:yczhang@nigpas.ac.cn)

**The deadline for submission to Issue 71 is July, 31th, 2021**

| Age (Ma) | Series/stage             | Magnetic polarity units | Conodonts |  | Fusulines   | Radiolarians  |
|----------|--------------------------|-------------------------|-----------|--|---|---|
|          |                          |                         |           |  |   |   |
| 250      | Triassic                 | Lopingian               | I2        | <i>Isarcicella isarcica</i>  |   |   |
| 252      |                          |                         | I1        | <i>Hindeodus parvus</i>  |   |   |
| 254      |                          |                         | LP3       | <i>Clarkina changxingensis</i>   | <i>Palaeofusulina sinensis</i>                                  | Unzoned   |
| 254      |                          |                         | LP2r      | <i>Clarkina subcarinata</i>  | <i>Palaeofusulina minima</i>                                    | <i>Albaillella yaoi</i> <i>Neocalbaillella optima</i>               |
| 254      |                          |                         | LP2n      | <i>Clarkina wangii</i>   |   | <i>Albaillella triangulata</i> <i>Neocalbaillella ornithoformis</i> |
| 256      |                          |                         | LP1       | <i>C. longicupidata</i>  | <i>Gallowayinella meitiensis</i>                                |   |
| 258      |                          |                         | LP1.1r    | <i>Clarkina orientalis</i>   |   | <i>Albaillella excelsa</i>  |
| 258      |                          |                         | LP0r      | <i>Clarkina transcaucasica</i> <i>Clarkina liangshanaensis</i>             |   | <i>Albaillella levis</i>  |
| 258      |                          |                         | L7        | <i>Clarkina levenii</i>  |   |   |
| 260      |                          |                         | L6        | <i>Clarkina asymmetrica</i>  | <i>Nanlingella simplex</i> - <i>Codonofusiliella kwangsiana</i> |   |
| 260      | Permian-Mixed Superchron | Lengwan                 | L5        | <i>Clarkina dukouensis</i>   |   | <i>Albaillella cavitata</i>   |
| 260      |                          |                         | L4        | <i>Clarkina postbitteri postbitteri</i>                                    |   |   |
| 262      |                          |                         | L3        | <i>Clarkina postbitteri hongshuiensis</i>                                  | <i>Lantschichites minima</i>                                    |   |
| 262      |                          |                         | L2        | <i>Jinogondolella granti</i>   | <i>Metadolliolina multivoluta</i>                               |   |
| 264      |                          |                         | L1        | <i>Jinogondolella xuanhanensis</i>   |   | <i>Follicucillus charveti</i>                                       |
| 264      |                          |                         | G7        | <i>Jinogondolella prexuanhanensis</i>                                      |   | <i>Follicucillus scholasticus</i>                                   |
| 266      |                          |                         | G6        | <i>Jinogondolella altudaensis</i>  |   |   |
| 266      |                          |                         | G5        | <i>Jinogondolella shannoni</i>   |   |   |
| 268      |                          |                         | G4        | <i>Jinogondolella postserrata</i>  | <i>Yabeina gubleri</i>  |   |
| 270      |                          |                         | G3        |  | <i>Afghanella schencki</i> / <i>Neoschwagerina margaritae</i>   |   |
| 272      | Kuhfengian               | Kuhfengian              | G2        | <i>Jinogondolella aserrata</i>   | <i>Neoschwagerina craticulifera</i>                             |   |
| 272      |                          |                         | Gu1n      | <i>Illawarra Reversal</i>  |   |   |
| 274      |                          |                         | Cl3r.1n   | <i>Jinogondolella nankingensis</i>   |   |   |
| 274      |                          |                         | C15       | <i>Mesogondolella lamberti</i>   | <i>Neoschwagerina simplex</i>                                   | <i>Pseudoalbaillella ishigai</i>                                    |
| 276      |                          |                         | C14       | <i>Sweetognathus subsymmetricus</i> /<br><i>Mesogondolella siciliensis</i> | <i>Cancellina liuzhiensis</i>                                   | <i>Albaillella sinuata</i>  |
| 278      |                          |                         | C13       | <i>Sweetognathus guizhouensis</i>  | <i>Maklaya elliptica</i>  | <i>Albaillella xiaodongensis</i>                                    |
| 280      |                          |                         | C12       | <i>Neostreptognathodus pnevi</i>   | <i>Shengella simplex</i>  |   |
| 282      |                          |                         | C11       | <i>Neostreptognathodus exsculptus</i> /<br><i>N. pequopensis</i>           | <i>Misellina claudiae</i>                                       |   |
| 284      |                          |                         | C10       | <i>Sweetognathus aff. whitei</i>   | <i>Misellina termieri</i>                                       |   |
| 286      |                          |                         | C9        |  | <i>Pamirina (Brevaxina) dyrehfurthi</i>                         |   |
| 288      | Cisuralian               | Luodianian              | C8        |  |   | <i>Pseudoalbaillella rhombothoracata</i>                            |
| 290      |                          |                         | C7        | <i>Mesogondolella bisselli</i> /<br><i>Sweetognathus anceps</i>            | <i>Robustoschwagerina ziyunensis</i>                            | <i>Pseudoalbaillella lomentaria</i>                                 |
| 292      |                          |                         | C6        | <i>Mesogondolella manifesta</i>  |   | <i>-Ps. sakmarensis</i>   |
| 294      |                          |                         | C5        | <i>Mesogondolella monstra</i> /<br><i>Sweetognathus binodosus</i>          |   |   |
| 296      |                          |                         | C4        | <i>Sweetognathus aff. merrilli</i> /<br><i>Mesogondolella uralensis</i>    | <i>Sphaeroschwagerina moelleri</i>                              | <i>Pseudoalbaillella u-forma</i>                                    |
| 298      |                          |                         | C3        | <i>Streptognathodus barskovi</i>   | <i>Robustoschwagerina kahleri</i>                               | <i>-Ps. elegans</i>   |
| 300      |                          |                         | C2        | <i>Streptognathodus fusus</i>  | <i>Pseudoschwagerina uddeni</i>                                 |   |
| 300      |                          |                         | C1        | <i>Streptognathodus constrictus</i>  |   | <i>Pseudoalbaillella bulbosa</i>                                    |
| 300      |                          |                         | Cl1r.1n   | <i>Streptognathodus isolatus</i>   | <i>Triticites spp.</i>  |   |
| 300      |                          |                         | Cl1n      | <i>Streptognathodus wabaunsensis</i>                                       |   |   |

High-resolution integrative Permian stratigraphic framework (after Shen et al., 2019. Permian integrative stratigraphy and timescale of China. Science China Earth Sciences 62(1): 154-188. Guadalupian ages modified after Shen et al., 2020. Progress, problems and prospects: An overview of the Guadalupian Series of South China and North America. Earth-Science Reviews, <https://doi.org/10.1016/j.earscirev.2020.103412>.